Time Evolution of Holographic Observables

Memoria de Tesis Doctoral realizada por

João Aparício

y presentada ante el Departamento de Física Teórica
de la Universidad Autónoma de Madrid
para la obtención del Título de Doctor en Ciencias

Tesis Doctoral dirigida por **Esperanza López Manzanares,**
Investigador Científico del Instituto de Física Teórica UAM/CSIC

Departamento de Física Teórica
Universidad Autónoma de Madrid

Instituto de Física Teórica
UAM/CSIC

Diciembre de 2013

Acknowledgements

I am thankful to my supervisor Esperanza López for her scientific support and guidance and appreciative of her intuition that drove most of our work together.

I thank Javier Abajo-Arrastia, Daniel Grumiller, Esperanza López, Ioannis Papadimitriou and Stefan Stricker for collaborations that taught me a lot and contributed enormously to the way I understand physics.

Scientifically I am deeply indebted to Ioannis Papadimitriou for being an excelent physicist whose clarity of thought I have always found inspiring and who was always more than patient with my questions. I have also taken advantage of the insight and expertise of José Barbón, Germán Sierra and Karl Landsteiner in their respective fields, and thank them for always making me feel welcome in their offices.

I must thank my good friends Pablo Bueno, Amadeo Jiménez and Diego Regalado for always being ready to help. Their humor was a huge part of my life and shaped my own, and my experience in Madrid would have been significantly bleaker without them.

Over the years I have developed a few interesting subject-oriented relationships. With João Laia and Diego Regalado, our conversations about life, people, and society contributed to a lot to my understanding of our own species. For Sérgio Silva I have a special appreciation for generally being a very nice human being and programmer, and one of my oldest friends. Roberto Vidal has been a very wise man and a collaborator. Eoin Kerrane showed me that chaotic as society is, we can make predictions about it too. Tariq Nath taught me that getting people enthusiastic is an underestimated skill. Thank you all very much.

Finally, I am especially thankful to Snezhanna Trotsenko for being my tiny family for these past few years.

This work was supported by the Fundação para a Ciência e Tecnologia (FCT-Portugal) through the grant SFRH/BD/45988/2008.

Motivation

Why think about the AdS/CFT correspondence?

The AdS/CFT correspondence is a conjecture about the observables in a certain gravity theoriy and in a certain field theory. Defining a map between the observables in the two theories, we say that they are dual to each other if all observables match in the way specified by the map [1, 2, 3]. In practice however, we don't know how to calculate all observables on both sides of the correspondence. But if we think we have enough evidence to believe the correspondence to be true, then this is a reason to think harder about it: maybe we discover that an observable that we couldn't calculate in one of the descriptions can be calculated in the dual description.

Assuming two theories are dual to each other, or rather that they are dual descriptions of the same physics, the question exists of what exactly is the map between physical processes or observables on both sides. If one picks a specific physical process that he knows how to describe on one side of the correspondence, the motivation exists of the completeness of the holographic dictionary. The simple question "What does this physical phenomenon or setup correspond to on the other side?" is of interest in theoretical physics.

One such setup is that of the quantum quenches. Imagine that we take a quantum theory with a certain Hamiltonian which depends on a parameter $H(\lambda_0)$ in a state that is an eigenstate of the Hamiltonian. Then imagine that at some instant in time we change (or "quench") this Hamiltonian into a different one by changing that parameter, $\lambda_0 \to \lambda$. We will find the system in a state which is not an eigenstate of the new Hamiltonian and will thus evolve non-trivially in time. Some questions about this non-trivial evolution are by now textbook questions for the case of quantum mechanics[1], but on the gravity side the question is still open. So the motivation isn't only "I'm interested in quantum quenches, what can I learn about them by using AdS/CFT?", but also "I'm interested in AdS/CFT, lets see what a quantum quench looks like on the gravity side".

Quantum quenches

We will go into more depth into the quantum field theory description of quantum quenches in the following chapters, here we are just concerned with the motivation of the vague idea described in the previous paragraphs. With so many phenomena in nature, both in quantum theories and in gravity theories, why pick specifically quantum quenches to study?

For one thing, if one of the motivations is learning about AdS/CFT, then time-dependent scenarios are a lot less studied in the literature. As such, the things we might learn are more likely to have been open questions. A couple of such questions could be related for example to the thermodynamics of black holes. In static systems it's well understood that the geometric description of their temperature has the same nature as in quantum field theory: it comes from the fact that the imaginary time direction is compact with a certain length β, the inverse temperature. However, for time-dependent situations the story isn't so clear on neither side. The existence of an imaginary time direction demands the existence of an analytic continuation from real time which in a

[1] Although not as much for the case of quantum field theory, where the first results on the subject are relatively recent, depending on what questions you are asking about these non-trivial evolutions.

time-dependent situation needn't exist — and in our model doesn't. How far can we take this geometry interpretation of temperature then?

That was the motivation coming from learning about AdS/CFT, but we also have the motivation of learning about quantum quenches. One big source of interest in quantum quenches is that they have finally become experimentally feasible. Until recently, the question of how observables react to a quantum quench has been theoretical. Traditionally, isolation between the system under consideration and the rest of the universe wasn't good enough that quenches could be performed coherently. After the quench the state would decohere quickly and no unitary evolution could be observed, and so the question remained largely of academic interest. With the development of experimental tools for studying the behavior of optical lattices of ultracold atoms [4,5] there has been renewed interest in this problem.

Limits of the correspondence

When working with AdS/CFT dualities it's good to have in mind exactly how strong the kind of dualities are that we are considering; that is, it might be that two theories are dual in the full range of their free parameters, or it might be that that are dual only in some limit of these parameters. In the original paper by Maldacena several dualities are proposed. But what's the range of validity of these conjectured dualities? How general are they? Lets see a specific example.

The $\mathcal{N} = 4$ conformal SYM has two free dimensionless parameters: N and g_{YM}. The type IIB string theory has one dimensionless parameter, g_s and one parameter of dimension $(\text{length})^2$, α'. If we put this theory on $\mathrm{AdS}_5 \times \mathrm{S}^5$ with both AdS_5 and S^5 of radius L, the second dimensionless parameter of this theory becomes L^2/α'. The strongest form of the conjecture then says that this string theory describes the same reality as the $\mathcal{N} = 4$ conformal SYM if we identify the free parameters as $g_s = g_{\mathrm{YM}}^2$ and $L^2/\alpha' = \sqrt{4\pi g_s N} = \sqrt{4\pi N} g_{\mathrm{YM}}$ [1].

Given this most general version we can take some limit and consider the duality perturbatively around that limit. The 't Hooft limit is taken by defining the 't Hooft coupling, $\lambda \equiv g_{\mathrm{YM}}^2 N$ and taking the limit $N \to \infty$ while at the same time keeping λ fixed. Since we know how g_s is related to g_{YM}^2, we can use this to see what the 't Hooft perturbative expansion means for the string theory. We see that $g_s = \lambda/N$ and so we conclude that the 't Hooft perturbation in SYM translates into a weak coupling perturbation in string theory, also called string loop expansion.

We can take this further. After taking the 't Hooft limit our SYM has only one dimensionless parameter, λ. The limit $\lambda \to 0$ then corresponds to usual quantum field theory perturbative expansion. By our mapping of parameters it corresponds to string theory at large α'/L^2, which is a regime where the strings are large compared to the spacetime curvature. The opposite limit however corresponds to a regime where the strings are point-like compared to the curvature of the spacetime, i.e. gravity. In the SYM theory this is the strong λ coupling limit.

Here we see something which is what makes the AdS/CFT correspondence so hard to study and at the same time so powerful. We can study the theory as $\lambda \to 0$ using the usual perturbative techniques on the field theory side, and study $\lambda \to \infty$ by looking at the dual string theory which in this limit reduces to gravity. So on the one hand, if we believe it, the AdS/CFT correspondence allows us to describe (or define) physics in both limits

of the free parameter of our theory. But on the other hand, for a chosen λ it allows us to use either a field theory description, or a gravity description, but not both simultaneously. This makes it hard to compare observables one by one by doing a calculation and its dual, and comparing the results. Some times this can be done and over the past 16 years much work has focused on doing exactly this. Every time a calculation could be performed on both sides the result has been positive. Examples of quantities that have been tested on both sides of the correspondence because they don't depend on the coupling are the global symmetries, some correlation functions, anomalies, the spectrum of chiral operators, and the moduli space of the theory [6, 7].

Field-operator correspondence

Pairs of theories (typically a gauge theory and a gravity theory) exist such that it is believed that the complete set of their observables matches. Each of the elements of these pairs is known as the dual of one another. For different dualities, more or less convincing evidence for their accuracy exists. Ideally for every theory we would like to study we should find its dual. This would allow us to describe the theory in a different regime of coupling, or calculate the same observables in a different way and so extract different insight. However in general given a theory we don't know how to find its dual theory. What we can do in some cases is given a duality, modify it somehow. We have seen the case of taking limits on both sides of the duality in the previous paragraph. Another thing that can some times be done is truncating the spectrum of both theories. But before arguing for a specific one of these truncations, lets look at something else.

One of the ideas to come out of the AdS/CFT revolution was the relation between the partition function of the string theory and the generating functional of the gauge theory. Consider the partition function of the string theory in the AdS space. The fields need boundary conditions at the boundary of AdS, in the sense that we fix the value of a bulk field $\phi(\bar{x}, z)$ at the boundary $z = 0$ to $\phi_0(\bar{x})$, *i.e.* $\phi(\bar{x}, z)|_{z=0} = \phi_0(\bar{x})$. Therefore the partition function will depend on this boundary condition: $Z_{\text{string}}[\phi_0(\bar{x})]$. On the other hand, we can add to the gauge theory an external source that we couple to the operators in the gauge theory by adding the term $\int d\bar{x}\phi_0(\bar{x})\mathcal{O}(\bar{x})$ to the lagrangian. The claim of [3, 2] is that these are the same,

$$\langle e^{\int d\bar{x}\phi_0(\bar{x})\mathcal{O}(\bar{x})}\rangle_{\text{gauge}} = Z_{\text{string}}[\phi_0(\bar{x})] \tag{1}$$

One of the reasons why this expression is so important is that it gives us an algorithmic way to compute correlation functions. We know that in a field theory correlation functions are derivatives of the generating functional with respect to the external source $\phi_0(\bar{x})$. Therefore according to (1) if we manage to calculate the partition function of the string theory we can take derivatives with respect to the boundary condition $\phi_0(\bar{x})$ and the result will be correlator of the dual theory. In practice it is usually too difficult to calculate such partition function of a string theory. To try and calculate the a partition function exactly will motivate us to move away from a complicated string theory and towards a gravity theory where the problem might be more tractable.

There is therefore a one to one relation between fields in the string theory side and operators in the gauge theory side. The relation between their respective mass m and

scaling dimension Δ is

$$\Delta = \frac{d}{2} + \sqrt{\frac{d^2}{4} + R^2 m^2} \tag{2}$$

where d is the total number of dimensions in the gauge theory and R is the radius of AdS space. In other words, for every field on the gravity side there exists an operator in the dual field theory, correlators of which we can calculate by the use of (1).

Away from exact dualities

From here we can conjecture. If we know a supergravity and its dual, as described above, we can consider a truncation of supergravity. The simplest of these is Einstein's equations with negative cosmological constant

$$E_{\mu\nu} \equiv R_{\mu\nu} - \frac{1}{2} R g_{\mu\nu} + \Lambda g_{\mu\nu} = 0 \tag{3}$$

At present it isn't completely known how these truncations act on the gauge theory, but some partial things can be observed. As explained, a correspondence exists between fields on the gravity side and operators in the gauge theory side. Therefore, it's reasonable to expect that a truncation of fields on the gravity side will correspond to a truncation of operators in the gauge theory. If we could calculate the partition function of the gravity theory exactly, then by (1) we would know the generating functional of the gauge theory. But since we usually can't, we don't know how a truncation of some gravity fields acts on the gauge theory, apart from truncating the corresponding operators.

Of the many truncations of supergravity, why is Einstein's gravity interesting? Because it is relatively simple while at the same time still containing AdS as a solution. In the context of the AdS/CFT duality, the empty AdS solution is a gravity solution which is mapped into the vacuum of the CFT. Also, being a common feature to so many known examples of dualities allows us to blindly apply most of what is known about dualities at least to the gravitational side.

The history of physics reveals which strategies have proven records in scientific research and which ones failed. One good strategy is that given a certain phenomenon we want to study, *Make things as simple as possible, but not simpler.* In a broader philosophical perspective we are left to discuss what is meant by the word "simpler", but in physics one often takes this to mean computational simplicity; after all, once all concepts are understood what is left is doing the calculations.

This means that given a system that contains the phenomenon we want to study and other things, we should simplify our system by removing as many of the other things as possible. We will use this as a justification for the gravity system we choose to study. We start with Einstein's equations and ask *If we were to consider a quantum quench in whatever the dual of Einstein's gravity is, what would that look like in Einstein's gravity?* We hope that such a dual theory exists and argue for a specific answer to question. Then we calculate some quantities and ask ourselves whether the results we obtain seem reasonable.

Gravity in $2+1$ dimensions

Does a field theory dual to (3) even exist?

It's not known for sure[2], but many highly non-trivial results exist. A particularly important one is that of Brown and Henneaux. In 1986 they decided to check how the generators of the isometries of AdS_3 space act on its boundary. They discovered that it acts like the generators of the Virasoro algebra, and computed its central charge. The result is [10]

$$c = \frac{3R}{2G_N^{(3)}} \tag{4}$$

where c is the central charge, R is the AdS_3 radius and G_N^3 is Einstein's constant in three dimensions. So 11 years before the AdS/CFT paper of Maldacena, there already was evidence in the literature that a very subtle relation existed between AdS_3 and a some conformal field theory.

Note however that the regime where string theory reduces to gravity, i.e. R large, is the same where the central charge of the dual theory is large, and therefore out of reach of the powerful techniques to handle CFTs with $c < 1$ [11]. The CFT dual to pure Einstein gravity in asymptotically AdS_3 spaces isn't any well known field theory. It's not even known if it's well-defined except insofar as we can define its correlators to be whatever we can calculate on the gravity side using (1). But in any case, it is known what its central charge should be, (4).

The RHIC experiment and holographic modelling

An important motivation is also that of experiments such as the Relativistic Heavy Ion Collider (RHIC). It is known that while the RHIC data is compatible with the hydrodynamics description of a quark-gluon plasma [12], its transport quantities are not compatible with those predicted by perturbative QCD. This suggests that this high temperature quark-gluon plasma is not weakly-coupled as previously thought [13] but rather a strongly-coupled system [14, 15].

How long after the collision can hydrodynamics be applied? Hydrodynamic modelling of RHIC suggests that the produced plasma isotropizes over a time scale $\tau_{\text{iso}} \lessapprox 1\text{fm/c}$ [12]. This is circumstantial evidence that holographic plasmas could be good to model at least the fast thermalization aspect: they too display very fast thermalization at strong coupling [16, 17, 18, 19].

But we are interested in thermalization. And in the spirit of simplifying the problem, we do not ask "What is the gravitational process dual the collision of heavy nuclei, fireball formation, isotropization, thermalization, hadronization, and all the scales therein?" Instead we realize a lot of physics is involved each bit of which can be studied separately and using different tools. Therefore we take only one of these phenomena — thermalization — and wonder if it's possible to use the AdS/CFT duality to say anything about it. We do this by bringing the system out of equilibrium by what we conjecture is the gravitational dual of a quantum quench, and an especially simple one.

In a field theory, after a quench the system will generically evolve in time towards thermal equilibrium. We know what thermal equilibrium looks like in the context of AdS/CFT: if the gravitational theory is a static black hole, that is dual to a field theory at finite temperature [2]. Therefore one can conjecture that the dual to a quantum quench is a system that at early times has no black hole and at late times has a black hole [20, 21].

[2] See however the fascinating accounts of [8, 9].

There are several ways this can be done. In [16] the time evolution of a homogenous but non-isotropic initial state in a strongly-coupled large N SYM. They did this by turning on a time-dependent background field coupled to an operator of interest, in their case the background field is the metric and the operator of interest in the energy-momentum tensor. They do it in an translational-invariant way to avoid exciting hydrodynamic modes.

Another possible way to do this is by considering the collapse of a dust shell in $2+1$ dimensions. For a space of constant negative curvature dust shell collapse was first investigated numerically in [22], even before Maldacena's paper. Within the framework of holography it was done first in [20, 21], where the authors already give the collapse the interpretation of a thermalization process from the point of view of the boundary theory. As their favorite observables the authors pick the 2-point function of a scalar field, but only solve the problem in two different quasi-static limits of an in-falling dust shell: in [20] they consider the dust shell is moving slowly because it is located near the boundary and so just starting the free fall, and in [21] the dust shell is near the horizon and so it asymptotically freezes for an observer at the boundary. Regarding the infalling dust shell model, we note that translation invariance prevents hydrodynamic modes from being excited as in [16] and this is a good thing if one wants to narrow down the different kinds of physics the model includes.

After we pick the model, we still need to consider what observables we want to look at. In the case of a collapsing dust shell geometry, what kind of observables would be interesting? In [23] it is noticed that the situation might occur that different gravity solutions are identical outside some region, for example in the case of a spherically symmetric collapse of a dust shell to form a black hole. The scale-radius duality [24, 25, 26] suggests that we should be able to know the position of the dust shell from the boundary, since things near the interior (boundary) should correspond to things in the IR (UV) of the dual field theory. For solutions that are identical outside of some region, it seems that expectation values in the CFT can't distinguish such solutions. Therefore the authors of [23] conjecture (and in their chosen model of colliding particles, show) that the observables in the field theory side that contain the extra information required to completely reconstruct the bulk geometry should be non-local observables.

We take this as a hint to pick non-local observables and decide to compute the entanglement entropy [27] and 2-point functions [28][3].

Other models of quantum quenches

After the above, there are several possible generalizations. Apart from the obvious ones — for example, consider high-dimensional analogues where in addition to everything else one could play with the shape of the entangled subsystems — there are two main categories of generalizations possible. One is given the same model for a quench, look at other observables. The other is using different quenches.

How would one go about to consider different quenches? As mentioned, our holographic model of a quench is an Einstein solution interpolating between an empty AdS_3 space and an asymptotically AdS_3 black hole. The problem with generalizing this is that unless we want to consider inhomogeneous solutions, where the problem quickly becomes intractable, that's pretty much it in terms of solutions to pure Einstein gravity.

[3] We haven't defined entanglement entropy at this point, but for now suffice it to say that it is a non-local observable in quantum field theories.

Therefore one possible route is to consider more complicated theories. Specifically, we consider Einstein-dilaton gravity (EDG). There we present an algorithm go generate new solutions with the motivation that in the future they be used to quench between more general solutions. One possibility here is the exact analogue of what we did for pure Einstein gravity: quench from a soliton (empty AdS) and a black hole. Indeed we show that in EDG under certain reasonable assumptions, every $(n+1)$-parameter family of black hole solutions has an associated n-parameter family of solitons. Another possibility is quenching between solitons or between black holes of different solutions. This would correspond to a quench using a parameter of the scalar potential, for example.

This work is organized as follows. In Ch. 1 we recall general facts and results from the CFT literature. In particular, we show how to compute both the entanglement entropy and 2-point functions in both static scenarios and after quantum quenches using CFT techniques. There is no holography involved at that point. In Ch. 2 we recall known solutions which are asymptotically AdS_3 in pure Einstein gravity, and compute space-like geodesic lengths in those spaces. In Ch. 3 we present our model, explain how to compute the relevant observable there in a holographic way and discuss and interpret the results and compare them with the relevant CFT calculations in the literature. This chapter is based on the results of [27]. In Ch. 4 we treat the fast-quench limit of our model and compute general space-like 2-point functions there, thus in some sense generalizing our previous work. This chapter is based on results of [28]. In Ch. 5, based on [29], we present a new algorithm which we use to obtain new EDG solutions. In Ch. 5.4.3 we make a summary of the conclusions of this work and present an outlook.

Contents

1

Results from Conformal Field Theories

Here we show how to calculate two things using exclusively Conformal Field Theory (CFT) tools:

- First, on a CFT at finite temperature and living in 1 spatial dimension, calculate the entanglement entropy between a line segment in the spatial direction at fixed time, and its complement;
- Second, on a CFT also living in 1 spatial dimension and where we do a quantum quench, calculate the time evolution of the 2-point functions and entanglement entropy after a quantum quench.

There are several reasons why we want to do this. First, we want to keep this work as self-contained as possible up to a reasonable extent. Second, we need to understand such calculations from a traditional framework if we want to be able to have some interpretation for the quantities in our final expressions. From the holographic calculations their physical origin can often be mysterious. And third, a favorable agreement between holographic results and traditional results serves as circumstantial evidence that our holographic assumptions and conjectures are probably on the right track.

1.1 General statements regarding 2D CFTs

1.1.1 2- and 4-point functions on the complex plane

The 2-point functions of primary operators of conformal weights h and $\bar{h}$ on the complex plane are [30]

$$\langle \phi(z_1, \bar{z}_1)\phi(z_2, \bar{z}_2)\rangle_{\mathbb{C}} = \frac{1}{(z_1 - z_2)^{2h}(\bar{z}_1 - \bar{z}_2)^{2\bar{h}}} \tag{1.1}$$

if the conformal dimensions of the two fields are equal, and vanishing otherwise, and where $z_i = x_i + iy_i$ represent complex coordinates on the plane. Often one is interested in a particular case of the above expression where it's assumed that $2h = 2\bar{h} = \Delta$. In this case the 2-point function has different expressions which are often seen in the literature,

$$\begin{aligned} \langle \phi(z_1, \bar{z}_1)\phi(z_2, \bar{z}_2)\rangle_{\mathbb{C}} &= \frac{1}{|z_1 - z_2|^{2\Delta}} && (1.2)\\ &= \frac{1}{|\Delta x^2 + \Delta y^2|^{\Delta}} && (1.3)\\ &= \frac{1}{|l^2 - \Delta t^2|^{\Delta}} && (1.4) \end{aligned}$$

The first expression is the special case we are considering, the second expression we used real coordinates to cover the Euclidean plane, and in the third expression we Wick rotated the coordinates $it = y$ and defined $x_1 - x_2 = l$ and $t_1 - t_2 = \Delta t$.

The 4-point functions on the plane however are not completely constrained by the conformal symmetry. Instead, they depend on a function F [30]

$$\langle \phi(z_1, \bar{z}_1)\phi(z_2, \bar{z}_2)\phi(z_3, \bar{z}_3)\phi(z_4, \bar{z}_4)\rangle_{\mathbb{C}} = \left| \frac{z_{13}z_{24}}{z_{12}z_{23}z_{34}z_{14}} \right|^{2\Delta} F(\eta) \tag{1.5}$$

with $\eta \equiv \frac{z_{12}z_{34}}{z_{13}z_{24}}$ and $z_{ij} = z_i - z_j$ and where again we specialized for the case where all the holomorphic and anti-holomorphic conformal dimensions coincide for all the operators, $2h_i = 2\bar{h}_i = \Delta$.

Although the F functions are not completely constrained, they are still very constrained in certain limits of the argument. Specifically [31], F has singular points for $\eta = 0, \infty, 1$ corresponding to placing two operators insertions at the same point, $z_1 \to z_2, z_3, z_4$. At these points $F(\eta) \sim \eta^\alpha$ with the α's given by the OPE of the theory. We will look at these facts more in detail in Sec. 1.2.1 where we apply them to the quantum quench calculation.

1.1.2 Transformation law

In a CFT, under a map $z \to w(z)$, $\bar{z} \to \bar{w}(\bar{z})$, primary operators with conformal dimensions h_i and $\bar{h}_i$ transform in the following way [30]:

$$\phi'(w, \bar{w}) = \left(\frac{dw}{dz}\right)^{-h} \left(\frac{d\bar{w}}{d\bar{z}}\right)^{-\bar{h}} \phi(z, \bar{z}) \tag{1.6}$$

In the present introduction this transformation law is used in the following way. If an n-point is known in a certain Riemann surface, typically either the Euclidean plane or the Euclidean half-plane, then by using (1.6) we can relate it to an n-point function on a different Riemann surface.

The energy momentum tensor is not a primary. Instead, it is a quasi-primary. This means that it transforms like (1.6) for $\mathrm{SL}(2, \mathbb{C})$ transformations, but not for general conformal transformations. Instead, for a general conformal transformations the (holomorphic part of) the energy momentum tensor transforms as

$$T'(w) = \left(\frac{dw}{dz}\right)^{-2} \left[T(z) - \frac{c}{12}\{w; z\}\right] \tag{1.7}$$

where $\{w; z\}$ is the Schwarzian derivative of the map $z \to w(z)$, defined as[1]

$$\{w; z\} = \frac{d^3w/dz^3}{dw/dz} - \frac{3}{2}\left(\frac{d^2w/dz^2}{dw/dz}\right)^2 \tag{1.8}$$

[1]Fun fact: what is the significance of the Schwarzian derivative? If the energy-momentum tensor is not a primary, what terms can we add to its transformation law? First, it should vanish for $\mathrm{SL}(2, \mathbb{C})$ transformations, by definition of quasi-primary. Second, if we want a symmetry group, then it should obey the group property $\{u; z\} = \{w; z\} + \left(\frac{dw}{dz}\right)^2 \{u; w\}$. The Schwarzian derivative is the only such function with these two properties!

Some maps between popular Riemann surfaces

The map

$$z \to w = \frac{L}{2\pi} \log z \tag{1.9}$$

goes from z coordinates on the complex plane to w coordinates on the cylinder of circumference L. $\mathrm{Re}\, w = \frac{L}{2\pi} \log |z|$ is the position along the cylinder and varies between $-\infty$ and $+\infty$, while $\mathrm{Im}\, w = \frac{L}{2\pi} \arg z$ is the position around the cylinder and so goes from 0 to L as $\arg z$ goes from 0 to 2π. It is useful for example to go from a theory on the Euclidean complex plane (that is, zero temperature), to a theory on the cylinder (finite temperature).

Similarly, the map

$$z \to w = \frac{L}{\pi} \log z \tag{1.10}$$

goes from z coordinates on the upper half complex plane (UHP) to w coordinates on an infinite length strip (or equivalently, half a cylinder) of width L. This map will be applied in Sec. 1.2.2 to the calculation of the time-evolution of a state living on the boundary a the strip.

2-point function on a cylinder

As an example of an application of (1.6), lets compute the 2-point function on a cylinder of width L. This object is important because if we identify the infinite length of the cylinder with the infinite length of a spatial dimension and the periodicity of the cylinder with the periodicity of the imaginary time direction, then a cylinder is the Riemann surface appropriate for finite temperature calculations if we set $L = \beta$. On the complex plane, the 2-point function of two primaries of conformal dimensions h and $\bar{h}$ is (1.1)

A map to the cylinder is (1.9). The insertion points on the cylinder are $w_i = (L/2\pi) \log z_i$. The derivatives that we have to calculate in (1.6) are $dw/dz = (L/2\pi) e^{-\frac{2\pi w}{L}}$. To simplify the expressions consider further that the $z_{1,2}$ insertion points are on the real line and that the conformal dimensions of the operators we are considering are equal, $\bar{h} = h$. Direct substitution into (1.6) then gives us the 2-point function on the cylinder

$$\langle \phi'(w_1, \bar{w}_1) \phi'(w_2, \bar{w}_2) \rangle_{\text{Cyl.}} = \left(\frac{2\pi}{L} \right)^{4h} \frac{e^{\frac{4\pi}{L}(w_1+w_2)h}}{\left| e^{\frac{2\pi}{L} w_1} - e^{\frac{2\pi}{L} w_2} \right|^{4h}} \tag{1.11}$$

Consider $w_1 = 0 + i0$ and $w_2 = r + i0$. Substituting above and then taking the large r limit we find

$$\langle \phi\phi \rangle_{\text{Cyl.}} \to \left(\frac{2\pi}{L} \right)^{4h} e^{-\frac{4\pi h}{L} r}, \quad \text{large } r \tag{1.12}$$

and we call this a thermal 2-point function: it's nothing but an exponential decay with a decay constant proportional to the temperature.

1.2 Boundary Conformal Field Theories (BCFTs)

It is known that in a conformal field theory, the presence of a boundary breaks exactly half of the symmetries. Instead of two copies of the Virasoro algebra, we have one Virasoro

algebra. Specifically, if we consider a theory living on UHP this can be seen by considering, of all the conformal transformations, only those that leave the real axis invariant. This means that we allow, instead of complex holomorphic functions, only real holomorphic functions, since those are the functions that map the real axis into itself. Hence we are halving the number of symmetry transformations we are considering.

Consider how one can use a symmetry to constraint correlators. One knows how an operator transforms under general symmetry transformation, in this case (1.6) and so one knows how correlators transform under such transformations. One knows how to relate a correlator to its transformed version. Thus, by considering infinitesimal versions of such transformations, one can obtain differential equations that said correlators must obey. To obtain correlators for a BCFT one has just to obtain such differential equations, not when the relevant symmetry is generated by complex holomorphic functions, but when it is generated by real holomorphic functions.

Exploring the above ideas, in [31] Cardy shows that n-point functions in BCFTs obey the same differential equations as $2n$-point functions in CFTs. Because of this, even though in a CFT conformal symmetry completely fixes (apart from a multiplicative factor) 1-, 2- and 3-point functions and 4-point functions depend on a free function of an anharmonic ratio, in BCFTs only 1-point functions are completely constrained and 2-point functions depend on this free function.

Of course, even though the differential equations are closely related in the two cases, to obtain a specific solution boundary conditions have to be specified. In particular, for physically interesting applications are usually imposed on the boundary of the system. On the one hand, for CFTs the boundary conditions are more or less always that correlators should vanish at infinity, but on the other hand for BCFTs a lot of variety is introduced depending on what one chooses as his boundary conditions.

1.2.1 1- and 2-point functions

1-point functions on the UHP are [31]

$$\langle \phi(z,\bar{z})\rangle_{\text{UHP}} \propto (2\,\text{Im}(z))^{-\Delta} \tag{1.13}$$

where Δ is the bulk scaling dimension of the primary operator ϕ. The constant of proportionality depends both on the operator ϕ and on the boundary conditions we choose on the real axis.

By using the map (1.10) we can get the 1-point on a strip:

$$\langle \phi(z)\rangle_{\text{strip}} \propto \left(\frac{\pi}{2L}\frac{1}{\sin\frac{\tau\pi}{L}}\right)^{\Delta} \tag{1.14}$$

for a strip of width L and where we have used translation invariance along the strip to set the real part of the coordinate to zero, $z = 0 + i\tau$.

The 2-point functions on the UHP are [31,32]

$$\langle \phi(z_1,\bar{z}_1)\phi(z_2,\bar{z}_2)\rangle_{\text{UHP}} = \left(\frac{z_{1\bar{2}}z_{2\bar{1}}}{z_{12}z_{\bar{1}\bar{2}}z_{1\bar{1}}z_{2\bar{2}}}\right)^{\Delta} F(\eta) \tag{1.15}$$

with

$$\eta \equiv \frac{z_{1\bar{1}}z_{2\bar{2}}}{z_{1\bar{2}}z_{2\bar{1}}} \tag{1.16}$$

$z_{ij} \equiv z_i - z_j$. As is the case for 4-point functions on a traditional CFT, symmetry isn't enough to completely determine a 2-point function in a BCFT.

The function F depends on the particular BCFT under consideration. But an important point to us is that in both limits that we will want to take the function F is determined by the OPE of the theory. Lets look at some limits of the argument of the F function [32]:

- The limits $\bar{z}_1 \to z_1$ or $\bar{z}_2 \to z_2$ independently correspond to putting one operator on the boundary of the UHP while leaving the other one in the bulk. This corresponds to the limit $\eta \to 0$. It is known that the behavior of F in this limit is controlled by the bulk-boundary expansion, $F \sim \eta^{\Delta_b}$, where Δ_b is called a boundary scaling dimension;
- The limit $z_2 \to z_1$ means both points are relatively far away from the boundary and shouldn't feel its presence. This means $\eta \to 1$ and in this limit $F \to 1$.

The 2-point function on a strip of width L will also be useful. Repeating the usual procedure, we get

$$\begin{aligned} \langle \phi(0,\tau)\phi(r,\tau)\rangle_{\text{strip}} &\propto \left[\left(\frac{\pi}{L}\right)^2 \frac{\left(-1+e^{\frac{\pi(r+2i\tau)}{L}}\right)\left(-e^{\frac{\pi r}{L}}+e^{\frac{2i\pi\tau}{L}}\right)}{\left(-1+e^{\frac{\pi r}{L}}\right)^2\left(-1+e^{\frac{2i\pi\tau}{L}}\right)^2}\right]^{\Delta} F(\eta) \\ \eta &= -\frac{e^{\frac{\pi(r-i\tau)}{L}}\left(-1+e^{\frac{2i\pi\tau}{L}}\right)^2}{\left(-1+e^{\frac{\pi(r+2i\tau)}{L}}\right)\left(e^{\frac{\pi(r-i\tau)}{L}}-e^{\frac{i\pi\tau}{L}}\right)} \end{aligned} \tag{1.17}$$

1.2.2 Extrapolation length

The presence of a boundary breaks half of the symmetries of the system. One consequence of this is that even though a 1-point function should be either zero or constant if the full conformal group were to be preserved, this isn't the case near the boundary. Now, even when a boundary is present one expects that far away from the boundary its effect is not noticeable, that is, deep in the bulk 1-point functions are still zero or constant in some approximation. Near the boundary we find deviations to this; the 1-point function isn't constant but has non-trivial profile instead. The story as usually told in the condensed matter literature is that in the presence of boundaries a new scale appears in the system. The bulk value of some expected value, for example the magnetization, in the bulk goes to constant only up to corrections of order $\approx \exp(-x/\tau_0)$ where τ_0 is this scale introduced by the presence of the boundary and is called the *extrapolation length* of this state; see Fig. 1.1.

To look at it from a different point of view consider the following argument, which can be found in [33]. Consider a transformation that moves the boundary of the UHP down from $\operatorname{Im} z = 0$ to $\operatorname{Im} z = -\tau_0$, for example the transformation $z \to z + \epsilon(z)$ with $\epsilon(z) = -\tau_0$ for $\operatorname{Im} z > 0$ and $\epsilon(z) = 0$ for $\operatorname{Im} z < 0$; this implies $\partial\epsilon = -\tau_0\delta(\operatorname{Im} z)$. We know how these transformations act on the action, namely $\delta S = -\int dz d\bar{z} T\partial\epsilon$, and so moving the boundary of the UHP down by a distance τ_0 is the same as adding a boundary term to our theory,

$$S \to S + \tau_0 \int dx T \tag{1.18}$$

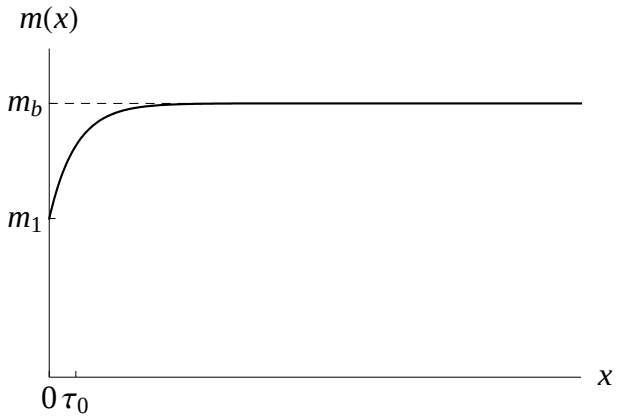

Figure 1.1: Non-trivial profile of the magnetization due to the presence of a boundary at $x = 0$. m_1 is the magnetization at the boundary. m_b is its value deep in the bulk up to corrections of order $\approx \exp(-x/\tau_0)$.

Now, from the thorough discussion in [34, 35] we know how boundary terms of this kind behave under RG-flows: τ_0 always flows to either 0 or $\pm\infty$ at a critical point. $\tau_0 = 0$ would correspond to the 1-point function being constant in the bulk and all the way to the boundary, but this fixed point is actually unstable. The stable fixed points, $\tau_0 = \pm\infty$ correspond to the 1-point function vanishing or diverging, respectively, depending on boundary conditions. So if we see a profile like Fig. 1.1 we know that we are not at a critical point.

Therefore, we again conclude that having a boundary state that is not RG-invariant corresponds to having a finite extrapolation length. In this sense, the extrapolation length *characterizes the RG distance of the actual boundary state from the RG-invariant one* [36].

There are other ways to understand the relation between τ_0 and non-criticality. The integral of T on a spatial section of the system is the Hamiltonian. Therefore, keeping in mind the path integral representation of a wave functional (1.32), perturbing the action as in (1.18) is the same as acting on a state with the operator $e^{-\tau_0 \hat{H}}$. If we want to consider a state $|\psi_0\rangle$ that is not in general conformal invariant, then we should instead use the state $e^{-\tau_0 \hat{H}}|\psi_0\rangle$.

Another way to understand the above replacement is that the effect that the operator $e^{-\tau_0 \hat{H}}$ has on a state is to suppress modes that correspond to distances smaller than τ_0. If the state is in some sense near a IR fixed point then applying that operator to it will erase the information that distinguishes it from a IR fixed point. That is, $|\psi_0\rangle$ and $e^{-\tau_0 \hat{H}}|\psi_0\rangle$ are the same at large distances, but the short distances are additionally conformally invariant in the second case.

In any case, even before we consider the above more or less abstract arguments, we already knew that some kind of regularization would be necessary. We know what the 1-point function on the UHP is, (1.13). But this diverges at the boundary. One way to fix it is to substitute $z \to z + \tau_0$:

$$\langle \phi(z, \bar{z}) \rangle_{\text{UHP}} \propto (2\,\text{Im}(z) + 2\tau_0)^{-\Delta} \tag{1.19}$$

so that the 1-point function is well defined at every point of the UHP. It would instead diverge at $-\tau_0$, but this is not contained in the UHP. The extrapolation length can therefore

also be interpreted as a UV cutoff (additional to the usual lattice cutoff) that we have to introduce whenever boundary effects are present. In condensed matter applications the extrapolation length is usually of the order of the lattice cutoff itself, but *independent from it*. It depends on the details of the state, the system, and the boundary conditions we are considering; see for example [33] for many pedagogical examples.

1.3 Entanglement entropy

Before defining the entanglement entropy, lets say a few words about density matrices.

1.3.1 Density matrices

For the calculation of the entanglement entropy we will need a few observations about density matrices.

In quantum-mechanical ensemble theory, the density matrix is defined to be

$$\hat{\rho} = \sum_n p_n |\psi_n\rangle\langle\psi_n| \tag{1.20}$$

where p_n is the probability that we will find the state $|\psi_n\rangle$ upon measurement.

If we want to consider the canonical ensemble the probability of each state is given by the Boltzmann factor. Then, if we take $|\psi_n\rangle$ to be an eigenvalue of the Hamiltonian, the density matrix is

$$\hat{\rho} = \sum_n Z^{-1} e^{-\beta E_n} |\psi_n\rangle\langle\psi_n| = Z^{-1} e^{-\beta \hat{H}} \tag{1.21}$$

If we want to consider a pure state then we have

$$\hat{\rho} = |\psi_0\rangle\langle\psi_0| \tag{1.22}$$

that is, we have probability 1 of finding the state $|\psi_0\rangle$ and zero of finding any other.

However, the story is more complicated if we want to consider the density matrix in a system with a boundary, for a state $|\psi_0\rangle$ which might in general not be an invariant state, at least if one wants to apply CFT techniques there. In this case it's not enough to plug $|\psi_0\rangle$ into (1.22). Instead, we must bring our non-conformally invariant state $|\psi_0\rangle$ into a conformally invariant one by acting on it with the operator $e^{-\tau_0 \hat{H}}$ as discussed in Sec. 1.2.2. The density matrix to use in this case is then

$$\hat{\rho} = Z^{-1} e^{-\tau_0 \hat{H}} |\psi_0\rangle\langle\psi_0| e^{-\tau_0 \hat{H}} \tag{1.23}$$

where $Z = \langle\psi_0| e^{-2\tau_0 \hat{H}} |\psi_0\rangle$, the partition function on a strip of width $2\tau_0$.

1.3.2 Definition of entanglement entropy

Imagine we want to study quantum entanglement. What would be an appropriate measure for this end? If we consider an imaginary division of the whole system Ω into a subset A and its complement B, we can ask What would be a measure of quantum entanglement

between the degrees of freedom living in A and those living in B? The entanglement entropy of A is defined with this role in mind.

To give a quantitative concretization of these ideas, the entanglement entropy is defined in the following way. Consider a spacial subsystem of the system A and its complement B. Consider that the Hamiltonian of the full system can be written as a direct product of the Hamiltonians of the two subsystem, $H = H_A \otimes H_B$. Calculate the reduced density matrix of the subsystem A defined by integrating out all degrees of freedom localized outside of A, that is in B:

$$\hat{\rho}_A = \mathrm{Tr}_B\, \hat{\rho} \tag{1.24}$$

Even though the total system density matrix $\hat{\rho}$ might or might not be pure, the matrix $\hat{\rho}_A$ will in general not be pure. With respect to this reduced density matrix, we calculate the entropy in the same way one would do an average over macroscopically indistinguishable states in statistical mechanics; the entanglement entropy is therefore defined to be the Von Neumann entropy of this reduced density matrix:

$$S_A = -\,\mathrm{Tr}\; \hat{\rho}_A \log \hat{\rho}_A \tag{1.25}$$

In other words, the entanglement entropy *is the logarithm of the number of states of the inaccessible part of the universe that are consistent with all measurements restricted to the accessible part* [37]. Because the entanglement entropy will in general depend on the geometry of the subsystem A that we consider, it is also sometimes called geometric entropy.

Note that (1.25) really means the sum

$$S_A = -\sum_i \lambda_A^i \log \lambda_A^i \tag{1.26}$$

where λ_A^i are the eigenvalues of $\hat{\rho}_A$. We can therefore see that if the matrix $\hat{\rho}_A$ is pure then the entanglement entropy is zero, and it is non-zero otherwise.

In this sense, the entanglement entropy is thus a measure of how entangled a subsystem A of the total system Ω is with its complement B. However, it isn't so for a mixed state, as the above argument doesn't go through in that case. In this sense, and according to Sec. 1.3.1, we can say that at finite temperature the entanglement entropy contains contributions both from quantum and from statistics. In particular for high temperature, we must recover an extensive results, which has nothing to do with quantum entanglement.

The entanglement entropy is always divergent in a continuum theory. Intuitively, the reason for this is that since a) for any finite region of the theory we have infinitely many degrees of freedom, and b) degrees of freedom closer to each other are more entangled than degrees of freedom farther away, then it follows that any finite region of the theory, no matter how small, will contain infinite entanglement. The entanglement entropy therefore contains a UV divergence. For this reason it's usual to regularize it by introducing a lattice-spacing-like hard cutoff a. In our previous picture, this means that a finite region of the theory will contain a finite number of degrees of freedom. About this regularization it was pointed out [38, 39] that the coefficient of the leading term is proportional to the area of the boundary ∂A of the subsystem. For a d-dimensional system,

$$S_A = f \frac{\mathrm{Area}(\partial A)}{a^{d-1}} + \text{subleading} \tag{1.27}$$

where f is a number that depends on the theory. Intuitively, the explanation for this behavior is that only degrees of freedom entangled across the boundary of the system A contribute to the entanglement entropy, and those near the boundary contribute more. This is true for systems with finite length correlations, but for systems with long correlations, (1.27) actually fail. For example, for 2-dimensional CFTs, the dependence on the cutoff enters through $\log l/a$, where the length l contains all the information about subsystem A: the length of the line segment. In this case the area of A is just two points, thus contributing to S_A with a factor of 2.

We point out a property of entanglement entropy. If the density matrix is pure, then the entanglement entropy of a subsystem A is equal to that of its complement B,

$$S_A = S_B \tag{1.28}$$

As such, at finite temperature we have that $S_A \neq S_B$.

Even though an object with a logarithm of an operator acting on an infinite-dimensional Hilbert space might be scary, we will see that in 2D CFTs the power of symmetry is such that this quantity can sometimes be calculated exactly.

1.3.3 The replica trick

The *replica trick* [37, 40] is the name given to a way to do this calculation that relies on a set of related observations:

- First, we observe that if we manage to calculate $\operatorname{Tr} \hat{\rho}^n$ (and the result is analytical around $n = 1$), then the Von Neumann entropy is

$$S = -\operatorname{Tr} \hat{\rho} \log \hat{\rho} = -\lim_{n \to 1} \frac{d}{dn} \operatorname{Tr} \hat{\rho}^n; \tag{1.29}$$

- The second observation is that the trace of the n-th power of the density matrix is proportional to the partition function of a theory that lives on a Riemann surface constructed by appropriately gluing n copies of the complex plane and considering an n-sheeted theory instead;

- The third observation is that this gluing of planes can also be seen as insertions of certain operators called "branch point twist fields" in a theory that lives on the complex plane.

If we go through these steps we see that we started with a complicated operator on the plane and ended up with the same theory on the plane but with some operators inserted. These operators turn out to be primaries with known conformal dimensions, on the correlator of which we will take derivatives as (1.29) instructs.

Partial traces in quantum field theory

How exactly do we do this selective sum over degrees of freedom of (1.24)? It just so happens that in the path integral formalism this is very natural. If we want to calculate an expected value using the thermal density matrix $\hat{\rho}$ (1.21), we will have inside the path integration the usual weighting factor e^{-S_E}. If instead we want to calculate an expected

value using the reduced density matrix $\hat{\rho}_A$ then we have just to add a path integral over degrees of freedom that live in A's complement, B, at some fixed time t_0:

$$e^{-S_E[\phi]} \to \int_{x\in B} \mathcal{D}\phi(x,t_0) e^{-S_E[\phi]} \tag{1.30}$$

while specifying the boundary configuration $\phi(x,t_0) = \phi_0(x)$ for $x \in A$. Equivalently this can be implemented by introducing appropriate Dirac delta functions that restrict the integration over all paths to an integration over "some paths":

$$\int_{x\in B} \mathcal{D}\phi(x,t_0) e^{-S_E} = \int_{x\in\Omega} \mathcal{D}\phi(x,t_0) e^{-S_E} \prod_{x\in A} \delta(\phi(x,t_0) - \phi_0(x)) \tag{1.31}$$

We can then apply this to the reduced density matrix $\hat{\rho}_A$ to obtain the entanglement entropy S_A. We will see below that there exists a natural representation of an arbitrary power of the density matrix in the path integral formalism.

In the particular case of zero temperature the domain of integration is the plane. The wave functional is then similar, only changing the boundary conditions adequately:

$$\Psi(\phi_0(x)) = \int_{t_E=-\infty}^{\phi(t_E=0,x)=\phi_0(x)} \mathcal{D}\phi e^{-S_E} \tag{1.32}$$

Path integral and Riemann surfaces

In this section we will see how defining the path integral on complicated Riemann surfaces can enable us to compute complicated observables. We will first use this to compute the entanglement entropy between a line segment and its complement on a system defined on an infinite spatial direction. Schematically,

$$\begin{aligned} & n\text{-th power of the density matrix on the plane} \longrightarrow \\ \longrightarrow\ & \text{Vaccum of theory on an } n\text{-sheet Riemann surface} \longrightarrow \\ \longrightarrow\ & \text{Twist operators } \sigma_n \text{ on the plane} \end{aligned} \tag{1.33}$$

With little extra effort we can Wick rotate to obtain the entanglement entropy for theory at finite temperature.

Various quantities on the complex plane have been shown to be related to simpler quantities on more complicated surfaces. This observation has enormous computational power. If you have a complicated observable whose expected value you want to calculate on the complex plane and you believe it might be related to something simple on a Riemann surface, the only tricky part is to determine the relevant Riemann surface. Done that, find the conformal dimension of an operator which would implement such identifications between the n sheets, and identifications between n fields on a single sheet. The initial quantity is then just the expected of these operators on the plane.

For the remaining of this section we will focus on the case of finite temperature. The zero temperature case being $\beta \to \infty$ or equivalently, unrolling our cylinder into a plane. Consider the matrix elements of the thermal density matrix (1.21), $\langle\phi'|\hat{\rho}|\phi''\rangle$. Textbooks[2]

[2]Many textbooks. See for example [41]

tell you that in path integral formalism this is the sum over all paths restricted to a configuration ϕ'' at imaginary time 0 and configuration ϕ' at imaginary time β:

$$\langle\phi'|\hat{\rho}|\phi''\rangle = Z^{-1}\int_S \mathcal{D}\phi(x,\tau)e^{-S_E^\beta}, \quad \text{with } S = \begin{cases} \phi(x,0) = \phi''(x) \\ \phi(x,\beta) = \phi'(x) \end{cases}, \quad \forall x \in \Omega \tag{1.34}$$

Geometrically, this corresponds to computing a sum over paths on an infinite strip. The infinite direction corresponds to the spatial direction, and the width β corresponds to the imaginary time direction.

These boundary conditions can be implemented in the following way:

$$\begin{aligned} \langle\phi'|\hat{\rho}|\phi''\rangle &= Z^{-1}\int \mathcal{D}\phi(x,\tau)e^{-S_E^\beta} \times \\ &\times \prod_{x'\in\Omega}\delta(\phi(x',0)-\phi'(x'))\prod_{x''\in\Omega}\delta(\phi(x'',\beta)-\phi''(x'')) \end{aligned} \tag{1.35}$$

As for the partial trace in (1.24), it consists in taking (1.34) and changing the restriction $\forall x \in \Omega \to \forall x \in B$. This restriction can be implemented in (1.35) as exemplified in (1.31):

$$\begin{aligned} \langle\phi'|\hat{\rho}_A|\phi''\rangle &= Z^{-1}\int \mathcal{D}\phi(x,\tau)e^{-S_E^\beta} \times \\ &\times \prod_{x'\in A}\delta(\phi(x',0)-\phi'(x'))\prod_{x''\in A}\delta(\phi(x'',\beta)-\phi''(x'')) \end{aligned} \tag{1.36}$$

This partial trace in turn has its own geometrical interpretation. It corresponds to taking the infinite strip of (1.34) and identifying the points x along the cylinder such that $x \in B$ at imaginary time 0 with the points $x \in B$ at imaginary time β. Therefore the matrix element $\langle\phi'|\rho_A|\phi''\rangle$ is computed by doing a sum over paths on a cylinder where we made cuts in points $x \in A$ and put there boundary conditions ϕ' and ϕ''.

The next thing that we need to calculate is the power of the reduced density matrix. Now, the matrix element of a power of a matrix can be calculated from the matrix elements of the matrix itself by summing over the appropriate free indices: $(M^2)^i{}_j = \sum_k M^i{}_k M^k{}_j$. For the case at hand, this is

$$\langle\phi^{(1)}|\rho_A^n|\phi^{(n+1)}\rangle = \int \mathcal{D}\phi^{(2)}\cdots\mathcal{D}\phi^{(n)}\langle\phi^{(1)}|\rho_A|\phi^{(2)}\rangle\cdots\langle\phi^{(n)}|\rho_A|\phi^{(n+1)}\rangle \tag{1.37}$$

Therefore geometrically this quantity corresponds to computing the path integral on a Riemann surface obtained by taking n cylinders with cuts in A and gluing one side of cylinder 1 with one side of cylinder 2, the other side of cylinder 2 with one side of cylinder 3 etc all the way up to $n+1$. On the parts of cylinders 1 and $n+1$ that are not glued to anything we put configurations $\phi^{(1)}$ and $\phi^{(n+1)}$.

The trace, the quantity that we want, is then

$$\text{Tr }\rho_A^n = \int \mathcal{D}\phi^{(1)}\cdots\mathcal{D}\phi^{(n)}\langle\phi^{(1)}|\rho_A|\phi^{(2)}\rangle\cdots\langle\phi^{(n)}|\rho_A|\phi^{(1)}\rangle \tag{1.38}$$

In the above formulas, we use $|\phi^{(i)}\rangle$ and $\langle\phi^{(i)}|$ to refer to the in- and out-going state in the i-th copy of the theory. What is happening here is that we are taking our field theory,

integrating over field configurations outside of the subset A and leaving field configurations inside of A without integrating. Then we consider n copies of this setup and impose that the outgoing state of the i-th copy equals de ingoing state of the $i+1$-th copy, and that the outgoing state of the n-th copy equals the ingoing state of the 1st copy, and then integrate the field configurations in A.

To be explicit, we write down the full expression below once with all its details. We will use $\phi(x,\tau,k)$ to refer to the field $\phi(x,\tau)$ in the k-th copy:

$$\begin{aligned}\langle\mathcal{O}(z)\rangle_{\mathcal{R}_A^n} \equiv & \int\prod_{k=1}^{n}\mathcal{D}\phi'(x',k)\mathcal{D}\phi''(x'',k)\prod_{x'''\in A}\delta(\phi'(x''',k+1)-\phi''(x''',k))\times \\ \times & \left(\int\mathcal{D}\phi(x,\tau,k)e^{-S_E^\beta}\prod_{x'\in A}\delta(\phi(x',0,k)-\phi'(x',k))\times\right. \\ & \left.\times\prod_{x''\in A}\delta(\phi(x'',\beta,k)-\phi''(x'',k))\times\mathcal{O}(z,k)\right), \quad k+n\sim k \end{aligned} \tag{1.39}$$

Inside the big parentheses we have n copies of our theory, n copies of (1.36). For each of those copies we insert our operator $\mathcal{O}$ inside the path integration. The Dirac deltas inside the parenthesis impose that we evaluate the path integral on a cylinder with a cut; in other words the parenthesis represent $\langle\phi'|\rho_A\mathcal{O}|\phi''\rangle$. The Dirac delta outside the parenthesis impose that the outgoing field in the k-th copy be equal to the ingoing field in the $k+1$-th copy. Finally, the outer path integration sums over configurations at the gluing points. As a result, the above expression can be interpreted as $\mathrm{Tr}\,(\rho_A^n\mathcal{O})$. In short:

$$\langle\mathcal{O}(z)\rangle_{\mathcal{R}_A^n}\equiv\mathrm{Tr}\ (\rho_A^n\mathcal{O}(z)) \tag{1.40}$$

In the expression above, ρ_A^n is the (reduced) density matrix in the n-replicated theory.

There is another way to look at this expected value computed on this Riemann surface (1.39). We can think that it is instead a path integral on a theory on a complex plane but with n-replicated $\phi_k(z)$ fields which obey some twisted boundary conditions:

$$\phi_k(e^{2\pi i}(w-u)) = \phi_{k+1}(w-u) \tag{1.41}$$
$$\phi_k(e^{-2\pi i}(w-v)) = \phi_{k-1}(w-v) \tag{1.42}$$

These twisted boundary conditions are clearly local, and so can be thought of as being implemented by appropriate insertions of local operators called branch-point twist fields. These fields have been studied before [40, 42, 43] and are known to be primary fields with conformal dimensions

$$h_n=\bar{h}_n=\frac{c}{24}\left(n-\frac{1}{n}\right) \tag{1.43}$$

which implies scaling dimension

$$\Delta_n=\frac{c}{12}\left(n-\frac{1}{n}\right) \tag{1.44}$$

From this way of thinking about it, (1.39) can equivalently be thought of as being the expected value of operator $\mathcal{O}$ inserted together with two of these branch-point twist fields:

$$\langle\mathcal{O}(z)\rangle_{\mathcal{R}_n}\equiv\langle\mathcal{O}(z)\sigma_n(u)\sigma_{-n}(v)\rangle \tag{1.45}$$

From here we can easily find a number of results regarding the entanglement entropy in different systems: we take the 2-point function calculated on the appropriate Riemann surface, together with knowledge of the conformal dimensions of twist fields, (1.43), and plug it into (1.29).

The question arises of what is the meaning of the limit $n \to 1$ in expression (1.29) if n is supposed to be an integer. Turns out the interpretation is unique. Since i) the eigenvalues of $\hat{\rho}$ are $0 \leq \lambda_i < 1$ and ii) $\operatorname{Tr} \hat{\rho} = 1$, then it follows that $\operatorname{Tr} \hat{\rho}^n = \sum_i \lambda_i^n$ is absolutely convergent and analytic for $\operatorname{Re} n > 1$. Therefore its derivative, which is the quantity we're really interested in, also exists and is unique.

A particular case of putting together (1.40) and (1.45) is the following:

$$\operatorname{Tr} \hat{\rho}_A^n = \langle \sigma_n(u) \sigma_{-n}(v) \rangle \tag{1.46}$$

1.3.4 Results

For an infinite length system at some time, the entanglement entropy can be obtained by substituting the 2-point function on the complex plane (1.1) with the correct scaling dimensions (1.44) into (1.29). After appropriate regularization we obtain

$$S_A = \frac{c}{3} \log \left(\frac{l}{a} \right) \tag{1.47}$$

where we defined $l = w_1 - w_2$ to be the separation between insertion points on the real axis or equivalently the size of the subsystem A.

For an infinite length, finite temperature system, take the 2-point function on the cylinder with width $L = \beta$, (1.11), to obtain:

$$S_A^\beta = \frac{c}{3} \log \left(\frac{\beta}{\pi a} \sinh \frac{\pi l}{\beta} \right) \tag{1.48}$$

For a finite temperature system, the low temperature corresponds to $\beta \to \infty$ and so we recover (1.47). This is because non-local observables corresponding to distances smaller than β don't know the system has a certain temperature. The explanation of this in the context of CFTs is that the limit of putting two insertions in the same point depends only on the OPE of the theory and in particular that is not sensitive to whether the theory is on a plane or on a cylinder.

The high temperature limit corresponds to $\beta \to 0$ and the result is

$$S_A^\beta = \frac{c}{3} \log \frac{\beta}{2\pi a} + \frac{\pi c l}{3\beta} \tag{1.49}$$

A finite system at zero temperature differs from the above in that the insertion point separation is across the cylinder, instead of along. This can be obtained by doing a rotation by i on the conformal map (1.9), $w = \frac{iL}{2\pi} \log z$. This is the same as taking (1.48) and doing $\beta \to iL$. The entanglement entropy for a periodic system is then

$$S_A^L = \frac{c}{3} \log \left(\frac{L}{\pi a} \sin \frac{\pi l}{L} \right) \tag{1.50}$$

1.4 Quantum quenches

This thesis is mostly about out of equilibrium physics, and in particular about thermalization. The way to study thermalization is to pick an observable, pick an initial out of thermal equilibrium state, and see how our observable evolves in time.

The one popular way to do this, especially used in condensed matter physics for its proximity to experimental setups, is called a quantum quench. The idea is to start with the system in an initial eigenstate state $|\psi_0\rangle$ of the Hamiltonian $H(h_0)$. h_0 is a parameter of the Hamiltonian that can be externally manipulated. For example, h_0 could be the external magnetic field of an Ising chain. At some moment $t = 0$ the value of h_0 is instantaneously changed to h in a way to make the new Hamiltonian $H(h)$ a critical one. The initial state $|\psi_0\rangle$ will not in general be an eigenstate of $H(h)$, and so will evolve in a non-trivial fashion which can formally be expressed as

$$|\psi_0(t)\rangle = e^{-itH(h)}|\psi_0\rangle \tag{1.51}$$

The expected value of any observable will then be time dependent:

$$\langle\mathcal{O}(t)\rangle = \frac{\langle\psi_0(t)|\mathcal{O}|\psi_0(t)\rangle}{\langle\psi_0(t)|\psi_0(t)\rangle} \tag{1.52}$$

If we have a state $|\psi_0\rangle$ at some position in (complex) time, then we can evolve it in time by acting on it with $e^{-\tau\hat{H}}$. We will consider τ to be real and positive in all the intermediate calculations and treat the theory as Euclidean. At the end we analytically continue the result to complex values of time. The (real) time evolution will be done here when we add to τ an imaginary part it. The validity of the final result therefore depends on the technical assumption that this analytical continuation is allowed.

At this point we have all the results we need to compute the time evolution of 2-point function after a quench. From Sec. 1.3.1 we know the density matrix that we should consider for the initial state and what boundary conditions we should put on the path integral. From Sec. 1.2 we know what a 2-point function on the UHP looks like, and in Sec. 1.1.2 we saw a map from the UHP to the infinite strip, which happens to be the correct Riemann surface for this calculation (because remember, starting in Sec. 1.2.2 and ending in (1.23) we argued that we should act with $e^{-\tau_0 H}$ on our initial bra and kets, displacing them in the imaginary time direciton.)

1.4.1 Results

To study a quantum quench we need to specify a boundary state at $t = 0$. This can be done by doing all calculations on an Euclidean strip of width twice the extrapolation length of the boundary state, $L = 2\tau_0$. This boundary state on the Euclidean strip will play the role of the initial state in real time. It is therefore through this quantity τ_0 named extrapolation length that our choice of the initial state will enter the final result.

Additionally, in the end we analytically continue to real time by adding an imaginary part to complex time

$$\tau = \tau_0 + it \tag{1.53}$$

1-point function

Taking the 1-point function on the strip (1.14) and doing analytic continuation (1.53) we get

$$\langle\phi(t)\rangle_{\text{quench}} \propto \left(\frac{\pi}{4\tau_0}\frac{1}{\cosh\frac{t\pi}{2\tau_0}}\right)^{\Delta} \tag{1.54}$$

We then find the result that for late times $t \gg \tau_0$ we have exponentially decaying 1-point functions

$$\langle\phi(t)\rangle_{\text{quench}} \propto \left(\frac{\pi}{2\tau_0}\right)^{\Delta} e^{-\frac{\Delta\pi}{2\tau_0}t}, \quad t \gg \tau_0 \tag{1.55}$$

This approximation is justified because the extrapolation length is a UV cutoff. We say that the extrapolation length is a UV cutoff in the sense that there's a scale, τ_0, below which we have modified our initial state in order to make our calculations more convenient, namely so that we can use the tools of CFT. In this sense, we shouldn't bother looking at lengths below τ_0 because the short-distance characteristics of the initial state will have been erased.

Equal-time 2-point function

We will now see the calculation of a 2-point function for equal-time insertions following a quantum quench [32]. For this specific application we want the 2-point function on the strip, i.e. (1.17). According to the discussion of Sec. 1.2.2 the only thing we need to do now is say that the width of the strip is twice the extrapolation length, $L = 2\tau_0$ and do the analytic continuation $\tau = \tau_0 + it$. The 2-point function on the strip (1.17) is a big expression so lets look at it in by parts.

The argument of the F function is

$$\eta = \frac{e^{\frac{\pi}{L}(l-i\tau)}\left(-1+e^{\frac{2i\pi\tau}{L}}\right)^2}{\left(1-e^{\frac{\pi}{L}(l+2i\tau)}\right)\left(e^{\frac{\pi}{L}(l-i\tau)}-e^{\frac{i\pi\tau}{L}}\right)} \tag{1.56}$$

We analytically continue to real time, $\tau = \tau_0 + it$, and do the approximation $l/\tau_0, t/\tau_0 \gg 1$. Then

$$\eta \approx \frac{e^{\frac{\pi t}{\tau_0}}}{e^{\frac{l\pi}{2\tau_0}} + e^{\frac{\pi t}{\tau_0}}} \tag{1.57}$$

We now recall the limits of Sec. 1.2.1. We know that we should pay attention to the limits $\eta \to 0, 1$ because those cases correspond to different physical situations where F is known:

- $\eta \to 0$ can be obtained by $l/2 - t \gg \tau_0$ and $l/2\tau_0 \gg 1$. Therefore in this case $F \approx e^{-(l/2-t)\frac{\pi\Delta_b}{\tau_0}}$;
- $\eta \to 1$ can be obtained by $t - l/2 \gg \tau_0$ and $t/\tau_0 \gg 1$. Therefore in this case $F \approx 1$.

The factor in front of (1.17) after analytical continuation of 2-point function on the

strip relevant for the calculation of a quantum quench is

$$\left(\frac{\pi}{2\tau_0}\right)^{2\Delta}\left[\frac{\left(e^{\frac{l\pi}{2\tau_0}}+e^{\frac{t\pi}{\tau_0}}\right)\left(1+e^{\frac{\pi(l+2t)}{2\tau_0}}\right)}{\left(-1+e^{\frac{l\pi}{2\tau_0}}\right)^2\left(1+e^{\frac{t\pi}{\tau_0}}\right)^2}\right]^{\Delta} \tag{1.58}$$

We now do the limit $l/\tau_0, t/\tau_0 \gg 1$ which is justified since τ_0 is an UV cutoff

$$\left(\frac{\pi}{2\tau_0}\right)^{2\Delta}\left[\frac{e^{\frac{l\pi}{2\tau_0}}+e^{\frac{t\pi}{\tau_0}}}{e^{\frac{l\pi}{2\tau_0}}e^{\frac{t\pi}{\tau_0}}}\right]^{\Delta} \tag{1.59}$$

Putting this together with the above limits, we find the equal-time 2-point function following a quantum quench [32, 36]:

$$\langle\phi(0,t)\phi(l,t)\rangle_{\text{quench}} \propto \begin{cases} e^{-\frac{l\pi\Delta}{2\tau_0}} & t > l/2 \\ e^{-\frac{t\pi\Delta}{\tau_0}}e^{-(l/2-t)\frac{\pi\Delta_b}{\tau_0}} & t < l/2t \end{cases}, \quad l/\tau_0, t/\tau_0 \gg 1, \quad |l-2t| \gg \tau_0 \tag{1.60}$$

Entanglement entropy following a quantum quench

In particular this will allow us to calculate the evolution of the entanglement entropy following a quench by virtue of the discussion in Sec. 1.3, specifically because we know how to write the entanglement entropy in terms of the n-power of the trace (1.29) and in turn know how to write this in terms of a 2-point function (1.46) of primaries of known scaling dimensions $x = \Delta_n$, (1.44). The entanglement entropy following a quantum quench can be obtained by plugging (1.59) into (1.29). The result is

$$S_l(t) \sim -\frac{c}{6}\log\left(e^{-\frac{l\pi}{2\tau_0}}+e^{-\frac{t\pi}{\tau_0}}\right) \tag{1.61}$$

where we dropped a non-universal term. Then, again under the assumption that $l/\tau_0, t/\tau_0 \gg 1$, we see that the above is [44]

$$S_l(t) \sim \begin{cases} \frac{\pi ct}{6\tau_0} & t < l/2 \\ \frac{\pi cl}{12\tau_0} & t > l/2 \end{cases} \qquad l/\tau_0, t/\tau_0 \gg 1, \quad |l-2t| \gg \tau_0 \tag{1.62}$$

More general 2-point function

The question of more general 2-point function is equally simple in principle but algebraically more complex. The map from the UHP to the strip (1.10) is now used for two completely independent points on the UHP. Namely for two points $w_1 = 0 + i\tau_1$ and $w_2 = l + i\tau_2$ with $\tau_1 = \tau_0 + it_1$ and $\tau_2 = \tau_0 + it_2$ where t_1 and t_2 are now independent numbers which denote the independent insertions in real time. This is more complex only because the algebra is more involved and more different limits have to be considered separately, but the idea is the same. Therefore we will just quote the result here. It is, for l, t_1, t_2, $|t_1 - t_2| \gg \tau_0$ [36]:

$$\langle\phi(0,t)\phi(l,s)\rangle_{\text{quench}} \propto \begin{cases} e^{-\pi\Delta(t_1+t_2)/4\tau_0}e^{-\pi\Delta_b(t_1+t_2-l)/4\tau_0} & l > t_1+t_2 \\ e^{-\pi\Delta l/4\tau_0} & t_1-t_2 < l < t_1+t_2 \\ e^{-\pi\Delta|t_1-t_2|/4\tau_0} & l < |t_1-t_2| \end{cases} \tag{1.63}$$

2
Gravity in AdS_3

In this chapter we recall known asymptotically AdS_3 solutions to pure Einstein gravity. We introduce the WKB approximation for the holographic calculation of 2-point functions and compute space-like geodesics in these spaces.

2.1 Solutions to $2+1$-dimensional gravity

The general spherically symmetric static solution in $2+1$ gravity can be written as

$$ds^2 = -\left(\frac{r^2}{L^2}+\gamma\right)dt^2 + \left(\frac{r^2}{L^2}+\gamma\right)^{-1}dr^2 + r^2 d\phi^2, \quad 0<\phi<2\pi \tag{2.1}$$

whose Euclidean version is

$$ds^2 = \left(\frac{r^2}{L^2}+\gamma\right)d\tau^2 + \left(\frac{r^2}{L^2}+\gamma\right)^{-1}dr^2 + r^2 d\phi^2, \quad 0<\phi<2\pi \tag{2.2}$$

For $\gamma = 1$ these are AdS_3:

$$ds^2 = -\left(\frac{r^2}{L^2}+1\right)dt^2 + \left(\frac{r^2}{L^2}+1\right)^{-1}dr^2 + r^2 d\phi^2, \quad 0<\phi<2\pi \tag{2.3}$$

and its Euclidean counterpart.

For $\gamma > 0$ we have that $0 < r < \infty$. We introduce the coordinate $\frac{r}{L} = \sqrt{\gamma}\sinh\frac{\rho}{L}$, where $r = 0$ coincides with $\rho = 0$. The metric becomes in these coordinates

$$ds^2 = -\gamma\cosh^2\frac{\rho}{L}dt^2 + d\rho^2 + \gamma L^2\sinh^2\frac{\rho}{L}d\phi^2 \tag{2.4}$$

Around the origin we have

$$ds^2 \approx -\gamma dt^2 + d\rho^2 + \gamma\rho^2 d\phi^2 \tag{2.5}$$

which shows that if $\gamma > 0$ then for $\gamma \neq 1$ this space has a conical singularity at the origin, since the perimeter of a circle around the origin is then $\int_0^{2\pi}\sqrt{g_{\phi\phi}}d\phi = 2\pi\sqrt{\gamma}\rho$. These spaces are known to be point particles in AdS_3 [45].

For $\gamma < 0$ and defining $m = -\gamma > 0$ we have the BTZ black hole [46, 47]

$$ds^2 = -\left(\frac{r^2}{L^2}-m\right)dt^2 + \left(\frac{r^2}{L^2}-m\right)^{-1}dr^2 + r^2 d\phi^2, \quad 0<\phi<2\pi \tag{2.6}$$

The metric (2.6) is interesting in Lorentzian space. However if we want it to be analytical we have to worry about possible conical singularities in its Euclidean version, which in this case might occur at the horizon. To study this possibility we go to the Euclidean where there $mL^2 < r < \infty$ and define the coordinate $r = L\sqrt{m}\cosh\frac{\rho}{L}$ and we get

$$ds^2 = m\sinh^2\frac{\rho}{L}d\tau^2 + d\rho^2 + mL^2\cosh^2\frac{\rho}{L}d\phi^2 \tag{2.7}$$

where now the horizon is placed at $\rho = 0$. Expanding around this point we get

$$ds^2 \approx \frac{m}{L^2}\rho^2 d\tau^2 + d\rho^2 + mL^2 d\phi^2 \tag{2.8}$$

Now to avoid a conical singularity as ρ goes to zero, around that point we must have an angle of 2π. This means that τ must be periodic,

$$\tau \sim \tau + \beta, \quad \beta = \frac{2\pi L}{\sqrt{m}} \tag{2.9}$$

This is the correct periodicity to use, as can be checked by the fact that we can then reproduce the formula for the perimeter of a circumference of radius ρ: $\int_0^\beta \sqrt{g_{\tau\tau}}d\tau = 2\pi\rho$.

In summary, two types of conical singularities could in principle arise. The first type are in the compact coordinate ϕ and if $\gamma > 0$ their absence fixes the γ parameter. Incidentally, we mention that this also shows that the $2+1$-dimensional asymptotically AdS space with compact spatial direction has a mass gap. Again taking $m = -\gamma$ we see that this implies states have either $m = -1$ or $m \geq 0$. The case $m = -1$ corresponds to pure AdS space and the case $m \geq 0$ corresponds to a continuum of BTZ black holes. The second type of conical singularities are in the imaginary time direction τ and fixes the β parameter (which in turn fixed the temperature of the BTZ black hole).

Regarding the Poincare patch, we define it as saying that the ϕ coordinate is not compact (and calling it x instead). The metric for Poincare AdS is

$$ds^2 = -\frac{r^2}{L^2}dt^2 + \frac{L^2}{r^2}dr^2 + r^2dx^2 \tag{2.10}$$

and the Poincare black hole is

$$ds^2 = -\left(\frac{r^2}{L^2} - m\right)dt^2 + \frac{dr^2}{\frac{r^2}{L^2} - m} + r^2dx^2 \tag{2.11}$$

Since the spatial coordinate is no longer compact, we can't consider a cycle contractible to a point and so the first type of conical singularities can't occur and so in the Poincare coordinates we don't have a mass gap and $m = 0$ corresponds to pure AdS. However, the second type can and so (2.9) also applies to (2.11).

From now on we will take all of the above expressions with $L = 1$.

Vaidya AdS$_3$

Here we superficially describe Vaidya in asymptotically AdS spaces. We won't spend much time on it in this section because a detailed description is the subject of much of what is ahead.

Starting from (2.6) (with $L = 1$) we transform to Eddington-Finkelstein "time" coordinate v, which is related to the global time t by

$$v = t + f(r)\,, \qquad \frac{df(r)}{dr} = \frac{1}{r^2 - m} \tag{2.12}$$

In these coordinates the BTZ metric is

$$ds^2 = -(r^2 - m)dv^2 + 2dvdr + r^2dx^2 \tag{2.13}$$

From here we can make m depend on Eddington-Finkelstein "time" v. This is called Vaidya AdS_3

$$ds^2 = -(r^2 - m(v))dv^2 + 2dvdr + r^2dx^2 \tag{2.14}$$

This geometry will be solution to Einstein's equations (3) provided on the rhs we include a matter energy-momentum tensor

$$T_{vv} = \frac{1}{2r}\frac{dm(v)}{dv} \tag{2.15}$$

with all other components being equal to zero. The energy-momentum tensor characteristic of null dust satisfies $T_{\mu\nu} \propto k_\mu k_\nu$ with $k^2 = 0$. The previous expression is of this form with $k_\mu = \delta_{\mu v}$. This generates infalling radial null geodesics and therefore (2.14) describes the formation of a black hole out of collapsing null dust. This metric was first obtained in [48].

We note that the null energy condition constrains (2.15). This condition says that the local energy density measured by a null observer always has to be non-negative,

$$T_{\mu\nu}k^\mu k^\nu \geq 0\,, \qquad \text{for any null vector } k^\mu. \tag{2.16}$$

This requirement constraints the mass function. It has to obey

$$\frac{dm(v)}{dv} \geq 0 \tag{2.17}$$

that is the mass function is a monotonically increasing function of v and so that the null matter that collapses has positive energy density.

2.2 WKB approximation and regularization of correlators

We have introduced the canonical way to compute correlators in AdS/CFT in Sec. . However this involves computing a gravity partition function which although feasible in simpler cases, doesn't appear so for the case of the Vaidya metric. There is however a different procedure which although approximate is much simpler.

WKB approximation

A different way from [2,3] to calculate CFT propagators has been proposed in [26]. Consider bulk correlators and take the external points to the boundary, being careful with the proper normalization which is necessary due to the diverging Weyl factor at the boundary

$$G_{\text{boundary}}(b_1, \ldots, b_n) = \prod_{i=1}^{n} \lim_{y_1 \to b_i} r^{d_i} G_{\text{bulk}}(y_1, \ldots, y_n) \tag{2.18}$$

where obviously b_i are points in the boundary and y_i are points in the bulk. For an asymptotically AdS space rescalings in the radial direction are asymptotically a symmetry. We then expect G_{bulk} to transform covariantly at least asymptotically under these rescalings, *i.e.* for large r doing $r \to \lambda r$ implies $G_{\text{bulk}} \to \lambda^{-x} G_{\text{bulk}}$ where x is a positive number which depends on the number of entries in G and on the mass dimension of the relevant field in the field-operator correspondence. For a 2-point function, $x = 2\Delta$ where the scaling dimension Δ in the field theory is related with the mass of the relevant field through (2). Of course, this vanishes at the boundary, and so the r^{d_i} factors in (2.18) are necessary: compensating for the polynomial divergence of the metric Weyl factor at the boundary is equivalent to compensating for the polynomial vanishing of the bulk correlators at the boundary.

G_{bulk} can be represented as an integral over paths in a gravity theory. For a particle with lowest AdS_3 eigenvalue Δ,

$$G_{\text{bulk}} = \int \mathcal{D}\mathcal{P} e^{i\Delta L(\mathcal{P})} \tag{2.19}$$

where $L(\mathcal{P})$ is the proper length of a certain path $\mathcal{P}$, $L(\mathcal{P}) = \int (-g_{\mu\nu}\dot{X}^\mu \dot{X}^\nu)^{\frac{1}{2}}$, here defined to be imaginary for spacelike paths.

In the WKB approximation the CFT propagator is dominated by bulk geodesics [23],

$$\langle \phi(x_1)\phi(x_2)\rangle = \lim_{r_b \to \infty} r_b^{2\Delta} \sum_g e^{-\Delta L_g(x_1,x_2)} \tag{2.20}$$

where L_g is a real proper length connecting the appropriate geodesic end-points and the sum is over the several geodesics that might exist for the same pair of points.

Regularization

We are therefore primarily interested in calculating geodesic lengths. These are however divergent due to the metric divergence at the boundary. One way to regularize this is to put the end-point of these geodesics not at the boundary but at a point at a finite but large point in the radial direction, r_b. The scale-radius duality suggests that in the bulk theory things that happen near the boundary correspond in the boundary theory to things in the UV. Therefore we expect that this regularization corresponds to some kind of UV regulator in the boundary theory. Indeed, we will see by comparison between the holographic results, for example (2.33) and (2.41), and the CFT calculations, for example (1.47), (1.48) and (1.50), that this is exactly what happens. This is another incarnation ofthe scale-radius duality, and suggests that we must be doing something right.

We mentioned that (2.18) vanishes polynomially in the radial direction r. This means that the leading order of the sum in (2.20) is $r_b^{-2\Delta} \approx e^{-\Delta L(r_b)}$ or equivalently

$$L(r_b) \approx 2 \log r_b \tag{2.21}$$

In other words, the regularization procedure for the correlator G_{bulk} of multiplying by factors of r^{d_i} is equivalent to regularizing the proper length L by subtracting a logarithmic divergence:

$$L = L_{\text{reg}} + 2 \log r_b \tag{2.22}$$

Finally, our main expression for the calculation of 2-point functions will be, in the limit that the Δ in (2.20) is large,

$$\langle \phi(x_1)\phi(x_2)\rangle = e^{-\Delta L_{\rm reg}(x_1,x_2)} \tag{2.23}$$

2.3 Spacelike geodesics in asymptotically AdS_3 spaces

In this section we present spacelike geodesics in the asymptotically AdS Poincare black hole as described by the metric (2.11). In every geodesic equation we use dot $\dot{}$ to denote derivation with respect to the proper length parameter λ and prime $'$ to denote derivation with respect to the AdS radius r.

We say that a solution to the equation,

$$\nabla_{\boldsymbol{K}} K^\mu = 0\,, \qquad \text{with } K^\mu = dx^\mu/d\lambda \tag{2.24}$$

is called a geodesic $x^\mu(\lambda)$. Since (2.24) is invariant under affine transformations $\lambda \to a\lambda+b$ then that equation additionally selects a preferred parametrization. We say therefore that solutions to (2.24) are geodesics that come equipped with an affine parameter λ.

The geodesic equations of (2.11) are

$$\dot{t} = \frac{A}{r^2-m} \tag{2.25a}$$

$$\dot{r} = \pm\frac{1}{r}\sqrt{A^2r^2+(r^2-m)(Br^2-r_*^2)} \tag{2.25b}$$

$$\dot{x} = \frac{r_*}{r^2} \tag{2.25c}$$

For $m=0$ we have the equations for geodesics in pure AdS_3.

Equation (2.24) implies [49] that the vector tangent to a geodesic is constant,

$$\boldsymbol{K}\cdot\boldsymbol{K} \equiv K^\mu K^\nu g_{\mu\nu} = B \tag{2.26}$$

which we choose to set to $B=-1,0,+1$ for timelike, null and spacelike geodesics respectively. From (2.25b) we can see only geodesics for which $B=1$ can reach the boundary, that is, spacelike geodesics. These are the geodesics we will be interested in, and so we set $B=1$ in (2.25b) from now on.

In a geometry with an isometry, motion along geodesics leaves constant the scalar product between its tangent vector and the Killing vector describing the isometry. The geometry (2.11) is left invariant by translations in the x and t coordinates, with associated Killing vectors $\boldsymbol{\partial}_x$ and $\boldsymbol{\partial}_t$. We have therefore the associated constants of motion

$$\boldsymbol{K}\cdot\boldsymbol{\partial}_t = g_{\mu\nu}K^\mu\delta^\nu_t = -A\,, \quad \boldsymbol{K}\cdot\boldsymbol{\partial}_x = g_{\mu\nu}K^\mu\delta^\nu_x = r_* \tag{2.27}$$

Therefore $-A$ is the constant associated with invariance of the metric under time translations, that is an energy, where the sign has been chosen for convenience. The constant r_* has the interpretation of a conserved momentum. By choosing appropriately the sign of the affine parameter, we can always impose $A>0$. Using invariance under parity, which will be also preserved by the dynamical metric we will later consider, we can take $r_*>0$ without loss of generality.

2.3.1 Poincare AdS_3

The metric for the Poincare patch of pure AdS_3 is (2.11) with $m = 0$, and the corresponding geodesic equations are (2.25). The solutions to these equations are

$$t_\pm(r) = t_0 \pm t^{\rm AdS}(r)\,, \qquad x_\pm(r) = x_0 \pm x^{\rm AdS}(r) \tag{2.28}$$

where

$$\frac{t^{\rm AdS}}{A} = \frac{x^{\rm AdS}}{r_*} = \frac{\sqrt{A^2 + r^2 - r_*^2}}{r|r_*^2 - A^2|} \tag{2.29}$$

Given the translational invariance in t and x of the geometry, the integration constants t_0 and x_0 do not have any influence on the geodesic length. The separation between the geodesic end-points (t_1, x_1) and (t_2, x_2), is related to the constants of motion by

$$|\Delta t| = \frac{2A}{|r_*^2 - A^2|}\,, \qquad l = \frac{2r_*}{|r_*^2 - A^2|}\,, \tag{2.30}$$

where $\Delta t = t_1 - t_2$ and $l = |x_1 - x_2|$.

When $r_* > A$, the geodesics extend from the boundary to the minimal value of the radial coordinate

$$r_m = \sqrt{r_*^2 - A^2}\,, \tag{2.31}$$

where both branches join.

As can be seen from (2.30), the geodesic end-points are spacelike separated in this case. When instead $r_* < A$ the branches $\pm$ describe disconnected branches that reach down to $r = 0$, where $t, x = \pm\infty$. In this case the end-points at the boundary would have a timelike separation but we don't understand in what sense disconnected branches can be though of as being part of the same geodesic. In particular in this case we are not able to reproduce the correct correlator that would be associated under the WKB approximation [28]. We won't study the timelike case any further.

The proper length of the geodesic is given by

$$L = 2\int_{r_0}^{r_b} \frac{dr}{\dot r} = 2\int_{r_0}^{r_b} \frac{dr}{\sqrt{A^2 + r^2 - r_*^2}}\,, \tag{2.32}$$

with the lower integration limit equal to r_m in (2.31) for $r_* > A$ and zero otherwise. For r_b going to infinity this integral does not converge and so we regularize it as explained in Sec. 2.2. The result for the regularized geodesic length (2.22) is

$$L_{\rm reg} = -\log\frac{|r_*^2 - A^2|}{4} = \log|l^2 - \Delta t^2|\,. \tag{2.33}$$

where we used (2.30).

2.3.2 Poincare black hole

The metric we consider now is again (2.11) but now with general m. These black holes are given different names in the literature, like planar BTZ or BTZ in Poincare coordinates. They are in fact very different from BTZ black holes and so we choose to call them simply Poincare black holes, with the understanding that we implicitly mean that these black holes are asymptotically AdS.

The geodesic equations (2.25) can also be integrated for general finite m (below we use indistinctly $\sqrt{m} = r_h$):

$$t_\pm(r) = t_0 - \frac{1}{2r_h} \log\left[m^{-1}\left(\epsilon X_t(r) \mp \text{sign}(r^2-m)\sqrt{X_t^2(r) - C}\right)\right] , \tag{2.34a}$$

$$x_\pm(r) = x_0 - \frac{1}{2r_h} \log\left[m^{-1}\left(\tilde{\epsilon} X_x(r) \mp \sqrt{X_x^2(r) - C}\right)\right] , \tag{2.34b}$$

where we have defined

$$\begin{gathered} X_t(r) = r_*^2 - A^2 - m - \frac{2A^2 m}{r^2 - m} , \qquad X_x(r) = r_*^2 - A^2 + m - \frac{2r_*^2 m}{r^2} , \\ C = (r_*^2 - A^2 - m)^2 - 4A^2 m = (r_*^2 - A^2 + m)^2 - 4r_*^2 m , \end{gathered} \tag{2.35}$$

together with

$$\epsilon = \text{sign}(r_*^2 - A^2 - m) , \qquad \tilde{\epsilon} = \text{sign}(r_*^2 - A^2 + m) . \tag{2.36}$$

The value of the radial coordinate ranges from infinity to the zero of the square root in the functions (2.34) with larger r

$$r_m^2 = \frac{1}{2}\left(r_*^2 - A^2 + m + \sqrt{C}\right) , \tag{2.37}$$

whenever this quantity is real and positive. Otherwise we have two separated trajectories, both reaching the black hole singularity $r = 0$. A necessary condition for this not to happen is that C is positive, which we will assume in this subsection — keep in mind that some of the statements made below are only valid in this case. This is the only case relevant for geodesics of the eternal black hole spacetime, but we will consider more general scenarios in Sec. 4.2.2. In order to describe the geodesics we will need to consider the extended Penrose diagram of the eternal black hole, which has a second asymptotic region (wedge III) and a past singularity (wedge IV). The time t acquires a non-vanishing imaginary part in three of the four wedges that compose the extended diagram, as shown in Fig. 2.1; see [50] and also [51].

The different geodesic types can be classified by the signs ϵ and $\tilde{\epsilon}$ in (2.36):

- When $\epsilon = \tilde{\epsilon} = 1$ the minimal value of the radial coordinate satisfies $r_m > r_h$, implying that these geodesics stay always outside the event horizon and are therefore completely contained in either wedge I or III.

- When $\epsilon = -1$ and $\tilde{\epsilon} = 1$ the associated geodesics reach behind the event horizon but they do not fall into the singularity, since for them $0 < r_m < r_h$. Close to the horizon the two branches of the geodesic time behave respectively as

$$t_\pm(r) \simeq \mp \frac{1}{2r_h} \log(r - r_h) . \tag{2.38}$$

  Therefore crossing the horizon adds an imaginary part of $-i\pi/2r_h$. Comparing with (2.9) we see that this is exactly the $-i\beta/4$ in the complex description of the eternal black hole of [51] when going from wedge I to wedge II (which they call going from wedge I to wedge III in that paper), or equivalently two crosses add up to the $-i\beta/2$ of [50] when going from wedge I to wedge III (which they call going from wedge

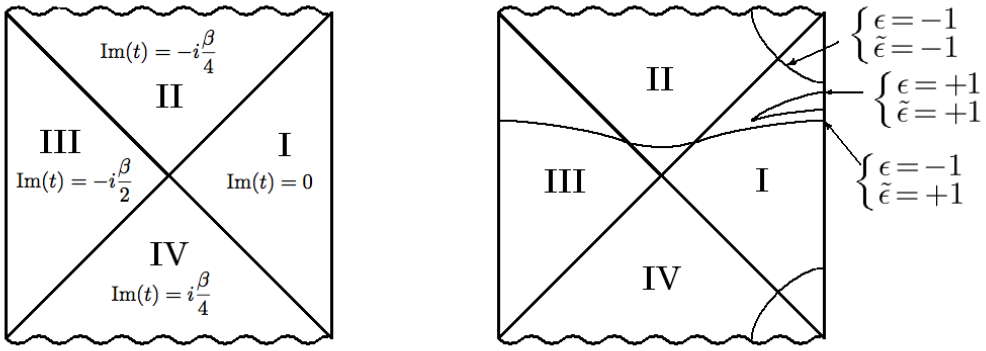

Figure 2.1: On the left we show the imaginary part of $t(r)$ in the different wedges of the Penrose diagram of the eternal BTZ. On the right we draw qualitatively different types of BTZ geodesics according to our classification.

1_{++} to wedge 1_{+-} in that paper). In any case, the fact that the time coordinate jumps in the imaginary direction by an amount given by (2.38) when crossing the horizon means in our language that to glue geodesic branches that enter the horizon we might need to adjust the time integration constants of (2.34a) adequately. For example, for a geodesic that connects wedge I with wedge III we would need to choose $t_{0-} = t_{0+} - i\beta/2$, with t_{0+} real. These geodesics connect two separated boundaries.

The conserved quantities A and r_* are related the separation between the end-points for the three types of geodesics described above by

$$\cosh\frac{2\pi\Delta t}{\beta} = \frac{|r_*^2 - A^2 - m|}{\sqrt{C}}\,, \qquad \cosh\frac{2\pi l}{\beta} = \frac{|r_*^2 - A^2 + m|}{\sqrt{C}}\,, \tag{2.39}$$

where for geodesics ending on opposite boundaries we have defined $\Delta t = \mathrm{Re}(t_1 - t_2)$. When the end-points lie on the same boundary, their separation is spacelike (timelike) when $\epsilon = \tilde{\epsilon} = 1(-1)$. For geodesics connecting both AdS boundaries, there is no restriction on the values of Δt and l.

The proper length of the geodesic in the BTZ background is

$$L = 2\int_{r_m}^{r_b}\frac{dr}{\dot{r}} = \int_{r_m^2}^{r_b^2}\frac{dr^2}{\sqrt{A^2r^2 + (r^2-m)(r^2-r_*^2)}}\,. \tag{2.40}$$

Notice that this expression also applies to geodesics with $\epsilon = \tilde{\epsilon} = -1$ if we analytically prolong them to negative values of the radial coordinate square, $r^2 \geq r_m^2$. The integration can be explicitly performed, with the result for the regularized length

$$L_{\mathrm{reg}} = -\log\frac{\sqrt{C}}{4}\,. \tag{2.41}$$

Using (2.39) to express C in terms l and Δt, and substituting into (2.23) we obtain

$$\langle\mathcal{O}(l,t_1)\mathcal{O}(0,t_2)\rangle = \left[\left(\frac{2\pi}{\beta}\right)^2\frac{1}{2|\cosh(2\pi l/\beta) - \epsilon\tilde{\epsilon}\cosh(2\pi\Delta t/\beta)|}\right]^{\Delta}\,. \tag{2.42}$$

When $\epsilon\tilde{\epsilon} = 1$, (2.42) correctly reproduces the 2-point function at thermal equilibrium for a 2-dimensional CFT with a compact spatial direction for spacelike separations [52].

It has been proposed that geodesics connecting the two asymptotic AdS boundaries of the eternal black hole are associated with eld theory correlators in the Schwinger-Keldysh, or real-time formalism [51, 53]. In this formalism the tensor product of two copies of the original eld theory is considered. The following pure but entangled state is associated with the system at thermal equilibrium

$$|\Psi\rangle = \frac{1}{Z^{1/2}} \sum_i e^{-\frac{1}{2}\beta E_i} |E_i\rangle_1 \otimes |E_i\rangle_2 \tag{2.43}$$

with $|E_i\rangle$ energy eigenstates of the theory. Ordinary thermal correlators are obtained when all operators are inserted on the same copy of the system. In the state (2.43), correlators with operators acting on different copies of the system can be related with ordinary ones by

$$\langle\Psi|\mathcal{O}_1(l,t_1)\mathcal{O}_2(0,t_2)|\Psi\rangle = \langle\Psi|\mathcal{O}_1(l,t_1)\mathcal{O}_1(0,-t_2 - i\beta/2)|\Psi\rangle \tag{2.44}$$

The holographic 2-point function (2.42) agrees with this relation. Using the bulk to boundary propagator, 2-point function between operators inserted on both copies have been obtained in the context of the AdS/CFT correspondence in [51, 50].

2.4 Holographic Entanglement entropy

In [54, 55] a holographic formula was proposed by Ryu and Takayanagi (RT) to compute the entanglement entropy in an Euclidean space. Consider a subsystem A of the boundary theory. Consider also the minimal surface γ_A of dimension d (or equivalently co-dimension 2) that lives in the bulk and is homologous to A, i.e. such that there exists a region r_A with $\partial r_A = A \cup \gamma_A$. Then in the boundary theory, the entanglement entropy between subsystem A and its complement is given by

$$S_{\mathrm{A}} = \frac{\text{Area of } \gamma_A}{4G_N^{(d+2)}} \tag{2.45}$$

$G_N^{(d+2)}$ is Newton's constant in the bulk theory.

For the particular case of $\mathrm{AdS}_3/\mathrm{CFT}_2$, the subsystem A is a line segment and its boundary ∂A is a set of two points where the line segment ends, and the minimal surface γ_A in question is a spacelike geodesic that starts and ends in the two points at the boundary that correspond to ∂A. The "area" of this minimal surface is the geodesic length. The geodesic length of geodesics that go from any point in the bulk to a point in the boundary is infinite and so we regularize it as described in Sec. 2.2.

When we try to consider RT's formula in a time-dependent (Lorentzian) geometry we will have to think about how to generalize it. When we consider geodesics in an Euclidean geometry we can talk about minimal curves. That is because there extremal points of the action are minimal length curves. Consider for example that in two dimensions a geodesic in the Euclidean plane to be characterized by $x(\lambda) = \lambda\cos\theta + x_0$, $y(\lambda) = \lambda\sin\theta + y_0$ with proper length element $L = \sqrt{g_{\mu\nu}\dot{x}^\mu\dot{x}^\nu} = 1$. By doing perturbations $x(\lambda) = \lambda\cos\theta + x_0 + \delta x(\lambda)$, $y(\lambda) = \lambda\sin\theta + y_0 + \delta y(\lambda)$ we learn that geodesics are minimal length curves: $\delta L \approx \frac{1}{2}(\delta\dot{x}(\lambda))^2 + \frac{1}{2}(\delta\dot{y}(\lambda))^2$.

Geometry		Compact	Zero temp.	Geo.	WKB	RT
AdS	(2.3)	✓	✓	[54]	[52]	[54]
BTZ	(2.6)	✓	×	[52]		[57]
Poincare AdS	(2.10)	×	✓	(2.33)	(1.4)	(1.47)
Poincare BH	(2.11)	×	×	(2.41)	(2.42)	(1.48)

In Lorentz geometry this isn't the case. Considering now a spacelike geodesic which again has proper length element $L = \sqrt{g_{\mu\nu}\dot{x}^\mu\dot{x}^\nu} = 1$ and doing perturbations $x(\lambda) = \lambda + \delta x(\lambda)$, $t(\lambda) = \delta t(\lambda)$ we instead find in this case that $\delta L \approx \frac{1}{2}(\delta\dot{t}(\lambda))^2 - \frac{1}{2}(\delta\dot{x}(\lambda))^2$, which shows that in a Lorentz geometry geodesics are extremal solutions to the action. However, in [56] the authors argue that (2.45) still holds, *simply interpreting γ_A as an extremal surface.*

We point to a similarity between RT formula and WKB approximation that will pervade all this work. The WKB approximation in general deals with geodesics that connect two end-points at the boundary. The RT formula deals with a co-dimension 2 minimal surface that anchors in a certain subset of the boundary. However, it just so happens that in $2+1$ gravity co-dimension 2 minimal surfaces are geodesics and so for the specific case of AdS_3/CFT_2, for the case at hand both formulas deal with geodesics.

Even for $2+1$ gravity these two formulas aren't exactly the same however. On the one hand, WKB tells us to take all geodesics between given end-points lengths and sum them, exponentially weighted, (2.20). On the other hand RT formula tells us to only take the smallest geodesic of all the geodesics that are homologous equivalent to the boundary subsystem.

We don't have a complete proof for RT's formula, but we can perform consistency checks. For example, we can calculate the holographic entanglement entropy between a line segment and its complement in a 1-dimensional system both in the vacuum and at finite temperature. Because of the similarity between RT and WKB in $2+1$, most of the computational work is done since we already computed geodesic lengths for some different scenarios.

As far as holographic computations go, our geodesic solution allows us to obtain the following results. In Sec. 2.3.1 we have the proper length for pure AdS geodesics, (2.33). Substituting into the WKB formula we recover 2-point functions on the plane, which agree with the CFT result (1.4), see [23]. Setting $\Delta t = 0$ and substituting into the RT formula we obtain the entanglement entropy of a system with one non-compact spatial direction and at zero temperature, which again agrees with CFT result (1.47).

In Sec. 2.3.2 we calculated the proper length for geodesics living on a Poincare black hole background and end-points at the boundary, (2.41). Substituting into the WKB formula we recover 2-point functions, (2.42). Into the RT formula at equal time we get the entanglement entropy for a system with non-compact spatial direction and finite temperature equal to that of the black hole, (1.48); see [54].

For the vacuum and zero temperature these geodesics have been calculated in Secs. 2.3.1 and 2.3.2 and the relevant results are formulas (2.33) and (2.41) respectively. As explained, for the calculation of geodesics we would plug these results into the WKB approximation, (2.23). By contrast, for the entanglement entropy we instead plug these results into RT's formula, (2.45). This was done in [54] and was shown that universal part

of the CFT results (1.47) and (1.48), respectively, are recovered.

Plugging the regularized geodesic length (2.33) into WKB approximation, the two-point function of primary operators for spacelike separations in vacuum (1.4) is reproduced [23].

3

Thermalization of Holographic Entanglement Entropy

Lets go over some ideas we have seen before but that are worth keeping in mind. We already mentioned the proviso that we are accepting we don't exactly know what field theory we're studying. We claim only that we are studying whatever it is that's dual to pure gravity in a $2+1$-dimensional asymptotically AdS space and that we assume it exists.

We also mentioned that how we model a thermalization process is largely a conjecture. We have however reasons to believe that a Vaidya geometry could do the trick: in the distant past it reduces to empty AdS_3, which corresponds to having our theory at zero temperature, and in the distant future it is an asymptotically AdS black hole which corresponds to having our theory at finite temperature. *This Vaidya geometry therefore interpolates between zero temperature and finite temperature*, with the understanding that at some point in between energy is introduced into the system to bring it out of equilibrium, only to let it equilibrate afterwards.

Lets go into some more depth about the Vaidya geometry. The following is based on the results of [27].

3.1 Vaidya AdS_3

In AdS_3 the minimal extremal surfaces relevant to the Ryu-Takayanagi formula (2.45) are spacelike geodesics which for equal-time boundary end-points live at constant time t. This can be seen first from remembering that equal-time boundary end-points have integration constant $A = 0$ (see (2.30)) which by (2.25a) implies that spacelike geodesics are completely contained in slices of $t = \text{const}$. It is also true to the asymptotically AdS_3 static black hole geometry. However it is not true for a time-dependent setup, like Vaidya AdS_3. Instead we have introduced the v variable, which we used to write the metric of this space in Sec. 2.1:

$$ds^2 = -(r^2 - m(v))dv^2 + 2dvdr + r^2dx^2 \qquad \text{(2.14 revisited)}$$

In the v variable the Vaidya AdS_3 metric is very simple. If we could invert the Eddington-Finkelstein change of coordinates (2.12), which connects the usual time t with the coordinate v in which the Vaidya AdS_3 metric is written, then we could write that metric in the t coordinate. In general (that is, for a general v-dependent mass function) we don't know how to integrate this change of coordinates. Instead we will describe everything in terms of the v coordinate: the geodesics and the AdS_3 and asymptotically AdS_3 black hole geometries.

We observe that the Eddington-Finkelstein change of coordinates (2.12), which connects the usual time t with the coordinate v in which the Vaidya AdS_3 metric is written, can be integrated for both the empty AdS and the black hole geometries. The explicit expression is

$$v = \begin{cases} t - 1/r & \text{Poincare AdS} \\ t + \frac{1}{2r_h} \log \frac{|r-r_h|}{r+r_h} & \text{Poincare Black hole} \end{cases} \tag{3.1}$$

where r_h is the horizon radius. Near the boundary (i.e. $r \to \infty$) the two coincide. However as we go away from the boundary and into the interior the coordinates v and t can differ significantly. Namely, for finite t as we approach the horizon $r \to r_h$ we have $v \to -\infty$.

The Vaidya geometry depends on a free function, the mass function $m(v)$, with the understanding that the matter energy-momentum tensor on the gravity side is whatever it needs to be, (2.15), such that Einstein equations will be obeyed.

In (2.25) we have shown the geodesic equations for the Poincare black hole (2.11). That is a very particular case of a Vaidya metric, one for which the mass function is constant, $m(v) = m$ and so the obtained geodesic equations aren't valid for more general $m(v)$. Below we present the geodesic equations for a metric with general $m(v)$, (2.14). Using dot $\dot{}$ to denote derivation with respect to the proper length parameter λ and prime $'$ to denote derivation with respect to x, then for a general mass function, the geodesic equations are

$$\frac{d}{d\lambda}\left(-(r^2 - m(v))\dot{v} + \dot{r}\right) = \frac{1}{2}\frac{dm(v)}{dv}\dot{v}^2 \tag{3.2a}$$

$$\dot{x} = \frac{r_*}{r^2} \tag{3.2b}$$

$$\ddot{v} = -r\left(\dot{v}^2 - \frac{r_*^2}{r^4}\right) \tag{3.2c}$$

The above equations are already incorporating the information that this space has the Killing vector $\boldsymbol{\xi}_x = \boldsymbol{\partial}_x$ and an associated constant of motion

$$\boldsymbol{\xi}_x \cdot \boldsymbol{K} = r_* \tag{3.3}$$

where $\boldsymbol{K}$ is the vector tangent to the geodesic (check (2.24)). Three second-order equations would in principle need 6 integration constants to uniquely define a solution, but this Killing vector allows us to reduce this number to 5, as we can recover the sixth by generating translations along the x direction. We already included this information in (3.2).

With an affine parametrization, the normalization of the tangent vector is constant (check the argument leading to (2.26)):

$$\boldsymbol{K} \cdot \boldsymbol{K} = B = g_{\mu\nu} K^\mu K^\nu = -(r^2 - m(v))\dot{v}^2 + 2\dot{v}\dot{r} + r^2\dot{x}^2 \tag{3.4}$$

where of course the metric used to do the inner product is (2.14). This fact allows a great simplification. We recall that according to the discussion of Sec. 2.3, if we want equal-time geodesics, then they are spacelike, i.e. $B = +1$. Then using the chain rule from (3.4) a common factor of $\dot{x}^2$ on the rhs can be extracted, which according to (3.2b) equals r_*^2/r^4. Therefore from (3.4) we have obtained that

$$\frac{r^4}{r_*^2} = r^2 + 2r'v' - (r^2 - m(v))v'^2 \tag{3.5}$$

which will prove very convenient.

If we want to think about boundary-spacelike geodesics, it is simpler to parametrize the geodesics not with the proper length parameter λ, but with the spatial coordinate x. This can be done by applying the chain rule to (3.2). The equations of motion become

$$\frac{d}{dx}\left\{\left[-(r^2-m(v))v'+r'\right]\dot{x}\right\} = \frac{1}{2}\frac{dm(v)}{dv}v'^2\dot{x} \tag{3.6a}$$

$$r^2 - r^2v'^2 - rv'' + 2v'r' = 0 \tag{3.6b}$$

For the numerical integrations we use (3.5) and (3.6b).

3.2 The horizon and the collapse

The Vaidya metric depends on an arbitrary function $m(v)$, subject to the constraint that it is a monotonically increasing function. What function should we pick? We want to interpolate between $m(v) = 0$ at $v = -\infty$ and $m(v) = m$ at $v = +\infty$, but there are many ways to do so.

But now a question arises: what gravity object should we look at as a measure of the progression in time of the collapse? One possibility would be the event horizon. At $v \to -\infty$ there is no event horizon, and at $v \to +\infty$ an event horizon exists at position $r = m$. As the collapse progresses we would then see the event horizon grow from $r = 0$ to $r = m$. However, this is suspicious. An event horizon is what is called a "teleological" object, which is taken to mean that to locate the event horizon at a certain moment in time we need to know the causal structure of the entire spacetime. As is amusingly put in [58], our intuitive definition that an event horizon is something from which nothing can ever escape runs into problems once we start carefully thinking about what we mean by "ever" and "escape": we need to wait an infinite amount of time for something to get infinitely far away from a black hole if we want to say that it has escaped.

The point is that the event horizon is a global object and we would like a local one. Many definitions of dynamical horizons exist [58]. None of them is completely satisfactory since they aren't covariantly defined.

Definition of apparent horizon

The calculation of the apparent horizon in AdS Vaidya was done in [56] and we recall it here summarily, starting with its definition. Consider spacelike slicing and in a certain slice, a co-dimension 2 spacelike surface with induced metric $h_{\mu\nu}$. Take two orthogonal null vectors to this surface, $N^\mu_\pm$. The extrinsic null curvatures are defined in the usual way

$$(\chi_\pm)_{\mu\nu} = h^\rho{}_\mu h^\lambda{}_\nu \nabla_\rho (N_\pm)_\lambda \tag{3.7}$$

and the expansions of an orthogonal null geodesic congruences to the surface are defined to be the traces of the null extrinsic curvatures:

$$\theta_\pm = (\chi_\pm)^\mu{}_\mu \tag{3.8}$$

If we have surfaces such that

$$-\theta_+ = \theta_{\text{in}} \leq 0\,, \quad -\theta_- = \theta_{\text{out}} \leq 0 \tag{3.9}$$

they are called *(outer) trapped surfaces*, the co-dimension 1 regions composed by the union of all such surfaces are called *trapped regions* and *apparent horizons* are defined to be the boundaries of the connected components of such regions. The physical intuition behind this definition is the following. Consider a spherical surface from which two spheres formed by photons leave emitted outwards and inwards. Usually an instant after the emission the area of the outwards sphere of photons is larger than that of the emitting spherical surface which in turn is larger than that of the inwards sphere. But if the areas of both the inwards and the outwards spheres are smaller than that of the emitting surface, that surface is called a trapped surface [59].

In [56] these calculations are done for AdS_3 Vaidya. There they look at the apparent horizon and note that the choice of spacelike slicing along the translationally invariant direction seems especially natural and that in this case most of the horizon definitions coincide. They obtained the apparent horizon to be at

$$r_{\rm A} = \sqrt{m(v)} \tag{3.10}$$

We make two remarks. First, while the apparent horizon doesn't coincide with the event horizon for general time-dependent spacetimes, it does for static spacetimes. Second, the position of the event horizon is given by

$$\frac{dr_{\rm E}(v)}{dv} = \frac{1}{2}(r^2 - m(v))\,, \quad \lim_{v\to\infty} r_{\rm E}(v) = \sqrt{m} \tag{3.11}$$

By integrating (3.11) we can show that in this simple case the event horizon always lies outside the apparent horizon, but in fact this has been shown to be true in general [59].

The collapse

Quantum quenches are very fast processes. If we want to model the evolution under a certain Hamiltonian of a system that was in the eigenstate of a different Hamiltonian, then the process of changing Hamiltonians should be fast compared to the scale where dissipation occurs. In our model we have no dissipation and the time-evolution is unitary (we will argue for this in Sec. 3.5). Because of this it might also be interesting to study the other regime where the crossover from AdS to black hole geometries is slow; we just have to keep in mind that this isn't usually called a quantum quench.

We still have to choose our $m(v)$ function. Based on the discussed above, a suitable choice is

$$m(v) = \frac{m}{2}\left(\tanh\,(v/a) + 1\right) \tag{3.12}$$

It has the appropriate limits, $m(-\infty) = 0$, $m(+\infty) = m$ and it has a free parameter a which lets us adjust how fast the transition between the two regimes is: small a corresponds to instantaneous transition (quantum quench) and large a corresponds to a slow perturbation. Finally, we note that according to (2.9) the temperature of the final state will be $T = \sqrt{m}/2\pi$.

The expectation value of the field theory energy-momentum tensor can be read from the variation of the dual gravity action, properly regularized, with repect to the boundary metric [60, 61]. We obtain for the field theory energy density and pressure

$$\epsilon(t) = p(t) = m(t) \tag{3.13}$$

3.3 Entanglement entropy in Vaidya$_3$

In Sec. 2.4 we introduced Ryu-Takayanagi's conjecture [54] to compute the entanglement entropy in a field theory-gravity duality scenario. Together with the generalization to Lorentz space of [56] it says that the entanglement entropy S_A is

$$S_A = \frac{\text{Area of } \gamma_A}{4G_N^{(d+2)}} \qquad \text{(2.45 revisited)}$$

where A is the subset of the CFT for which we want to calculate the entanglement entropy, and γ_A is the area of the *extremal* co-dimension 2 surface contained in the AdS space and with a boundary that coincides with the boundary of A, that is $\partial(\gamma_A) = \partial A$ and such that γ_A is homologous to A, and with the understanding that A is contained on an equal-time slice at the boundary, and so is $\partial(\gamma_A)$. In the case of a CFT$_2$/AdS$_3$ duality, A would be a line segment, γ_A would be a spacelike geodesic and their boundaries would be two points.

Given this we want to calculate equal-time geodesics. We parametrize them as a function of the space coordinate x, that is $r(x)$ and $v(x)$. We call l the size of the line segment A, and t the time at which the geodesic end-points live. Thus

$$r(0) = r(l) = \infty\,, \qquad v(0) = v(l) = t \tag{3.14}$$

As always, the proper length of a line is given by

$$L = \int \sqrt{g_{\mu\nu}(x)\frac{dx^\mu(\lambda)}{d\lambda}\frac{dx^\nu(\lambda)}{d\lambda}}d\lambda \tag{3.15}$$

Using the line elements of (2.14) and parametrizing with x we get

$$L = \int_0^l \sqrt{r^2 + 2r'v' - (r^2 - m(v))v'^2}dx \tag{3.16}$$

Fortunately (3.5) simplifies this a lot:

$$L = \frac{1}{r_*}\int_0^l r^2(x)dx \tag{3.17}$$

This is then to be substituted into (2.45) to obtain

$$S_A = \frac{1}{4G_N}\frac{1}{r_*}\int_0^l r^2(x)dx = \frac{c}{6}\frac{1}{r_*}\int_0^l r^2(x)dx \tag{3.18}$$

where c is the central charge of the field theory and we used (4).

As explained in Sec. 2.2, the integral in (3.18) has a logarithmic divergence coming from the part of the geodesic that reaches the boundary. This is logarithmic because the space is asymptotically AdS which we regularized in steps: we introduce a cut-off in the radial direction of the integral, subtract from the integrand a logarithm as in (2.22), and then send the cut-off to infinity. The resulting quantity is well defined and doesn't depend on the cut-off.

The cut-off is introduced by replacing the limits of integration

$$\int_0^l r^2(x)dx \to \int_{0+\eta}^{l-\eta} r^2(x)dx \tag{3.19}$$

Now the result contains a term proportional to $\log \eta$. This is the same term as in (2.22). If we want to take $\eta \to 0$ we have a divergence. This is the same divergence that we see in the CFT calculations of the entanglement entropy: if in for example (1.47) we take the cut-off a to zero keeping l fixed, the same thing happens. Now the regularization of the holographic calculation can be done by just subtracting $\log \eta$. The formula we will use is

$$\tilde{L}(l,t) = \frac{2}{r_*} \int_{\eta}^{l/2} r^2(x) dx - 2 \log r(\eta) \tag{3.20}$$

Lastly we mention that in Vaidya we don't have a well define A parameter as in geodesic solutions in the AdS_3 (2.29) and Poincare black hole (2.34). In those cases for equal-time geodesics it does follow that $A = 0$. The parameter A is the conserved quantity associated with a time-like Killing vector which we don't have in Vaidya. This is the reason why here unlike there we can't simplify the EOMs to two first-order equations, but instead have to numerically integrate a first-order (3.5) and a second-order (3.6b) equations.

3.4 Results

We now discuss our numerical results. What we will do is take the regularized version of (3.18) and plot it for different values of the parameters. The parameters are (check (3.14)) l the spatial distance between end-points of the geodesic living at the boundary, t the position in time where the geodesic end-points live with the understanding that we are using a mass function $m(v)$ of (3.12) which varies quickly around $t = 0$, and a which is the parameter of $m(v)$ which regulates how fast the quench is (smaller a being faster quench). We will see our results have all the expected properties and a few more unexpected ones.

For example, we can ask: If we place our observable at constant $t > 0$ how does it vary with size? On the field theory side we expect that observables of very small size see only the UV of the theory, which is a CFT, and so we expect the holographic entanglement entropy to grow logarithmically, like the entanglement entropy of the vacuum of a CFT would; check (1.47).

But what happens for larger sizes *a priori* is not obvious. Before we discuss our results lets take a look at the results of Calabrese and Cardy (CC) in [44] to see what they got from their CFT calculation, and their heuristic explanation of the result; recall (1.62). Of course, they were studying the entropy as usually defined, not its holographic counterpart, but as we will see the two have much in common.

Entangled quasiparticles

The system that CC studied in [44] is that of a quantum quench done to a Hamiltonian which depends on a parameter h_0. This parameter brings the Hamiltonian away from criticality. At some moment $t = 0$ they instantaneously change the parameter from h_0 to h, so that after this abrupt change (called quench) the Hamiltonian is critical. Immediately after the quench we expect that this initial state will have correlations over a finite length, say τ_0. To simplify the discussion assume in the following that τ_0.

CC propose the following model of entanglement propagation. Suppose that immediately before the quench only local correlations exist, and then suppose that the effect of the quench is to produce pairs of free entangled quasiparticles that separate in space with

constant velocity. If the entanglement entropy is a good measure of quantum entanglement between a subset A of the full system and its complement B, then it's reasonable to expect that *the entanglement entropy will be larger the larger the number of pairs of entangled quasiparticles such that one element of the pair is in A and the other in B. Pairs of these entangled quasiparticles that have both quasiparticles in A or both in B will not contribute to the entanglement between A and B.*

At a fixed time t after the quench, how many pairs of quasiparticles will have one quasiparticle in A and the other in B? Suppose the size of A is small, $l < 2vt$. If the quasiparticles move with velocity v then at time t we will have inside A left-moving quasiparticles belonging to pairs which at time zero were between positions $x = 0 + vt$ and $x = l + vt$ and right-moving quasiparticles which at time zero were between positions $x = 0 - vt$ and $x = l - vt$. Then the total length that emits such entangled pairs that contribute to the entanglement entropy is $(l + vt) - (0 + vt) + (l - vt) - (0 - vt) = 2l$. This is how CC explained that the growth in entanglement entropy at fixed t should be linear in l.

However, if we continue to increase the size of A at some point A will be big, $l > 2vt$. It will be big in the sense that pairs of quasiparticles exist such that they were emitted from inside A at time zero and at time t both of those entangled quasiparticles are contained inside A. These pairs don't contribute to the entanglement between A and B and so we shouldn't take them into account. Pairs that at time t have one quasiparticle in A and the other in B were emitted at time 0 between $x = l - vt$ and $x = l + vt$ if they are left-moving and between $x = 0 + vt$ and $x = 0 - vt$ if they are right-moving. The total quantity of pairs contributing to entanglement between A and B should then be proportional to $(l + vt) - (l - vt) + (0 + vt) - (0 - vt) = 4vt$.

One could think that for this big A systems increasing their size l further would increase the number of entangled pairs that have one quasi-particle inside A and the other outside. Instead, for $l > 2vt$ increments in l brings inside A new left-moving entangled quasiparticles at the same rate that includes right-moving quasiparticles whose respective left-moving quasiparticles were already inside A and these two contributions cancel out. This is why for $l > 2vt$ the entanglement entropy is constant in l. The transition between the two regimes takes place at

$$l = 2vt \tag{3.21}$$

This is indeed what they get [44]. There they obtain

$$S_l(t) \sim \begin{cases} \frac{\pi c t}{6\tau_0} & t < l/2 \\ \frac{\pi c l}{12\tau_0} & t > l/2 \end{cases} \qquad l/\tau_0, t/\tau_0 \gg 1, \quad |l - 2t| \gg \tau_0 \qquad \text{(1.62 revisited)}$$

We see that for fixed t the entanglement entropy is extensive if $l < 2t$ and is constant if $l > 2t$. Comparing (1.62) with (3.21) we notice that the coefficient between l and $2t$ is 1 and so we conclude that after a pair of entangled quasiparticles is created, they propagate with velocity $v = 1$. This would be expected in a CFT.

Formula (1.62) depends on τ_0. In the calculations of [44] they show that this quantity is the extrapolation length of the state, a microscopic parameter which measures how far away the state is from a scaling covariant state. This quantity also plays the role of an effective temperature for the IR physics, and so the complement subsystem B acts as a thermal bath for the subsystem A.

We can expect that the equivalent quantity in our model is the temperature, as it is the only dimensionful quantity we have, and we will see this is indeed the case.

Evolution of HEE after a quench

In all of the above we made the approximation that only pairs of quasi-particles emitted from the same point were entangled. This is an approximation because in fact we know that the initial state has correlations of the order of τ_0 and so quasi-particles separated by this distance should be entangled as well. As we will see, this is an important point to discuss the results of our model.

But we note that if we take into consideration that their state does indeed have non-local entanglement over scales of the order of τ_0, then the entanglement entropy would still go to constant for $l > 2vt$, but with a smoothing of the transition at $l = 2t$ of the order of τ_0. For long range correlations the entanglement doesn't go to constant, that is because $l > 2vt$ a small increment in the size of l would still include pairs of left- and right-moving quasiparticles that were not emitted from the same point. These contribute zero if the only entanglement in the initial state is finite-range, and non-zero if it long-range.

Now the question is: Do our numerical results match (1.62) exactly or only qualitatively, and if the latter then does CC's entangled quasiparticles picture still hold?

In Fig. 3.1 we answer this question. From our numerical results we see that we

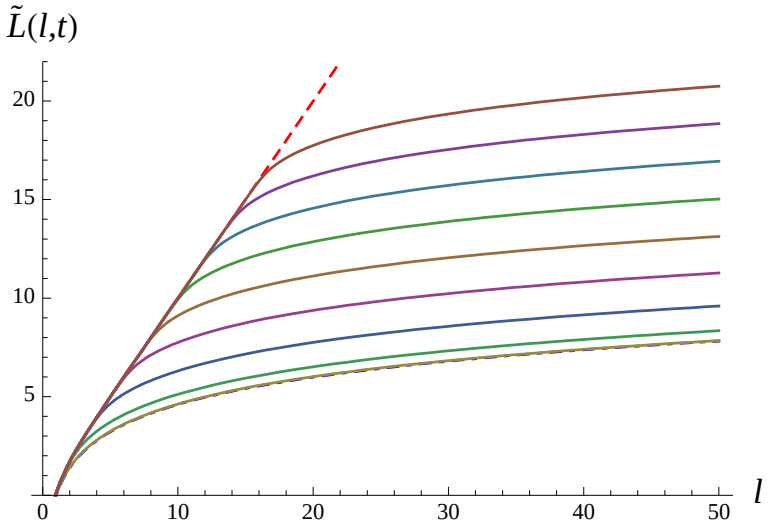

Figure 3.1: In solid lines we plot the regularized geodesic length (the holographic entanglement entropy) as a function of the geodesic end-point separation l for several fixed times $t = 0, 1, \ldots, 8$ from bottom to top and $a = 1/3$. The dashed line corresponds to the same quantity in a Poincare black hole geometry and the dot-and-dashed line corresponds to a pure Poincare AdS_3 geometry. $m(v) \to m = 1$.

also recover this behavior of CC: for a fixed time the (holographic) entanglement entropy grows linearly with the size of the system A that we are considering up to a size $l = 2t$. This means in particular that if we follow CC's model of entangled pairs of quasiparticles that propagate entanglement, then in our case too these quasiparticles move with velocity $v = 1$. However for $l > 2t$ we see that we have a logarithmic growth, instead of CC's

constant entanglement entropy. The reason for this is that as we explained in the previous subsection for $l > 2t$ we expect the entanglement entropy to reproduce the entangling characteristics of the state we had before the quench. In the case of CC that state is a state with finite-length correlations (order τ_0) and so the entanglement entropy should be constant. In our case, that state is the vacuum of the theory (since its dual is empty AdS) and therefore we expect to see for $l > 2t$ the entanglement entropy of the vacuum of a 2-dimensional CFT, which is a logarithm. This is exactly what we get.

If we trust our calculation, which we have good evidence is getting something right at least qualitatively, then from (3.18) we see that the holographic entanglement entropy is the regularized geodesic length multiplied by $c/6$. In our results, Fig. 3.1 we see that the linear regime of the holographic entanglement entropy in l has a proportionality factor 1 which means that the holographic entanglement entropy in this regime is $\sqrt{m}cl/6$. According to (1.62) it should be $\pi cl/12\tau_0$. For this to be true we must have that $\tau_0 = \pi/2\sqrt{m}$. According to (2.9) this implies

$$\beta = 4\tau_0 \tag{3.22}$$

where β is the (inverse) temperature.

There is an explanation why CC find correlation functions which coincide with those living at finite temperature despite the fact that they are dealing with pure states. The reason is that finite temperature correlation functions are computed in a cylinder geometry by mapping from the complex plane using (1.9) with $L = \beta$, while quench correlation functions are computed in a strip geometry by mapping from the UHP using (1.10) with $L = 2\tau_0$. Deep in the bulk of the strip the bulk-bulk correlators can't tell a cylinder from a strip, and comparing these two formulas we conclude that $\beta = 4\tau_0$.

It is highly non-trivial that the same fact holds for our holographic model. The above argument is based on the fact that in CC's model the late (real) time limit of the quench corresponds to the deep bulk of the strip with width in (imaginary) time (as discussed after (1.57)). We, however, have no such analyticity properties in our holographic model with Vaidya metric. And this is more circumstantial evidence that our model is getting something right.

Holographic interpretation

We have seen CC's interpretation for the linear growth of entanglement entropy at constant time and for subsequent constant behavior after it. What is the equivalent explanation from the holographic point of view for Fig. 3.1?

It is very convenient for clarity to have a mental picture of what the actual geodesics, and not just their proper length as in Fig. 3.1, look like. For this purpose we introduce Fig. 3.2.

At fixed time $t > 0$, small geodesics (which we will call geodesics such that the endpoints have a small spatial separation l, small in some sense to be specified in the following) live near the boundary. This means that the lowest radial position that they attain is not far into the bulk of the space; this can be checked in 3.2(a). Since this space is asymptotically AdS this geodesics are close to AdS geodesics, and so their proper length grows logarithmically with l. Pictorially it can be determined from Fig. 3.2 whether or not a segment looks like AdS by looking at whether or not it looks like part of a circle in

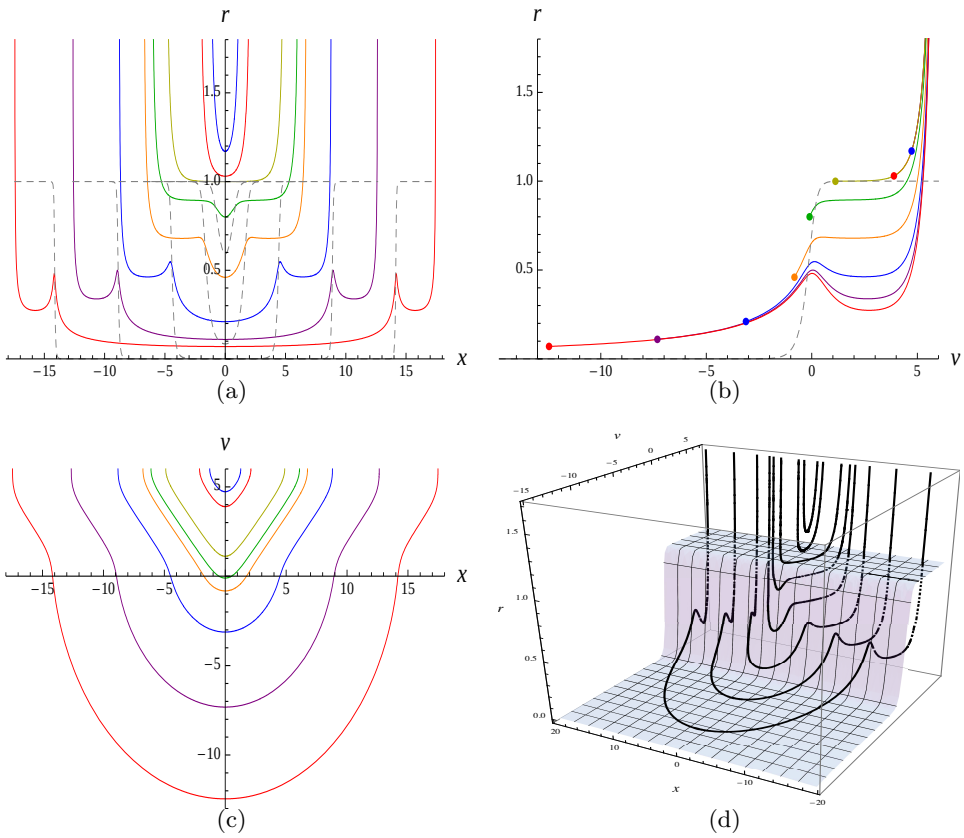

Figure 3.2: We plot profiles of geodesics for different boundary end-point separation l at $t = 6$ and $a = 1/3$. We project into the (a) $x - r$ plane, (b) $r - v$ plane and (c) $x - v$ plane. We also (d) plot the full three-dimensional profile of the geodesics. In (b) the dots represent the point of the geodesic with smallest r coordinate. The dashed line represent the position of the apparent horizon at the value v defined by the trajectory of each geodesic: $\sqrt{m(v(x))}$.

the $x - v$, Fig. 3.2(c). We see this is the case for both geodesic with small l and for those segments of geodesic which live in a part of space such that $v < 0$.

As l grows, the minimum value that the geodesics attain starts getting smaller and smaller — the geodesics feel more of the interior. For equal-time geodesics this minimum value (2.37) reduces to $r_m = r_*$. The earliest time v_* that these geodesics attain also gets earlier and earlier, according to (3.1) which together with taking the limit and inverting (2.34b) can be used to conclude that for an infinitely thin shell,

$$l = 2(t - v_*) \tag{3.23}$$

It holds for as long as the geodesics we are considering are completely contained in the black hole geometry, that is until they intercept the infalling shell, that is until $v_* = 0$. We conclude that the linear growth of the entanglement entropy with l in our holographic picture holds until

$$l = 2t \tag{3.24}$$

just as it did for both CC's CFT caculations [32] (also check (1.62)) and CC's entangled quasiparticles picture (3.21), and which is the same that we have in our numeric results, Fig. 3.1. This is extensive behavior. *This scale is related to the geodesic crossing of the shell.* Geodesics that reach the black hole horizon extend tangent to it, and induce an extensive behavior of entanglement entropy. So in our model too we have a temperature, which is the temperature that geodesics which are completely contained in the black hole geometry see, the black hole temperature. As another corollary we also conclude that the quasiparticles of CC also travel with velocity $v = 1$ in our case.

As l grows further, $v_* < 0$ and the geodesic first crosses enters the event and apparent horizons and then crosses the shell. That can be seen in Figs. 3.2(a) and 3.2(b). For the case of the static black hole this can never happen: there no solution for the geodesic EOMs exist such that the geodesic crosses the horizon and comes back to the boundary. The entanglement pattern among the sea of excitations and its causal propagation, determines that observables involving a length scale larger than $2t$ at time t can have an expectation value far from thermal. Hence equilibration cannot be achieved at the global level in a system of infinite size. We relate this property with the necessity to reach behind the apparent horizon in the holographic description of the field theory evolution. This behavior seems very generic for evolutions which admit a dual representation in terms of a process of gravitational collapse.

Inside the matter shell Gauss's law says there should be no gravity. This is why there the space is again AdS. Therefore now the geodesic length growth as a function of l goes back to that of a geodesic living in empty AdS: it's the logarithm we see in Fig. 3.1 for $l > 2t$. A way to pictorially "prove" that as l increases in this regime only the AdS part of the geodesic increases (thereby explaining the exactly logarithmic behavior) is by looking at Fig. 3.2(c) and checking that for these geodesics (for example, the first three counting from the outside) as l grows larger only the semi-circular $v > 0$ segment of the geodesic increases in size, while the segment that lives in $v > 0$ is just shifted in the x direction. An important point is that as l increases, eventually $v_* \to -\infty$, always. Therefore no matter what time the geodesics endpoints live at, a large enough geodesic will always cross the infalling shell.

For these large intervals there is an asymptotic return to a logarithmic dependence

on l and the effect of the infalling shell is encoded in a time dependent shift:

$$S(l,t) \to s(t) + \frac{c}{3}\log\frac{l}{\mu} \tag{3.25}$$

where μ is some UV scale — we have removed the cut-off dependence by our regularization procedure, but we must introduce some scale for dimensional reasons.

3.4.1 The thermal de Broglie time t_0

In the context of thermalization we are interested in finding relevant time scales. We can define one of them to be the time after which the entanglement entropy behaves like thermal, in some sense. Under what circumstances can this happen? Well, in the static case the exact formula for the entanglement entropy is (1.48), its large l regime is (1.49) and the transition between the two happens for $\frac{\pi l}{\beta} \gg 1$ and we can say that we are safely into the thermal regime when

$$\frac{l}{\beta} \gtrapprox \frac{1}{2} \tag{3.26}$$

This is a scale that exists in thermalized systems. That is, a geodesic in a static black hole geometry or equivalently the entanglement entropy at finite inverse temperature β, sees a thermal bath if (3.26) is verified.

However, our space isn't a static black hole. On the one hand, the proper length of small geodesics (in the sense that $\frac{\pi l}{\beta} \ll 1$; (3.26)) behaves like logarithms as a function of l, on the other hand large geodesics (in the sense that $l > 2t$; (3.23)) also behave like logarithms. That these two different qualitative changes exist can be seen clearly in Fig. 3.1: after some time geodesic lengths have first a logarithmic behavior on l, then linear, then logarithmic again.

But for very early times we can see that no geodesic will contain an extensive part; this can also be seen from Fig. 3.1. This suggests that a time exists after which regions of size $l < 2t$ have locally relaxed to a stationary state that can be identied as thermal equilibrium. So this will be our scale of interest: What is the time we have to wait such that geodesics exist which have a extensive behavior? The transition between a extensive behavior existing and not existing is given by putting (3.26) and (3.24) together. We obtain

$$t_0 \approx \frac{\beta}{4} \tag{3.27}$$

and call this special time the thermal de Broglie time t_0. Before time t_0 no subsystem A has an extensive entanglement entropy or equivalently no geodesic has a proper length that grows linearly with its boundary endpoint separation l.

This is the moment to say something about the conjecture that once in a while shows up in the literature that in AdS/CFT the apparent horizon is more appropriate than the event horizon as a measure of the entropy in an out of equilibrium setup. It is true that for late times the event and the apparent horizon coincide, but this isn't the case for early times. Consider early time geodesics, that is the ones with boundary end-points living at $t < t_0$, Fig. 3.3. Now, these early time geodesics of Fig. 3.3 (i) live after the $t = 0$ perturbation and (ii) differ significantly from their vacuum value as can be seen by looking at Fig. 3.1 (where we plotted $t = 1 < t_0$ geodesic proper lengths). However, they never touch the apparent horizon. That these three things can happen simultaneously seems

to discourage the idea that the apparent horizon might play a role in the holographic derivation of entanglement entropy.

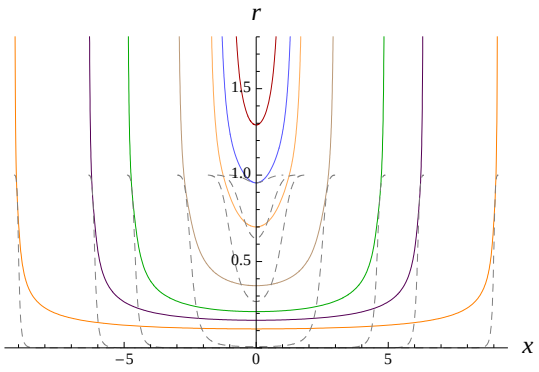

Figure 3.3: For $a = 1/3$, projection into the $r - x$ plane of early time geodesics of different spatial separation l at $t = 1.4 < t_0$. We also plot the apparent horizon and check that these early time geodesic never cross it.

Lastly, for the sake of a more transparent comparison with formula (1.62) we also plot the same information (that is, proper length depending on l and t) but instead of plotting the proper length as a function of l for several fixed t, here we plot the proper length as a function of t for several different l, Fig. 3.4. The prediction of (1.62) is that the entanglement entropy grows linearly in time while $t < l/2$ and is constant with a value which depends on l for $t > l/2$. In our model this growth in time for $t < l/2$ is only exactly linear in the limit where $\tau_0 = 0$.

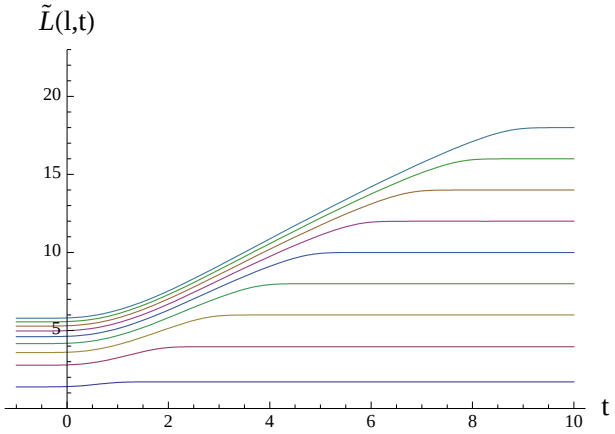

Figure 3.4: $\tilde{L}(l,t)$ as a function of t for $l = 2, \ldots, 18$ and $a = 1/3$.

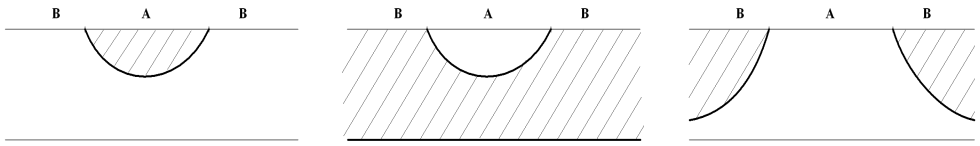

(a) (b) (c)

Figure 3.5: After dividing the whole system into subsystem A and its complement B, we show a) how to take the extremal surface in order to compute the holographic entanglement entropy of A, S_A. Note that this extremal surface is homologous to A. We also show b) and c) two different extremal surfaces. They are homologous to B if we imagine that b) the lower branch connects back to B "at spatial infinity" and c) the two branches join with each other "at spatial infinity".

3.5 Thermalization and unitarity

Entanglement entropy and unitarity

We have seen in Sec. (1.3.2) that for a pure state the entanglement of a subsystem A equals that of its complement B, that is

$$S_A = S_B \qquad \text{(1.28 revisited)}$$

If our initial state is a pure state (it's AdS, the vacuum of our theory) and if evolution is unitary then the state should stay a pure state for all times. We can use the entanglement entropy to check whether this is the case: if our state is pure at all times, then (1.28) should be true at all times. Is it?

To check this, we must first determine what is the entanglement entropy extremal surface corresponding to the complement of subsystem A, subsystem B. Done that, we compare it to the entanglement entropy of subsystem A.

Lets look at Figs. (3.5). The prescription says to pick the extremal surface of smallest area and which is homologous to the subsystem under consideration. For the system A it is clear that this is the one represented in Fig. (3.5(a)). For its complement, subsystem B, we see two possibilities, Figs. (3.5(b)) and (3.5(c)). The lower geodesic branch sits at $r = 0$ and $v \to -\infty$. They both are composed of disconnected geodesic pieces which are glued together at spatial infinity and they both are homotopic to B. Then we must pick the one with smaller area, which is the one in Fig. (3.5(b)). Furthermore in that case the geodesic piece that seats at $r = 0$ has proper length zero. Therefore of the two contributions to S_B the one that isn't zero is the one that coincides with S_A. This shows that (1.28) is true for all times, and therefore our time-evolution is unitary.

Thermalization?

An important question is: How does unitarity as we discussed above relates to a temperature in the final state? If our time-evolution is unitary, then in what sense can we say that our final state is at a certain temperature? After all, if we have a pure state at all

times, then system can't be described as a statistical superposition of states as one would need to describe a system with a temperature, that is with a density matrix like (1.21).

Lets again start by thinking about the setup of Calabrese and Cardy. There both the quantum quench itself and the subsequent time evolution of the system are manifestly unitarity processes. However, already there they have a sort of an effective temperature in their final state. Not explicitely, but the fact that the entanglement entropy for fixed time t has regimes where it behaves extensively, i.e. grows linearly, suggests that we can describe those regimes by considering an effective temperature (which they related to the extrapolation length, $\beta_{\text{eff}} = 4\tau_0$). So clearly that we have characteristics of a system with a temperature doesn't automatically imply our evolution was non-unitary. Even there, even though the entanglement entropy can behave extensively, it's questionable in what sense we can say something like an actual temperature is present: after all we have seen that the appearance of a temperature in their results is due to a technicality whereby the real time analytic continuation of the deep-bulk Euclidean 2-point function on a strip looks like that on a cylinder — not because the system actually has a compact imaginary time direction! So if one wants to study thermalization by looking at the behavior of entanglement entropy, maybe it's more correct to say "the entanglement entropy is extensive with a certain slope" than "the system has thermalized to a certain temperature". Certainly the system displays features of a system at a certain temperature, but other features differ; in particular, the final state after "thermalization" is a pure state, both in the case of CC and in ours. Another feature of the CC final state that differs from a state at finite temperature, is that the entanglement entropy isn't extensive for all scales; the entanglement entropy of very large systems $l > 2t$ is constant in l.

So regarding the question of unitarity we should turn things around. Maybe the good question is not "is evolution unitary?" but "evolution is unitary; what characteristics can the final state have in common with those of a thermal state, knowing that we started from a pure state?"

Lets turn our attention to our own model. How much of the above holds? In our case, the question of whether or not the imaginary time direction is compact can't be asked because we don't have an imaginary time direction. While CC do all their calculations in Euclidean time and at the end do an analytic continuation to real time, we do everything directly in real time. Therefore, in our case we model thermalization by *actual* time-evolution of an out-of-equilibrium system. But even so, other things that we have in common with CC differ from that of a thermal system. For example, in our case too the entanglement entropy stops behaving extensively if we consider a large enough subsystem, $l > 2t$.

One way to interpret all this is to say that in an out of equilibrium situation several processes occurs, all of which contribute towards stationarity of different characteristics necessary for a system to be indistinguishable from a thermal one.

One of them is propagation of entanglement. In the case of a dynamical situation, entanglement entropy gives a measure of the evolution of the quantum entanglement between degrees of freedom inside and outside a chosen subsystem. Propagation will make CC's entangled quasiparticles excitations initially localized in a small region spread over ever larger scales. Hence the entanglement entropy of a subsystem will strongly depend on the relation between its size and the typical separation of entangled degrees of freedom at a given time. Therefore, we conclude that during the evolution of CC's quench and ours what is happening is that this part of the thermalization process is happening but will

never be concluded, because large enough subsystem always see deviations from an extensive behavior, as if the information that the system hasn't really thermalized becomes contained in ever larger regions of space. Of course, for small observables can't distinguish the entanglement pattern they see from that of a thermal system.

Another phenomena we conjectured is occurring is that associated with the time scale t_0. We said that an early time exists such that for early times $0 < t < t_0$ our system never looks like a thermalized system in the sense that the entanglement entropy never behaves extensively, but still differs significantly from that of an unperturbed system, $t < 0$. It would be nice to know the underlying microscopical process that gives rise to this other aspect of thermalization. We conjecture that in terms of entangled quasiparticles, t_0 is the time it takes for two entangled quasiparticles to separate after production a distance larger than their wavelength; only for distances larger than the particle's wavelength does it make sense to say that they have "separated". In a thermal bath this particle wavelength, also called the de Broglie wavelength, is of a size of the order of the (inverse) temperature of the system. In the absence of other characteristic scales in the problem, the typical momentum of the these pairs should be set by the energy density $\epsilon(t)$ (3.13), explaining why it plays a role in determining t_0, (3.27). Our time t_0 would then be the time needed for an entangled quasiparticle of velocity $v = 1$ to cross a distance roughly of the order of the thermal de Broglie length.

3.6 Quenching, fast and slow

What happens if we play with the parameter a of (3.12) to see what happens for faster and slower quenches? All of the above discussion referred to a fast quench; we did all plots with $a = 1/3$ which is close to an instantaneous quenches, at least as far as the plots go. In Fig. 3.6 we have plotted the most relevant pictures for $a = 2$. This is slow enough that the slow build-up of the quench is noticeable.

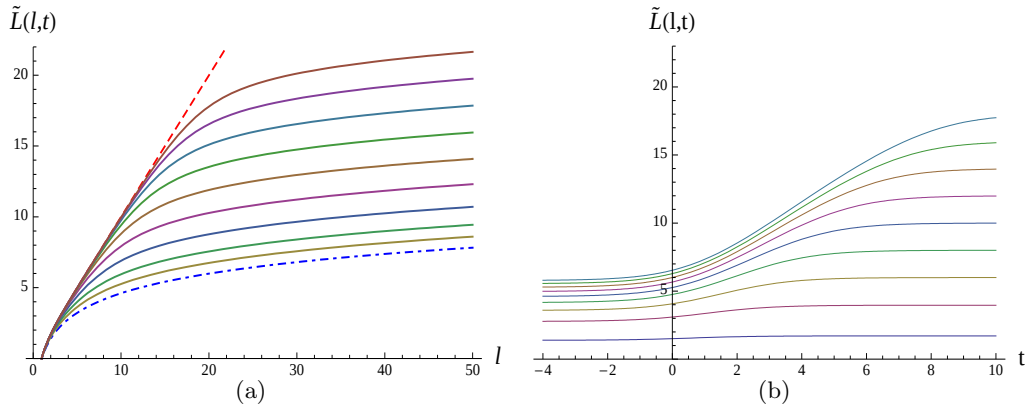

Figure 3.6: For $a = 2$, proper length (a) as a function of boundary end-points separation l for several fixed times t and (b) its time-evolution for several fixed subsystem sizes l. These are the slow quench analogs of Figs. 3.1 and 3.4.

From Fig. 3.6 we see that in the case of a slow quench the transition between behaviors (3.24) isn't respected. This isn't shocking, given the way that expression was obtained (assuming instantaneous quenches in the case of CC and assuming a instantaneous tran-

sition from AdS to black hole geometries in ours). In the case of the mass function we picked, (3.12), for $v \approx 2a$ the mass function $m(v)$ is almost at its final value. Taking this as the threshold at which we can say the slow perturbation has "almost ended", we obtain that geodesics which satisfy

$$l \lessapprox 2t - 4a \tag{3.28}$$

are completely contained in the black hole geometry in the case of a slow perturbation. This then becomes the new transtion point between behaviors.

We can then redo the argument preceeding (3.27) and conclude that for a slow perturbation the time t_0 is

$$t_0 \approx \frac{\beta}{4} + 2a \tag{3.29}$$

4

Thermalization of Holographic 2-point Functions

We have already said a few words about the motivation to study Vaidya. Interpreted as a thermalization process, Vaidya (2.14) looks like finite temperature (a static black hole) in the distant future and like a vacuum (empty AdS) in the distant past. Furthermore in the thin shell limit the separation between the two regimes happens instantaneously. Namely, for $v < 0$ the geometry is empty AdS and for $v > 0$ the geometry is a black hole. This is closer in spirit to the quantum quenches of Sec. 1.4 and therefore we are especially interested in this limit.

We want to check that working with an infinitely thin shell and still using the WKB approximation for geodesics (2.23) we can reproduce the behavior (1.63).

Lets do that. The following is based on the results of [28].

4.1 Non equal-time thermal geodesics

Even without doing any difficult calculations we can reproduce part of the behavior of (1.63), specifically the fact that the 2-point spatial separation l and the two times of the end-points t_1 and t_2 enter in a very precise combination: $l - t_1 - t_2$. In Ch. 3 we have seen that it's possible to study the time evolution of the quantum entanglement after a quantum quench (1.62) from the study of equal-time geodesics in a Vaidya geometry [27]. In particular we have seen that two regimes exist.

We showed that for geodesics completely contained in the black hole part of the geometry,

$$l = 2(t - v_*) \qquad \text{(3.23 revisited)}$$

where v_* is the minimal value of the v coordinate attained by the geodesic, l is the space separation of the geodesic end-points and t is the time coordinate where both geodesic end-points live. We saw that at $t \to +\infty$ the geodesic will be completely contained in the black hole part of the geometry and that at $t \to -\infty$ the geodesic will be completely contained in the empty AdS part of the geometry. We also saw that between the two limits geodesics exist that cross the infalling shell. How are the two regimes separated?

Suppose that we place the infalling Vaidya shell at $v = 0$ and consider a geodesic at very late time, completely contained in the black hole part of the geometry. If we start placing it at earlier time, when does it start feeling that the space isn't an eternal black hole but actually a Vaidya geometry? That happens when in (3.23) we have $v_* = 0$ because this is the v coordinate of the shell and so the geodesic contains exactly one point in the shell and the rest of the geodesic in black hole geometry. Any geodesic before that will be partly contained in the empty AdS part. Then if the quench is placed at $t = 0$ the

largest geodesics completely contained in the black hole geometry have $l = 2t$, and they signal the threshold between the two different behaviors in (1.62).

So for a fixed time t, small geodesics $l < 2t$ will not be able to tell that the space they live in is not really an eternal black hole, but Vaidya geometry, because they are completely contained in the black hole part of the geometry. Larger geodesics $l > 2t$ will cross the infalling shell.

Turning it around, we consider a geodesic of fixed length l. In order that the associated observables (that is, 2-point functions (1.60) and entanglement entropy (1.62)) can appear thermalized, a time $t = l/2$ has to be waited; this is in agreement with CFT calculations [44]. Before $t = l/2$ how much of the geodesic fall into empty AdS evolves with t, which is how we model thermalization. After that the proper length will be constant in time which means that, at least according to the common lore, the system will have thermalized. In Ch. 3 we suggested that maybe the situation isn't that simple, and an entanglement entropy constant in time, even when it displays linear growth with the system size, might not be enough to claim thermalization of the *system*. At most we could claim that observables at such scales can't see deviations from thermalization.

How do we generalize this for the case of non-equal time geodesics? In analogy with the above, we don't need to do calculations for geodesics that cross the shell, but instead we need only ask What is the earliest geodesic completely contained in the black hole geometry, and how does that depend on the time separation of its end-points, $t_1 - t_2$? Note that since the black hole part of the geometry is time invariant, then for geodesics which are completely contained in that part only the difference $t_1 - t_2$ is important, and not $t_{1,2}$ individually. This question is answered by finding the earliest v_* that a non-equal time geodesic can attain and how it is related to l, t_1 and t_2, and then setting it to zero.

It will be convenient to describe the geodesics as functions $t(r)$, $x(r)$ of the radial coordinate instead of using the affine parameterization. As it is clear from (2.25b) each function will have two branches, which we will denote as $\pm$. To fix notation, we choose them to be defined by the conditions

$$t_+(\infty) \geq t_-(\infty)\,, \qquad x_+(\infty) \geq x_-(\infty) \tag{4.1}$$

The integration constant r_* and A can have either sign. The reason for the criterion (4.1) is that the resulting functions $t_\pm(r)$ and $x_\pm(r)$ depend only on the modulus of the integration constants. Hence without loss of generality we can consider r_* and A to be always positive, and shift the information about their sign to the choice of branch. The signs of both constants are independent, and so is the choice of branch for the functions $t(r)$ and $x(r)$.

What about the boundary data of the end-point insertions? We decide to name the end-points (t_1, x_1) and (t_2, x_2) such that

$$t_1 > t_2\,, \quad x_1 - x_2 \equiv l > 0 \tag{4.2}$$

which according to (4.1) implies

$$v_+(\infty) = t_1\,, v_-(\infty) = t_2\,, \qquad x_+(\infty) = x_1\,, x_-(\infty) = x_2 \tag{4.3}$$

As we can see in for example (2.30) that equal-time geodesics are characterized by a vanishing parameter A such that the functions $v_\pm(r)$ coincide. The minimal value of the

radial coordinate that they can attain is r_* and by symmetry at this point v_* is reached: $v_* \equiv v(r_*)$. However, for geodesics with non-equal time end-points the two branches $v_\pm(r)$ are different, joining smoothly at the minimal value of the radial coordinate r_m (2.37), which now differs from r_*. Given the criterion (4.1) chosen to distinguish between branches, it is clear that the minimum value of the null coordinate must occur in the branch $(-)$. Putting together (2.25b) and (2.12), in Eddington-Finkelstein coordinates the derivative of the time coordinate is

$$\frac{dv_\pm}{dr} = \frac{dt_\pm}{dr} + \frac{1}{r^2-m} = \frac{1}{r^2-m}\left(1 \pm \frac{Ar}{\sqrt{A^2r^2+(r^2-m)(r^2-r_*^2)}}\right) \tag{4.4}$$

where according to our conventions A is always positive. Thus we should search for a zero of its $(-)$ minus branch. This expression has a zero at infinity, corresponding to a maximum. It has an additional zero at r_*, necessarily then a minimum, implying

$$v_* \equiv v_-(r_*) \tag{4.5}$$

We know the black hole solution in usual coordinates, $t_-(r)$ (2.34a), which we substitute into the Eddington-Finkelstein coordinate $v_-(r)$ (3.1), and evaluate at r_*. The result is

$$v_* = t_0 - \frac{1}{2r_h}\log\left[m^{-1}\left((r_*+r_h)^2 - A^2\right)\right] \tag{4.6}$$

where t_0 is an integration constant of the EOMs, not to be confused with the thermal de Broglie time of Sec. 3.4.1. This is the minimum v attained by a geodesic branch which in general will not be part of an equal-time geodesic, but which is however completely contained in the black hole part of the geometry. Now the integration constant t_0 is related to the boundary time of the geodesic end-points by (4.3). Therefore we plug (2.34a) into (3.1), take the $r \to \infty$ limit and equate to $t_{1,2}$ according to (4.3), and obtain

$$t_0 = \frac{t_1+t_2}{2} + \frac{1}{4r_h}\log\left(Cm^{-2}\right) \tag{4.7}$$

which substituted into (4.6) gives us

$$v_* = \frac{t_1+t_2}{2} + \frac{1}{4r_h}\log\frac{(r_*-r_h)^2-A^2}{(r_*+r_h)^2-A^2} \tag{4.8}$$

In turn r_* and A are related to boundary data l and Δt by (2.39). Inverting these and substituting into (4.8) we finally obtain

$$l = t_1 + t_2 - 2v_* \tag{4.9}$$

This expression is the generalization of (3.23) that we were looking for. It relates boundary data of the geodesic end-points, like time coordinates t_1 and t_2 where the end-points live and the space separation between them l with the earliest point in v-time that the geodesic attains. Now we repeat the previous reasoning. If we place the quench at $t = v = 0$ then the earliest geodesic that is completely contained in black hole geometry is

$$l = t_1 + t_2 \tag{4.10}$$

Notice that again we see we must be doing something right: the CFT calculation of a 2-point function after a quench, (1.63), displays the same threshold on its behavior at $l = t_1 - t_2$ that we see in (4.10).

4.2 The thin shell limit of Vaidya

For the case of the Vaidya metric (2.14) in all its generality we obtain similar equations (3.2) to those of the AdS black hole except now equation (3.2a) can't be integrated exactly as (2.25a) could. The reason for that is that in Vaidya we don't have the global Killing vector $\boldsymbol{\partial}_v$ or in other words, in (3.2a) it's not true that $dm(v)/dv = 0$ as it was for both the empty AdS and the eternal AdS black hole spaces. Instead what we will do is describe a geodesic that crosses the shell as being composed of different parts, some of which are empty AdS geodesics, other are AdS black hole geodesics.

In the infalling shell model of Vaidya AdS_3 (2.14), the infinitely thin shell is obtained by taking

$$m(v) = m\Theta(v) \tag{4.11}$$

where $\Theta(v)$ is the Heaviside function. As a bonus this also allows us to use analytical instead of numerical methods. We have already described the geodesic equations and their solutions in these two regimes. For $v < 0$ the geodesic equations are those in Sec. 2.3.1 and for $v > 0$ they are those in Sec. 2.3.2, which we solved there. Therefore we know almost everything we need to solve this problem. The last conceptual questions remaining are What criterion both solutions, empty AdS and black hole geodesic solutions, should obey at $v = 0$ so that we can think of these two geodesic pieces as being glued together into a single geodesic which has both end-points at the boundary of AdS while crossing the infalling shell?, and How are the integration constants of those solutions related?

4.2.1 Matching conditions

A short remark on notation. We will call the affine parameter λ. Anything with a c subscript will be a point at the shell crossing: λ_c, $r_c \equiv r(\lambda_c)$, $x_c \equiv x(\lambda_c)$. Also, the black hole part of the geodesic, which is on the outside of the shell, will have a 'out' subscript and AdS geodesics will have an 'in' subscript.

We have obtained previously the geodesic equations in the Vaidya background, (3.2). Of course, as they are now, there is a problem with the derivative of $m(v)$ with respect to v in the limit where $m(v)$ is the Heaviside function. Therefore to address this question we will regularize the problem by first considering that the shell thickness is finite and afterwards taking the limit of zero thickness.

Let λ_- be the maximum value of the affine parameter such that for $\lambda < \lambda_-$ we have that $m(v_{\text{in}}(\lambda)) = 0$ and λ_+ the minimum value of the affine parameter such that for $\lambda > \lambda_+$ we have that $m(v_{\text{out}}(\lambda)) = m$. The way we will take the infinitely thin shell limit at the end is

$$\lim_{\lambda_- \to \lambda_c} m(v_{\text{in}}(\lambda_-)) = 0 \tag{4.12a}$$

$$\lim_{\lambda_+ \to \lambda_c} m(v_{\text{out}}(\lambda_+)) = m \tag{4.12b}$$

Before going any further we should notice that the solutions to the geodesic equations for both empty AdS and black hole have 4 integration constants: t_0, x_0, r_* and A. For the case of the black hole geodesic we will use the fact that we have translation invariance in the x coordinate to set x_0 to zero. Then, given t_0, r_* and A for the outer (black hole)

geodesic we need to decide how to select t_0, x_0 and A for the inner (empty AdS) geodesic, namely some sort of matching conditions; from the geodesic equations (3.2) it is immediate that r_* on both the inner and the outer branches must be the same, as it is a constant of motion of the full geodesic.

We first demand that the geodesic be continuous at the shell, that is chosen a parameterization then

$$r_{\rm in}(\lambda_c) = r_{\rm out}(\lambda_c) \tag{4.13a}$$
$$v_{\rm in}(\lambda_c) = v_{\rm out}(\lambda_c) \tag{4.13b}$$
$$x_{\rm in}(\lambda_c) = x_{\rm out}(\lambda_c) \tag{4.13c}$$

If we decide to parameterize the geodesic with a metric coordinate (the useful coordinate is r) we see that the above gives us two matching conditions,

$$x_{\rm in}(r_c) = x_{\rm out}(r_c) \tag{4.14a}$$
$$v_{\rm in}(r_c) = v_{\rm out}(r_c) \tag{4.14b}$$

To get more conditions we will do some manipulations of the geodesic equations.

How do the derivatives of the geodesic match on both sides of the thin shell? We will think about $\dot{x}(\lambda)$, $\dot{v}(\lambda)$, $\dot{r}(\lambda)$ by using the geodesic equations to evaluate differences on both sides of the (regularized) shell. From (3.2b) we obtain

$$\dot{x}_{\rm out}(\lambda_+) - \dot{x}_{\rm in}(\lambda_-) = \frac{r_*}{r^2(\lambda_+)} - \frac{r_*}{r^2(\lambda_-)} \tag{4.15}$$

We now take the thin shell limit, $\lambda_\pm \to \lambda_c$ and using (4.13a) we obtain

$$\dot{x}_{\rm out}(\lambda_c) = \dot{x}_{\rm in}(\lambda_c) \equiv \dot{x}(\lambda_c) \tag{4.16}$$

that is, the derivative $\dot{x}(\lambda)$ is continuous across the shell.

We repeat the procedure for v. Take (3.2c) and integrate it across the shell

$$\dot{v}_{\rm out}(\lambda_+) - \dot{v}_{\rm in}(\lambda_-) = \int_{\lambda_1}^{\lambda_2} -r\left(\dot{v}^2(\lambda) - \frac{r_*^2}{r^4(\lambda)}\right) d\lambda \tag{4.17}$$

again taking $\lambda_\pm \to \lambda_c$ we find

$$\dot{v}_{\rm in}(\lambda_c) = \dot{v}_{\rm out}(\lambda_c) \equiv \dot{v}(\lambda_c) \tag{4.18}$$

We now take (3.2a) and integrate it across the shell

$$\left[-(r^2(\lambda) - m(v(\lambda)))\dot{v}(\lambda) + \dot{r}(\lambda)\right]_{\lambda=\lambda_1}^{\lambda=\lambda_2} = \int_{\lambda=\lambda_1}^{\lambda=\lambda_2} \frac{1}{2} m'(v(\lambda))\dot{v}^2(\lambda) d\lambda \tag{4.19}$$

The lhs can be evaluated in the following way:

$$\begin{aligned} \text{lhs}_{(4.19)} \quad = \quad & \left[-r^2_{\rm out}(\lambda_+)\dot{v}_{\rm out}(\lambda_+) + r_{\rm in}(\lambda_-)\dot{v}_{\rm in}(\lambda_-)\right] + \\ & + \left[m(v_{\rm out}(\lambda_+))\dot{v}_{\rm out}(\lambda_+) - m(v_{\rm in}(\lambda_-))\dot{v}_{\rm in}(\lambda_-)\right] + \\ & \dot{r}_{\rm out}(\lambda_+) - \dot{r}_{\rm in}(\lambda_-) \end{aligned} \tag{4.20}$$

Now take $\lambda_\pm \to \lambda_c$. Using the fact that the derivative $\dot{v}(\lambda)$ is continuous across the shell (4.18) and the way we defined our regularization (4.12) we find:

$$\text{lhs}_{(4.19)} = m\dot{v}(\lambda_c) + \dot{r}_{\text{out}}(\lambda_c) - \dot{r}_{\text{in}}(\lambda_c) \tag{4.21}$$

The rhs can be evaluated in the same limit by setting $m'(v) = m\delta(v)$ and direct substitution, yielding

$$\text{rhs}_{(4.19)} = \frac{1}{2}m\dot{v}(\lambda_c) \tag{4.22}$$

Putting the above two equations together we get

$$\dot{r}_{\text{out}}(\lambda_c) - \dot{r}_{\text{in}}(\lambda_c) = -\frac{1}{2}m\dot{v}(\lambda_c) \tag{4.23}$$

Putting (4.18) and (4.23) together we finally obtain the relation between the parameters A_{in} and A_{out} for a geodesic that crosses an infinitely thin shell. It depends on the mass of the shell and on the geodesic [62]

$$A_{\text{out}} = A_{\text{in}} - \frac{1}{2}m\dot{v}(\lambda_c) \tag{4.24}$$

We have now obtained all the matching conditions necessary, which are the result of this subsubsection.

4.2.2 Branch exclusion and constraints

In Sec. 2.3.2 we said some words about geodesics in black hole geometry. In particular, one of the things we mentioned for the eternal black hole geometry is that a necessary condition for the geodesics not to fall into the singularity is that the C of (2.35) be positive. Turning it around: if C is negative in an eternal black hole geometry, then the geodesic falls into the singularity, which for our applications we do not want. In that section we were exclusively thinking about geodesics completely contained in the eternal black hole geometry *and* that had both end-points at the boundary of AdS so naturally we excluded the possibility that $C < 0$.

However, in our work we found that if what we want to do is construct a full geodesic out of geodesic branches each of which are solutions to either the eternal black hole or the empty AdS geometries, and which have different parameters, and that the full geodesic has both end-points at the boundary of AdS and crosses the infalling shell, then under some circumstances it sometimes happens that the geodesic branches that we must use to achieve this have $C < 0$. Therefore in this subsection we study geodesics that live in the black hole geometry and which happen to fall into the singularity, because we will be using pieces of them to glue properly into our full geodesics in Vaidya geometry.

The relevant expression for the following arguments is (4.4), with values of m, r_* and A that determine C according to (2.35) and might or might not lead to $C < 0$, and also determine $\epsilon, \tilde{\epsilon}$ according to (2.36).

Instead of t_0, r_* and A as in Sec. 4.2.1, we find that to describe the behavior of geodesics branches which we will want to glue together it is better to parameterize them in terms of r_*, A and r_c, where r_c is the radial coordinate where the full geodesic will cross the infalling shell. Since the geodesics will be glued at r_c, this way we have parameters

which are closer to the decision criteria of which branches to use. If two crossing points exist (for example, when both $t_{1,2} > 0$ but small enough that the geodesic crosses the shell twice), then we choose r_c to be the smaller one and denote the bigger one by $\bar{r}_c$. Additionally we also need a sign. We know that on top of each set of parameters we also need to pick a branch, corresponding to both signs of (2.28) and (2.34). So together with r_*, A and r_c, we choose this sign d_{in} to be the sign of the branch of the inner geodesic that reaches the shell at r_c. We do so similarly for the outer branch, and parametrize it with a sign d_{out} which is the sign of the outer branch which reaches the shell at r_c.

Some geodesic branches contain problematic points. For example, a divergence of (4.4) signals that the corresponding geodesic branch goes $v = -\infty$ at finite r, while some other branches contain the point $r = 0$, the singularity. We will see that our gluing rules will tell us that imposing that the geodesic comes back to the boundary automatically excludes the problematic parts of these branches. For example on shell crossings where a black hole brach is glued to an AdS branch at r_c, or gluing either two black holes branches or two empty AdS branches, $(+)$ and $(-)$.

The exclusion criterion for geodesics that fall into the singularity is easy to implement in terms of our parametrization: geodesic branches must either have positive derivative at the crossing point, *i.e.* $v'(r_c) > 0$, or change branch before reaching infinity. If both of these simultaneously not happen, the geodesic falls into the singularity.

We then examine the derivatives of complete geodesics living in the black hole geometry.

- When $\epsilon = -1$ the branch $(+)$ has a minimum at r_*, having a positive derivative for $r > r_*$ and negative otherwise, while the branch $(-)$ always diverges to minus infinity at the horizon, having a positive derivative above it and negative below.
- When $\epsilon = +1$ the branch $(-)$ has a minimum at r_*, having a positive derivative for $r > r_*$ and negative otherwise. The $(+)$ always diverges to minus infinity at the horizon, having a positive derivative above it and negative below, but the horizon is only reached if $C < 0$.

Branch change when going to the boundary

The above points can be spelled out in terms of d_{out}. If $d_{\text{out}} = +1$ then we must have that $v'_+(r_c) > 0$ for that branch not to be exluded. If $d_{\text{out}} = -1$ and $v'_-(r_c) < 0$ then the outer geodesic segment must change into the branch $(+)$ before reaching the boundary.

Let us define an index η which equals $+1$ if there is no change of branches, and -1 if the branch changes from $(-)$ to $(+)$ between the shell crossing and the geodesic getting to infinity. If $d_{\text{out}} = +1$, equation (4.4) together with $\tilde{\epsilon} = 1$ implies that v'_+ is always positive and therefore $\eta = 1$.

When $d_{\text{out}} = -1$, Eq. (4.4) shows that v'_- is negative for $r < r_*$ when $\epsilon = 1$ and for $r < r_h$ when $\epsilon = -1$. Therefore we conclude:

$$d_{\text{out}} = +1 \quad \Longrightarrow \quad \eta = 1 \tag{4.25}$$

$$d_{\text{out}} = -1 \quad \Longrightarrow \quad \begin{cases} \eta = \text{sign}(r_c - r_*)\,, & \text{for } \epsilon = +1 \\ \eta = \text{sign}(r_c - r_h)\,, & \text{for } \epsilon = -1 \end{cases} \tag{4.26}$$

We will call d^x_{in} and d^x_{out} the signs of the branches that reach the shell, like d_{in} and

d_{out}, but this time for the inner and outer $x(r)$ functions. The choice (4.2) for the geodesic endpoints sets $d^x_{\text{in}} = d_{\text{in}}$. Combining the matching conditions (4.16) and (4.18) we have $d^x_{\text{out}} = \eta$.

A second crossing point of the geodesic with the shell will exist at

$$\bar{r}_c = \frac{r_c r_*^2}{r_*^2 - 2A_{\text{in}}\left(A_{\text{in}} + d_{\text{in}}\sqrt{A_{\text{in}}^2 + r_c^2 - r_*^2}\right)} \tag{4.27}$$

whenever the denominator is positive. The denominator is positive or negative depending on the precise relation between r_*, A_{in} and r_c:

$$\begin{cases} r_*^2 > 2A_{\text{in}}^2 \begin{cases} d_{\text{in}} = -1 \to \text{positive} \\ d_{\text{in}} = +1 \begin{cases} r_c < \frac{r_*^2}{2A_{\text{in}}} \to \text{positive} \\ r_c > \frac{r_*^2}{2A_{\text{in}}} \to \text{negative} \end{cases} \end{cases} \\ r_*^2 < 2A_{\text{in}}^2 \begin{cases} d_{\text{in}} = -1 \begin{cases} r_c > \frac{r_*^2}{2A_{\text{in}}} \to \text{positive} \\ r_c < \frac{r_*^2}{2A_{\text{in}}} \to \text{negative} \end{cases} \\ d_{\text{in}} = +1 \to \text{negative} \end{cases} \end{cases} \tag{4.28}$$

4.2.3 Branch parameter matching

Here we describe how the parameters we chose to parametrize the geodesic branches are related between them across the thin shell.

Eq. (4.24) gives us a relation between derivative of the radial coordinate on each side of the thin shell. This allows us to relate parameters A_{out} and d_{out} to A_{in} and d_{in}:

$$A_{\text{out}} = \frac{|A_{\text{in}}(2r_c^2 - m) - d_{\text{in}} m\sqrt{A_{\text{in}}^2 + r_c^2 - r_*^2}|}{2r_c^2} \tag{4.29}$$

$$d_{\text{out}} = \epsilon\,\text{sign}\left[\frac{m\sqrt{A_{\text{in}}^2 + r_c^2 - r_*^2} + d_{\text{in}}A_{\text{in}}(m - 2r_c^2)}{(m - 2r_c^2)\sqrt{A_{\text{in}}^2 + r_c^2 - r_*^2} + d_{\text{in}}A_{\text{in}}m}\right] \tag{4.30}$$

Contrarily to the thermal case, where the entire geometry is described by a black hole, we need now to allow both positive and negative values for the constant C (2.35) in order to construct the outer geodesic segment.

4.2.4 Geodesic solutions in thin shell Vaidya

Here we put together everything we learned so far about geodesics in Vaidya geometry and how they depend on the parameters we chose. This completely analytic solution to the thin shell limit of Vaidya was first obtained in [28].

We start with the inner segment. When $d_{\text{in}} = +1$, it is given by

$$\begin{aligned} r \in [r_m, r_c] \quad &: \quad \begin{cases} \hat{v}(r) = t_0 + t^{\text{AdS}}(r) - 1/r \\ \hat{x}(r) = x^{\text{AdS}}(r) \end{cases} \\ r \in [r_m, r_M] \quad &: \quad \begin{cases} \hat{v}(r) = t_0 - t^{\text{AdS}}(r) - 1/r \\ \hat{x}(r) = -x^{\text{AdS}}(r) \end{cases} \end{aligned} , \tag{4.31}$$

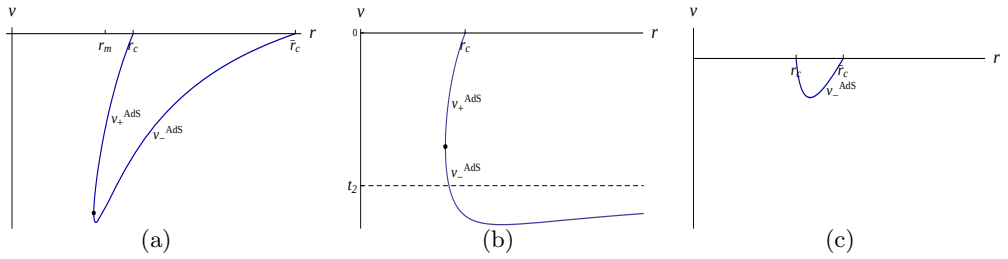

Figure 4.1: Examples of inner segments of a thin shell geodesic for different parameters. The $v = 0$ line denotes the shell, r_c and $\bar{r}_c$ denote crossings, and dots denote gluing points between $v_\pm^{\mathrm{AdS}}$ branches. (a) $d_{\mathrm{in}} = +1$ and two crossings, (b) $d_{\mathrm{in}} = +1$ and one crossing, (c) $d_{\mathrm{in}} = -1$ and two crossings.

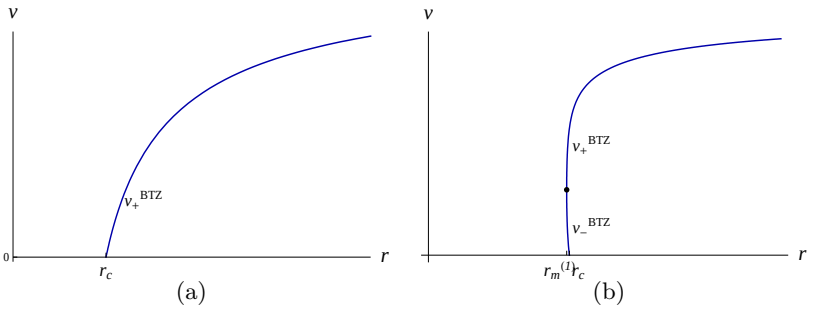

Figure 4.2: Examples of outer segments of a thin shell geodesic for different parameters. The $v = 0$ line denotes the shell, r_c denotes a crossing, and dots denote gluing points between $v_\pm^{\mathrm{BTZ}}$ branches. (a) $\eta = +1$ and $d_{\mathrm{out}} = +1$ ($d_{\mathrm{out}} = -1$ would look visually similar) and (b) $\eta = -1$ and $d_{\mathrm{out}} = -1$. For outer segments starting at a second crossing $\bar{r}_c$ all the pictures would be similar.

where r_m is given by (2.31), and $r_M = \bar{r}_c$ if there is a second crossing of the geodesic with the shell (see Fig. 4.1(a)) and infinity otherwise (see Fig. 4.1(b)). A second crossing exists if and only if $\bar{r}_c$ (4.27) is positive which is determined by (4.28). The functions $t^{\rm AdS}$ and $x^{\rm AdS}$ are given in (2.29). When instead $d_{\rm in} = -1$, we have

$$r \in [r_c, r_M] \quad : \quad \begin{cases} \hat{v}(r) = t_0 - t^{\rm AdS}(r) - 1/r \\ \hat{x}(r) = -x^{\rm AdS}(r) \end{cases} \tag{4.32}$$

(see Fig. 4.1(c)). The integration constant t_0 in (4.31) and (4.32) has to be chosen such that $v_{d_{\rm in}}(r_c) = 0$, and for simplicity we have set $x_0 = 0$ since it does not affect any relevant quantity.

The outer geodesic segment starting at the crossing point r_c has the following expression. When $\eta = 1$ we have

$$r \in [r_c, \infty] \quad : \quad \begin{cases} v(r) = t_1 - t_{d_{\rm out}}(\infty) + v_{d_{\rm out}}(r) \\ x(r) = x_+(r) - x_+(r_c) + d_{\rm in} x^{\rm AdS}(r_c) \end{cases} , \tag{4.33}$$

with t_d and x_d given by (2.34) (see Fig. 4.2(a)). For $\eta = -1$ we must have $d_{\rm out} = -1$ and then

$$\begin{aligned} r \in [r_c, r_m^{(1)}] \quad : \quad & \begin{cases} v(r) = t_1 - t_+(\infty) + v_-(r) \\ x(r) = x_-(r) - x_-(r_c) + d_{\rm in} x^{\rm AdS}(r_c) \end{cases} \\ r \in [r_m^{(1)}, \infty] \quad : \quad & \begin{cases} v(r) = t_1 - t_+(\infty) + v_+(r) \\ x(r) = x_+(r) - x_-(r_c) + d_{\rm in} x^{\rm AdS}(r_c) \end{cases} \end{aligned} , \tag{4.34}$$

with the minimal value of the radial coordinate $r_m^{(1)}$ defined in (2.37) (see Fig. 4.2(b)). The value of the time coordinate at the endpoint of this geodesic segment, t_1, is given by

$$t_1 = t_{\eta\, d_{\rm out}}(\infty) - v_{d_{\rm out}}(r_c) \,. \tag{4.35}$$

The outer geodesic segment starting at the second crossing point $\bar{r}_c$, when $\bar{\eta} = 1$ is given by

$$r \in [\bar{r}_c, \infty] \quad : \quad \begin{cases} \bar{v}(r) = t_2 - \bar{t}_{\bar{d}_{\rm out}}(\infty) + \bar{v}_{\bar{d}_{\rm out}}(r) \\ \bar{x}(r) = \bar{x}_-(r) - \bar{x}_-(\bar{r}_c) - x^{\rm AdS}(\bar{r}_c) \end{cases} , \tag{4.36}$$

where the bar over the functions indicates that the energy parameter should be taken to be $\bar{A}_{\rm out}$ instead of $A_{\rm out}$. For $\bar{\eta} = -1$ we have

$$\begin{aligned} r \in [\bar{r}_c, r_m^{(2)}] \quad : \quad & \begin{cases} \bar{v}(r) = t_2 - \bar{t}_+(\infty) + \bar{v}_-(r) \\ \bar{x}(r) = \bar{x}_+(r) - \bar{x}_+(\bar{r}_c) - x^{\rm AdS}(\bar{r}_c) \end{cases} \\ r \in [r_m^{(2)}, \infty] \quad : \quad & \begin{cases} \bar{v}(r) = t_2 - \bar{t}_+(\infty) + \bar{v}_+(r) \\ \bar{x}(r) = \bar{x}_-(r) - \bar{x}_+(\bar{r}_c) - x^{\rm AdS}(\bar{r}_c) \end{cases} \end{aligned} , \tag{4.37}$$

with

$$t_2 = \bar{t}_{\bar{\eta}\, \bar{d}_{\rm out}}(\infty) - \bar{v}_{\bar{d}_{\rm out}}(\bar{r}_c) \,. \tag{4.38}$$

From the previous expressions we can also immediately read off l, the spatial distance between the geodesics endpoints. If the geodesic crosses the shell twice we have

$$l = x_+(\infty) - x_\eta(r_c) + d_{\rm in} x^{\rm AdS}(r_c) + x^{\rm AdS}(\bar{r}_c) + \bar{x}_+(\infty) - \bar{x}_{\bar{\eta}}(\bar{r}_c) \,, \tag{4.39}$$

where we have used that $\bar{x}_{-\bar{\eta}}(\bar{r}_c) - \bar{x}_-(\infty) = \bar{x}_+(\infty) - \bar{x}_{\bar{\eta}}(\bar{r}_c)$. If the geodesic crosses the shell only once we have

$$l = x_+(\infty) - x_\eta(r_c) + d_{\rm in} x^{\rm AdS}(r_c) + x^{\rm AdS}(\infty) \,. \tag{4.40}$$

4.2.5 Time evolution of the thin shell 2-point function

In Sec. 4.2.4 we have put together all the information necessary to reconstruct a complete geodesic given the parameters of its inner segment and the position where it crosses the shell. Then the proper length of the geodesic is $\int d\lambda = \int dr/\dot{r}$. The length of the inner segment is given by

$$L_{\rm in} = d_{\rm in} \log\left[r_m^{-1}\left(r_c + \sqrt{r_c^2 - r_m^2}\right)\right] + \log\left[r_m^{-1}\left(r_M + \sqrt{r_M^2 - r_m^2}\right)\right]. \tag{4.41}$$

When the geodesics cross twice the infalling shell, $r_M = \bar{r}_c$. Otherwise r_M should be replaced by a large but finite value r_b, as explained in previous sections. Inverse powers of r_b are then to be neglected in the second term of the rhs. The length of the outer geodesic segment that starts at r_c is

$$\begin{aligned} L_{\rm out} \;=\; & \log 2\, r_b + \frac{1}{2}\log\left| C^{-1}\left(r_*^2 - A_{\rm out}^2 + m - 2r_c^2 + \right.\right. \\ & \left.\left. +2\eta\sqrt{r_c^4 + m r_*^2 - r_c^2(r_*^2 - A_{\rm out}^2 + m)}\right)\right|. \end{aligned} \tag{4.42}$$

In the case that the geodesic crosses the shell twice, there is an analogous expression for the length $\bar{L}_{\rm out}$ of the outer geodesic segment starting at $\bar{r}_c$.

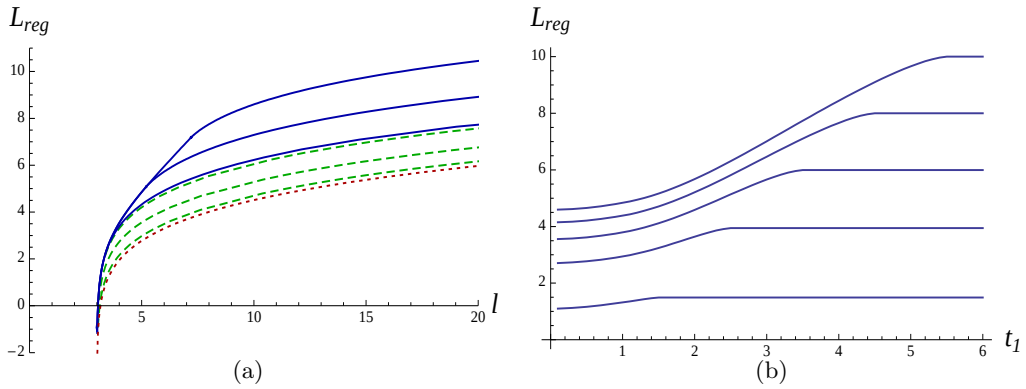

Figure 4.3: For $m = 1$ regularized geodesic length a) as a function of l for fixed $\Delta t = 3$ and $t_1 = 3.1, 4.1, 5.1$ from bottom up in solid lines ($t_2 > 0$), $t_1 = 0.9, 1.9, 2.9$ in dashed lines ($t_2 < 0$) and empty AdS geodesic in dotted line; b) as a function of t_1 for fixed $\Delta t = 1$ and $l = 2, 4, 6, 8, 10$ from bottom up respectively.

We previously discussed one of the thresholds present in the behavior of $L_{\rm reg}$ and obtained an important relation:

$$l = t_1 + t_2 - 2v_*\,, \tag{4.9 revisited}$$

where we keep in mind that in our calculations we placed the thin shell at $v = 0$. The idea is that to analyze these plots we set $v_* = 0$ and then write (4.9) in terms of t_1 and Δt:

$$l = 2t_1 - \Delta t\,. \tag{4.43}$$

In Fig. 4.3(a) we have plotted the regularized geodesic proper length (2.22) as a function of l for fixed $\Delta t = t_1 - t_2$. It diverges when the geodesics approach the lightlike limit, in this case $l = 3$. When $t_1 < 0$ the result is that of empty AdS_3. It doesn't depend on t_1 due to being completely contained in empty AdS and due to time translation invariance of this space. In dashed lines we have distinguished geodesics with positive t_1 and negative t_2, those associated to 2-point functions with one end-point after and one end-point before the perturbation acts. We can see these geodesics never have a thermal (linear) behavior: irrespectively of l they will never be completely contained in the black hole geometry since they always have one end-point on each side of the perturbation. In solid lines we have plotted the length of geodesic with both endpoints after the perturbation.

According to (4.9) geodesics with both $t_{1,2}$ positive and $l < t_1 + t_2$ lie completely outside the shell. They are completely contained in a black hole geometry and so they reproduce the results at thermal equilibrium. Namely for l bigger than Δt and such that the associated geodesics can reach the black hole horizon

$$L_{\text{reg}}(l; t_1, t_2) = 2 \log \frac{\beta}{2\pi} + \frac{2\pi l}{\beta} \,. \tag{4.44}$$

In our case β is given by (2.9), and we have further set $L, \sqrt{m} = 1$. Substituting this into (4.44) we get $L_{\text{reg}} = l$. This linear regime with this proportionality constant can clearly be seen in Fig 4.3(a). Geodesics with $l > t_1 + t_2$ cross the shell and lead to a result that deviates from thermal.

Plots of the geodesic length as a function of t_1 for fixed l and Δt are shown in Fig.4.3(b). It saturates to its thermal value at $t_1 = (l + \Delta t)/2$, when the associated geodesic stops reaching the infalling shell, (4.43)

Although our results are exact, L_{reg} is a complicated function of the geodesic data which can not be explicitly expressed in terms of the physical variables t_1, t_2 and l. Explicit results can be however derived for large intervals or late times. The next sections are devoted to analyzing the evolution of 2-point functions in these two limits, from which we will derive important physical information.

4.3 Large distance limit

Taking the large distance limit is straightforward now that we have the general solution, as presented in Sec. 4.2.4.

As we take the space separation of the geodesic end-points to be larger and larger, the geodesic will get closer and closer to $r = 0$. In the large l limit most of the geodesic will be contained in pure AdS_3 space. We can therefore use the formula (2.30) that in AdS_3 relates A and r_* with the space and time separation of the geodesic end-points. In that limit, it reduces to

$$r_* \approx \frac{2}{l} \,, \quad A_{\text{in}} \approx \frac{2a}{l^2} \tag{4.45}$$

for some finite constant a and $d_{\text{in}} = +1$. From (4.29) and (4.30) we get

$$A_{\text{out}} = \frac{m}{2r_c} \,, \quad d_{\text{out}} = \text{sign}(2r_c^2 - m) \tag{4.46}$$

and from (4.27) the second crossing will be at

$$\bar{r}_c = \frac{r_c}{1 - a r_c} \tag{4.47}$$

iff $a < 1/r_c$, in which case expressions like (4.46) apply.

The proper length in this limit can be found as follows. In all generality, the proper length of the inner and outer parts of the geodesics are given by (4.41) and (4.42) respectively. For the inner part we take (4.41)

$$L_{\text{in}} = 2\log l + \log r_c + \log r_M + \mathcal{O}(l^{-1}) \tag{4.48}$$

Here l strictly represents the spatial separation of the endpoints of the inner geodesic prolonged to the boundary in the absence of a shell. However, the difference between this separation and that calculated in the presence of the shell, having into account the matching conditions, is a finite number. Thus (4.48) applies equally with l being the space separation between the geodesic endpoints in the thin shell geometry. For the outer part we take (4.42) and so the length between a crossing r_c and the boundary r_b at time t_1 of one of the outer branches is

$$L_{\text{out}} = \log 2r_b - \log \frac{4r_c^2 - m}{2r_c}\,, \quad t_1 = \frac{1}{r_h}\log\frac{2r_c + r_h}{2r_c - r_h} \tag{4.49}$$

where the second expression allows us to write $r_c = f(t_1)$. There might be a second outer branch if there is a second crossing at $\bar{r}_c$. As before, in the formulas above r_M stands for $\bar{r}_c$ if a second crossing exists, and r_b if it doesn't. From these previous expressions we obtain

$$L_{\text{reg}} = 2\log l + \tilde{s}(t_1) + \tilde{s}(t_2) + \mathcal{O}(l^{-1}) \tag{4.50}$$

with

$$\tilde{s}(t) = \begin{cases} 2\log\cosh \pi t/\beta\,, & t > 0 \\ 0\,, & t < 0 \end{cases} \tag{4.51}$$

This is another generalization of a result of [27], where it was suggested that $L_{\text{reg}}(l; t_1, t_2) = 2\log l + s(t_1, t_2)$, in which case we can write

$$s(t_1, t_2) = \tilde{s}(t_1) + \tilde{s}(t_2) \tag{4.52}$$

Finally we can take formula (4.50) and substitute it into (2.23) to obtain the WKB approximation for 2-point functions in the large l limit:

$$\langle \phi(l, t_1)\phi(0, t_2)\rangle \approx \frac{1}{\left(l\cosh(\pi t_1/\beta)\cosh\pi(t_2/\beta)\right)^{2\Delta}} \tag{4.53}$$

Note how interesting it is that the *quantitative* mismatch between this formula and the CFT result of Calabrese and Cardy (1.63) actually reinforces our interpretation about the *qualitative* mismatch between the two models. Remember that in Ch. 3 we argued that the reason why for large l CC's entanglement entropy goes to constant while ours goes to a logarithm is because their initial state had finite-range correlations whereas ours had long-range correlations. The result (4.53) reinforces this, since it shows a 2-point function with a power-law dependence on l, characteristic of critical states, as opposed to that of CC, (1.63), which shows a 2-point function with an exponentially decaying dependence on l, characteristic of non-critical states.

4.4 Steady evolution

We have seen in the previous section that for $l > t_1 + t_2$ and taking the large l limit we are able to reproduce the $e^{-2\pi\Delta(t_1+t_2)/\beta}$ dependence of the 2-point function on $t_{1,2}$. Now lets see that we can actually uncover an even more general behavior of these objects.

Lets now focus on function (4.51). Define a time $\bar{t}$ such that for $t \gtrapprox \bar{t}$ that function can be approximated as

$$\tilde{s}(t) \approx -2\log 2 + \frac{2\pi t}{\beta} \tag{4.54}$$

Clearly for our model

$$\bar{t}_{\rm hm} \approx \beta \tag{4.55}$$

where 'hm' stands for holographic model.

We have shown how to obtain the 2-point function following a quench using CFT techniques, that is (1.63). There, for $l > t_1 + t_2$ we see that the l dependence enters the 2-point function only through the combination $l - t_1 - t_2$. Herein lies the significance of $\bar{t}$: in [28] we proved that if additionally we take $t > \bar{t}$ then in our model the dependence of the holographic 2-point functions on l enters through the combination $l - t_1 - t_2$, *even for finite* l.

The proof in [28] is algebraically intrincate and not very particularly illuminating and so here we simply quote the result. We proved that for $l > t_1 + t_2$ a time $\bar{t}$ and a function F exist such that after this time the entanglement entropy depends on l only through the combination $l - t_1 - t_2$:

$$L_{\rm reg} = \frac{2\pi}{\beta}(t_1 + t_2) + F(l - t_1 - t_2)\,, \qquad \text{for } t_i > \bar{t} \quad \text{and} \quad l > t_1 + t_2 \tag{4.56}$$

Actually, already in [27] we had numerically found hints of this behavior. We note that this time $\bar{t}$ is the same for both the holographic entanglement entropy and holographic 2-point functions.

We can identify two sources that drive the evolution of an out of equilibrium system towards equilibration: the interaction between its components and their propagation. In the sea of excitations sourced by the initial perturbation, quantum correlations will be stronger between excitations generated at close points. Propagation will tend to increase the separation between entangled excitations with time. On the other hand interaction will lead to the redistribution of energy, and other conserved charges in case they are present, among the different momentum modes. This is crucial in order that the state towards which the system evolves has properties in common to thermal equilibrium. The separation of entangled excitations with time is a process constrained by causality, implying that equilibration can only be achieved on regions of growing but finite size. On the contrary, the redistribution of energy among modes can be expected to require a finite time for its nearly completion. Could this time scale be $\bar{t}$?

The quasiparticle model that Calabrese and Cardy introduce and which we reviewed in Sec. 3.4 assumes that the excitations move as free particles according to their group velocities, $v = 1$. Since as we have seen that model is also applicable for our holographic model, it seems consistent that if 2-point function depend on l only through $l - t_1 - t_2$ (for $l > t_1 + t_2$), then all processes in the evolving plasma related with interaction have reached equilibrium. We therefore conjecture that this time scale $\bar{t}$ is associated with

time-evolution of the occupation numbers: if after $\bar{t}$ we have only propagation, then $\bar{t}$ should be the time it takes for the occupation numbers to stabilize.

As a consistency check, it's interesting to think about free bosons. For free bosons, we expect that the occupation numbers are always time independent, and in that sense we can say that $\bar{t}_{\text{free}} = 0$. In [36] the authors manage an exact calculation of the time-evolution of the 2-point function after a quench valid for all times for the case of the free boson and check that its dependence on l enters only through $l - t_1 - t_2$ for all times and so indeed $\bar{t}_{\text{free}} = 0$ according to our definition. This is an explicit example where we have enough control over the system to check that the time after which the 2-point function depends on l only through $l - t_1 - t_2$ and the time after which the occupation numbers are stationary in time, coincide.

5

Custom-made gravity solutions

We present an algorithm to generate new solutions to Einstein-dilaton gravity. For the case of asymptotically AdS solutions, which we focus on exclusively here, we remove the usual AdS divergences and properly define the variational problem. The following is based on the results of [29].

5.1 Motivation

In the previous chapters we proposed a holographic model of a quantum quench. A Vaidya metric represents an infalling shell of matter interpolating between an empty AdS space and an asymptotically AdS black hole. Then we considered two different observables, first the entanglement entropy and then 2-point functions, and studied their time evolution in the theory dual to the quenching process.

We are still interested in saying more things about quenches. We could take the same model and look at different observables. Or alternatively we could try to come up with new models.

What we want to consider is the possibility of "glueing" and AdS space to a different asymptotically AdS space along a constant time surface. If we can do this we can argue that we have a different holographic model of a quench, with different parameters that we can play with, and again compute observables. Alternatively we will see that we have not only introduced new candidates for the "after" geometry, but also for the "before geometry". We obtain solitonic states, the energy of which might the be lowest for a given theory, in which case they could be interpreted as the vacuum. The question of whether or not a given a certain state is that of lowest energy of course depends on the choice of boundary conditions of the problem.

As argued in the motivation for this work, from this we might learn not only about thermalization of strongly-coupled holographic plasmas, but turning things around, by trying to holographically reproduce known results we might also learn about the AdS/CFT duality itself.

Of course, for this we need the actual solutions to glue together with AdS. Therefore we have set out to look for new asymptotically AdS_3 solutions. On the one hand, to get new solutions we have decided to introduce a scalar field in AdS_3; we are studying Einstein-dilaton gravity (EDG). On the other hand we have decided to constrain the space of solutions in order to get exact solutions.

This chapter is organized in the following way. First we present the action for which we want to find solutions and we describe what constraints we'll accept in order to manage

to get exact solutions. Then we'll describe our algorithm: it allows us to generate new solutions to EDG given an input function $f_1(\rho)$ from which we demand a few properties. We describe how some physical properties of the solutions, like the asymptotics, or the presence or absence of horizons and singularities, are related to the choice of the input function. We will mention under which conditions solutions are asymptotically AdS and study exclusively those. In order to discuss other physical properties like mass and angular momentum of the solution we need to renormalize the theory, which we do, and again relate these with the (asymptotic behavior of the) input function. Lastly we review some EDG solutions present in the literature and show that they could've been obtained by choosing the input function appropriately and following our algorithm.

We haven't yet implemented using such solutions to generate new quenches, but in principle the idea is well defined and conceptually similar to what we've done in previously.

5.2 Einstein-dilaton gravity

The bulk action of Einstein-dilaton gravity (EDG) is

$$S = \int d^3x\sqrt{-g}\left(R + 2 - \frac{1}{2}(\partial\phi)^2 - V(\phi)\right) \tag{5.1}$$

where g is the determinant of the metric, R is the Ricci scalar, ϕ is a scalar field and $V(\phi)$ its potential.

Constraining solutions

Part of the trick to finding exact solutions to such a general action is considering only solutions with certain simplifying properties. In particular, solutions which depend only on a single direction and have a large symmetry group spanning the remaining normal directions. Given our motivation, we will choose this special direction to coincide with the radial direction of the asymptotically AdS solution and call it ρ. These solutions are called axi-symmetric solutions. An ansatz with captures all axi-symmetric solutions is that of [63]:

$$ds^2 = \lambda_{\mu\nu}dx^\mu dx^\nu + \frac{e^2 d\rho^2}{-\det\lambda} \tag{5.2}$$

where λ is the matrix

$$\lambda_{\mu\nu} = \begin{pmatrix} T+X & Y \\ Y & T-X \end{pmatrix} \tag{5.3}$$

with functions T, X and Y and e is the Einbein, and all of these depend on the single variable ρ.

We can rewrite the above by introducing the Minkowski metric $\eta = \mathrm{diag}(1,-1,-1)$ for the target space, and a vector $\mathbf{X} = (T,X,Y)$ with norm $\mathbf{X}^2 = -\det\lambda$ in that space. Then we can write the action (5.1) as that of a particle moving the 3-dimensional Minkowski space

$$S = \mathrm{Vol}\int_{\rho_0}^{\infty} d\rho e\left(\frac{e^{-2}}{2}\dot{\mathbf{X}}^2 + 2 - \frac{e^{-2}}{2}\mathbf{X}^2\dot{\phi}^2 - V(\phi)\right) \tag{5.4}$$

where 'Vol' refers to the volume of the 2-dimensional integration performed, dots denote $d/d\rho$ derivatives and the integration domain is bounded by some $\rho = \rho_0$ and $\rho = \infty$.

We vary (5.4) with respect to e, $\mathbf{X}$ and ϕ and then gauge-fix the Einbein to unity, $e = 1$. We obtain the following equations of motion (EOM)

$$\text{Einstein:} \quad \ddot{\mathbf{X}} = -\dot{\phi}^2 \mathbf{X} \tag{5.5a}$$

$$\text{Klein-Gordon:} \quad \mathbf{X}^2 \ddot{\phi} + 2\mathbf{X} \cdot \dot{\mathbf{X}} \dot{\phi} = V'(\phi) \tag{5.5b}$$

$$\text{Hamilton:} \quad -\frac{1}{2}\dot{\mathbf{X}}^2 + 2 + \frac{1}{2}\mathbf{X}^2 \dot{\phi}^2 - V(\phi) = 0 \tag{5.5c}$$

These EOMs have the following first integral:

$$\text{First integral:} \quad \eta^{nk} \epsilon_{ijk} X^i \dot{X}^j = J^n = \text{const} \tag{5.6}$$

meaning $\mathbf{J}$ does not depend on the independent coordinate ρ. We can call this the angular momentum of the particle described by action (5.4), not to be confused with the angular momentum of solutions of (5.1).

Note that (5.2) is manifestly $\mathrm{SL}(2,\mathbb{R})$ invariant. Instead of writing solutions to (5.4) in all generality, we restrict ourselves to writing one solution to each connected component of that group, then generating all the others by acting on a specific solution with group elements. The $\mathrm{SL}(2,\mathbb{R})$ invariance of (5.2) manifests itself in (5.4) as Lorentz invariance. We can use what we know about this to classify such components, and thus our solutions. Since $\mathbf{J}$ (5.6) is a first integral, then for each type of $\mathbf{J}$ (timelike, nulllike or spacelike), we can generate solutions by acting on $\mathbf{X}$ with elements of $\mathrm{SL}(2,\mathbb{R})$. We will see that most physically interesting solutions correspond to space-like $\mathbf{J}$.

Another feature of the EOMs is that (5.5a) implies planarity of the $\mathbf{X}$ vector, in the sense that the three dimensions decouple. For this reason, any independent solution to (5.5a) can be represented by a vector that doesn't depend on ρ times a scalar function which does. Since that equation is of second order, its solution space is spanned by a pair of independent solutions. Therefore, the most general solution to (5.5) can be written as

$$\mathbf{X}(\rho) = \mathbf{X}_1 f_1(\rho) + \mathbf{X}_2 f_2(\rho) \tag{5.7}$$

Picking a potential

The other part of the trick is not specifying the potential $V(\phi)$ and choosing it so that the metric and scalar EOM are satisfied. Usually one has the potential fixed and then looks for solutions. This is usually what makes sense: for a given theory, look for solutions. But given our motivation, what we really want is just obtaining solutions. Therefore we choose the theory (the potential) conveniently.

To pick the potential, one just has to notice that (5.5b) can be integrated, with its integration constant determined by (5.5c), to obtain the potential as a function of ρ, given $\mathbf{X}$:

$$V(\rho) = 2 - \frac{1}{4}\frac{d^2}{d\rho^2}\mathbf{X}^2 \tag{5.8}$$

Using symmetry to simplify

Lets see how use of symmetry simplifies the EOMs.

Take the general solution (5.7) and evaluate the integral (5.6):

$$\text{First integral:} \quad \dot{f}_2 f_1 - \dot{f}_1 f_2 = 2j = \text{const} \tag{5.9}$$

This is a Wronskian and so f_1 and f_2 are linearly independent if and only if $j = 0$.

Select

$$\mathbf{J} = (0, 0, -j) \tag{5.10}$$

This is discarding all solutions which have $\mathbf{J}$ either time-like or null-like; one the other hand, all other space-like solutions can be generated from Lorentz transformations. With this choice,

$$\mathbf{X}(\rho) = \begin{pmatrix} T \\ X \\ Y \end{pmatrix} = \frac{1}{2} \begin{pmatrix} f_1 - f_2 \\ -f_1 - f_2 \\ 0 \end{pmatrix} \tag{5.11}$$

$$\lambda_{\mu\nu} = \begin{pmatrix} -f_2 & 0 \\ 0 & f_1 \end{pmatrix} \tag{5.12}$$

The EOMs become

$$\text{Einstein:} \quad \ddot{f}_{1,2} + \dot{\phi}^2 f_{1,2} = 0 \tag{5.13a}$$

$$\text{Klein-Gordon:} \quad f_1 f_2 \ddot{\phi} - (f_1 \dot{f}_2 + f_2 \dot{f}_1)\dot{\phi} = V'(\phi) \tag{5.13b}$$

$$\text{Hamilton:} \quad \frac{1}{2}\dot{f}_1 \dot{f}_2 + 2 + \frac{1}{2} f_1 f_2 \dot{\phi}^2 - V(\phi) = 0 \tag{5.13c}$$

5.2.1 The algorithm

The algorithm to craft solutions works in the following way

- Pick a function f_1 such that
$$\ddot{f}_1 / f_1 \leq 0 \tag{5.14}$$
- f_2 is determined by integrating (5.9):
$$f_2 = \chi f_1 - 2j f_1 \int_\rho \frac{d\rho'}{f_1^2} \tag{5.15}$$
- The scalar is determined by integrating (5.13a):
$$\dot{\phi}(\rho) = -\sqrt{-\frac{\ddot{f}_1}{f_1}} = -\sqrt{-\frac{\ddot{f}_2}{f_2}} \tag{5.16}$$
- The potential as a function of ρ is given by (5.8):
$$V(\rho) = 2 - \frac{1}{2}\frac{d}{d\rho}(f_1 \dot{f}_2) \tag{5.17}$$
- $\phi(\rho)$ and $V(\rho)$ implicitly define $V(\phi)$

- The last step is to identify the $x^{0,1}$ coordinates of (5.2) with the physical boundary coordinates, which are defined by their periodicity properties, $(t, \varphi) \sim (t, \varphi + 2\pi)$, by using

$$t = ax^0 + bx^1\,, \qquad \varphi = cx^0 + dx^1 \tag{5.18}$$

With these steps done, our new solution to EDG is given by

$$ds^2 = -f_2(\rho)(dx^0)^2 + f_1(\rho)(dx^1)^2 + \frac{d\rho^2}{f_1(\rho)f_2(\rho)} \tag{5.19}$$

Given a specific solution new solutions can be generated by acting with $\mathrm{SL}(2,\mathbb{R})$ which amounts to choosing real numbers A, B, C and D:

$$\tilde{f}_1 = Af_1 + Bf_2\,, \quad \tilde{f}_2 = Cf_1 + Df_2 \tag{5.20}$$

The first integral transforms as $j \to \tilde{j} = j(AD - BC)$. The scalar does not transform but the potential does. This last fact will concern us later when we try to construct families of solutions to the same theory.

5.2.2 General features of the solutions

If we want to use our algorithm to cook up custom-made solutions with certain properties, it's convenient to study how certain features pop-up depending on the function f_1 that we choose. Specifically, we want solutions which have its asymptotic region as $\rho \to \infty$ and this region is AdS. If there are no horizons, then the solutions must be regular everywhere and without conical singularities or curvature singularities, or if these latter features are present, they must be shielded by an horizon. If an horizon is present at ρ_h then we take the radial coordinate $\rho \in]\rho_h, \infty[$ and if a center [1] is present at ρ_0 we take the radial coordinate $\rho \in [\rho_0, \infty[$.

For the following it's useful to write the curvature as a function of $f_{1,2}$:

$$R = -f_1\ddot{f}_2 - f_2\ddot{f}_1 - \frac{3}{2}\dot{f}_1\dot{f}_2 = 2f_1f_2\dot{\phi}^2 - \frac{3}{2}\dot{f}_1\dot{f}_2 \tag{5.21}$$

Restrictions from regularity

Regularity at a point $\bar{\rho}$ can be studied by checking what the EOM impose on functions $f_{1,2}$. If their leading behavior is a power law, then (5.9) imposes

$$f \propto (\rho - \bar{\rho})^\alpha\,, \quad \bar{f} \propto (\rho - \bar{\rho})^{1-\alpha} \tag{5.22}$$

and it follows from (5.16) that around this point and to leading order

$$\dot{\phi} \propto -\frac{\sqrt{\alpha(1-\alpha)}}{|\rho - \bar{\rho}|} \tag{5.23}$$

and therefore we must have $\alpha = 1$, or have a curvature singularity from (5.21).

[1] A "center at position ρ_0" is a position where the metric can written in polar coordinates where ρ is the radial coordinate and that furthermore isn't a conical singularity, that is $ds^2 = dr^2 + r^2 d\theta^2 + \dots$ with θ periodically identified in $0 \le \theta < 2\pi$.

A similar analysis can be done in the asymptotic region. Regularity of the scalar field at infinity implies f_1 and f_2 are linear combinations of functions whose leading behavior at large values of the radial coordinate is $f \propto \rho$ and $\tilde{f} \propto 1$, which leads to a constant value of the Ricci scalar at infinity, $R \to -\frac{3}{2}\dot{f}_1\dot{f}_2$. Therefore, the metric asymptotes to

- AdS when $f_{1,2}$ both asymptote to a linear function of ρ and furthermore with the same sign in from;
- dS when $f_{1,2}$ both asymptote to a linear function of ρ and with opposite signs;
- flat space when at least one of $f_{1,2}$ asymptotes to a constant.

We are mostly interested in asymptotically AdS solutions.

ADM metric

It's useful to write the metric (5.19) in the terms of the physical coordinates t and φ and in the ADM form. On the one hand this allows us to identify horizons by inspection of the metric elements, namely by looking at points where the coefficient of dt^2 vanishes. On the other hand provides a way to study solutions with more general first integral $\mathbf{J}$, (5.6). The relevant metric is

$$ds^2 = -N^2dt^2 + \frac{d\rho^2}{N^2R^2} + R^2(d\varphi + N_\varphi dt)^2 \tag{5.24}$$

and by writing $dr^2 = d\rho^2/R^2$ we obtain the usual ADM metric for the physical coordinates, where for the choice of $\mathbf{J}$ that we made in (5.10), the lapse function N and the shift vector N_φ are

$$R^2 = a^2 f_1 - b^2 f_2 \qquad N^2 = \frac{f_1 f_2}{R^2} \qquad N_\varphi = \frac{bdf_2 - acf_1}{R^2} \tag{5.25}$$

Regions of negative R^2 contain closed time-like curves. We will always want that R^2 is positive outside the outermost horizon if one is present, or everywhere otherwise.

For a general $\mathbf{J}$, or equivalently a general matrix λ (5.2)

$$R^2 = \mathrm{Tr}\,(\lambda M_R) \qquad N^2 = -\frac{\det\lambda}{R^2} \qquad N_\varphi = \frac{\mathrm{Tr}\,(\lambda M_N)}{R^2} \tag{5.26}$$

where we defined

$$M_R = \begin{pmatrix} b^2 & -ab \\ -ab & a^2 \end{pmatrix} \qquad M_N = \begin{pmatrix} -bd & bc \\ ad & -ac \end{pmatrix} \tag{5.27}$$

Gauge fixing

It's nice to gauge fix. By doing this, we guarantee that different $f_{1,2}$ functions, correspond to different solutions. The coordinate change (5.18) with the restriction $ad - bc = 1$ provides a realization of the $\mathrm{SL}(2,\mathbb{R})$ group of transformations of the matrix $\lambda_{\mu\nu}$ which locally preserves (5.2). For $ad - bc \neq 1$, λ is being multiplied by a constant. By rescaling of the radial coordinate we also preserve (5.2).

Equivalently we can implement the $\mathrm{SL}(2,\mathbb{R})$ by acting on $\mathbf{X}$. To keep things organized, for each orbit of $\mathbf{X}$ we pick a representative. Our choice in (5.11) doesn't completely

fix a representative, since solutions can still be generated by $(f_1, f_2) \to (\gamma f_1, f_2/\gamma)$ with $\gamma \in \mathbb{R}$. We can fix this by picking a relative normalization between f_1 and f_2. Specifically, when both grow linearly at infinity (the asymptotically AdS case) then we impose $f_1 \to \pm f_2$.

Horizons

Having the metric (5.24) looking for horizons amounts to looking for points where the lapse function can vanish: vanishing of the lapse function N is a sufficient condition for the existence of a Killing horizon at a point ρ_h of finite curvature. According to (5.25) this implies that f_1, f_2 or both must vanish at ρ_h.

A sufficient condition for the existence of a Killing horizon at a point ρ_h of finite curvature is the vanishing of the lapse function N at that point. This implies that f_1 or f_2 or both vanish. According to (5.6) $f_{1,2}$ might vanish simultaneously at a given point ρ_h if and only if $j = 0$.

If $j \neq 0$ we reparametrize the radial according to $y = \sqrt{2(\rho - \rho_h)/|j|}$ and obtain close to the zero

$$ds^2 = -\epsilon \frac{j^2}{R_h^2} y^2 dt^2 + \epsilon dy^2 + R_h^2 (d\varphi + N_{\varphi h} dt)^2 + \dots \tag{5.28}$$

where the subindex 'h' indicates that the corresponding function is evaluated at ρ_h. We defined $\epsilon = (-1)^i \operatorname{sign} j$ with $i = 1, 2$ for vanishing $f_{1,2}$ respectively. For $\epsilon = +1$ the first two terms are the 2-dimensional Rindler spacetime, which is known to be the correct near horizon approximation of any non-extremal black hole Killing horizon [64]. For $\epsilon = -1$, we have at ρ_h an inner black hole horizon or a cosmological horizon.

If $j = 0$ then both f_1 and f_2 vanish at ρ_h. Defining $y = \sqrt{\dot{f}_h(\rho - \rho_h)}$ we get

$$ds^2 = -y^2 dt^2 + y^2 (d\varphi + N_\varphi dt)^2 + \frac{4}{\dot{f}_h^2} \frac{dy^2}{y^2} + \dots \tag{5.29}$$

In particular extremal horizons can be obtained by writing $f_1 = 2(\rho - \rho_+) + 2\epsilon\rho_+$ and $f_2 = 2(\rho - \rho_+)$ and taking $\epsilon \to 0$. The result is

$$ds^2 = -\frac{2(\rho - \rho_+)^2}{\rho} d\rho^2 + \frac{d\rho^2}{4(\rho - \rho_+)^2} + 2\rho \left(d\varphi - \frac{\rho_+}{\rho} dt \right)^2 + \dots \tag{5.30}$$

from which we can in particular get the extremal BTZ by defining $r = \sqrt{2\rho}$.

In asymptotically AdS spaces with an horizon a restriction on our functions $f_{1,2}$ is obtained by demanding that outside the outermost horizon R^2 is positive. Then (5.25) imposes that it is f_2 which must vanish at the horizon.

As we have seen in the previous chapters, in a holographic quench, non-local observables like entanglement entropy and 2-point functions, are sensitive to things behind the horizon. One interesting thing would be to use our algorithm to find solutions with exotic behaviors which in the static case are hidden behind the horizon, but which in the time-evolving case could be sensed by these large observables and see what kind of behavior they induce.

Centers

If the radial function R vanishes at some point ρ_0 where the lapse function remains finite and furthermore we don't have a conical singularity, then we have a center. Since we want $R^2 > 0$ at infinity, then $b = 0$ and center are associated with zeroes of f_1. In coordinates $y = \sqrt{2(\rho - \rho_0)/|j|}$ near a center we have

$$ds^2 = -f_{2c}dt^2 + \frac{j^2}{f_{2c}}y^2 d\varphi^2 + dy^2 + \dots \tag{5.31}$$

To avoid conical singularities at ρ_0 we demand

$$f_{2c} = j^2 \tag{5.32}$$

Generating families of solutions

We have described a powerful algorithm which has the potential to give us many new solutions to EDG. The input of the algorithm is a function f_1 which has few restrictions and a choice of integration constants.

In this algorithm, the potential $V(\phi)$ is an *output* and will in general depend on our choice of integration constants. So we could think that by not specifying certain integration constants we would have an output that generates a family of solutions. But since the potential also in general depend on these integration constants, they will be labeling different solutions to different theories. We would like to know if it's possible to generate a family of solutions to the same potential. In principle this is non-trivial because in particular the potential is obtained by taking $\dot{\phi}(\rho)$ (5.16) and $V(\rho)$ (5.17), *both of which might depend on the integration constants*, and this provides an implicit definition of $V(\phi)$. So for $V(\rho)$ not to depend on the integration constants, a very precise cancellation of these would have to happen and this in general doesn't happen.

From the integration constants in the EOM we subtract those that are constrained by the Hamilton constraint and generated by $\mathrm{SL}(2,\mathbb{R})$ and shifts in ρ, and we are left with $8 - 1 - 3 - 1 = 3$, which can be thought of as being j and the leading and sub-leading modes of ϕ, $\phi_\pm$. How can we move in the space $\{j, \phi_\pm\}$ in a way that doesn't change $V(\rho)$?

We point out a symmetry of the EOMs:

$$\rho \to \Omega\rho \qquad f_{1,2} \to \Omega f_{1,2} \qquad j \to \Omega j \qquad \phi \to \phi \tag{5.33}$$

But now notice the interesting fact both $\phi(\rho)$ and $V(\rho)$ (5.17) don't transform, which means that $V(\phi)$ won't transform either. We found a way to go between two different solutions with the same potential. Therefore we define better integration constants in order to change the parametrization from $\{j, \phi_\pm\}$ to $\{\Omega, \xi, \lambda\}$:

$$\xi = j/\Omega \qquad \lambda = \phi_+/\phi_-^{\Delta_+/\Delta_-} \tag{5.34}$$

where $\Delta_\pm$ are the scaling dimensions of $\phi_\pm$. By using this parametrization of the integration constants we will obtain potentials which do not depend on Ω. λ is related to the fixing of boundary conditions in the sense that it fixes a relation between the leading and sub-leading behaviors of ϕ.

Static black holes and solitons

Smooth solutions with a Killing horizon or a center require $f_{1,2}$ to be at least twice di?erentiable down to its locus. In order to carry on a general analysis, we further assume now all functions to be analytic for $\rho > \rho_0$. Around a generic radial point $\bar{\rho}$, we have

$$f_1 = \sum_{n=0}^{\infty} a_n \frac{(\rho-\bar{\rho})^n}{\Omega^{n-1}} \qquad f_2 = \sum_{n=0}^{\infty} b_n \frac{(\rho-\bar{\rho})^n}{\Omega^{n-1}} \qquad \phi = \sum_{n=0}^{\infty} \phi_n \frac{(\rho-\bar{\rho})^n}{\Omega^{n-1}} \tag{5.35}$$

Our first integral implies

$$a_0 b_1 - a_1 b_0 = 2\xi \tag{5.36}$$
$$a_0 b_2 - a_2 b_0 = 0 \tag{5.37}$$
$$\dots \tag{5.38}$$

The potential as a function of the radial coordinate is given by

$$V = 2 - \frac{1}{4} \sum_{n=2}^{\infty} n(n-1) \sum_{m=0}^{n} a_m b_{n-m} \frac{(\rho-\bar{\rho})^{n-2}}{\Omega^{n-2}} \tag{5.39}$$

On the other hand, assuming that the potential $V(\phi)$ is also an analytic function of ϕ around $\phi(\bar{\rho}) = c_0$ yields

$$V = V(\phi_0) + (\phi-\phi_0)V'(\phi_0) + \frac{1}{2}(\phi-\phi_0)^2 V''(\phi_0) + \cdots \tag{5.40}$$

Equating the two previous equations we obtain to leading order

$$V(\phi_0) = 2 - \frac{1}{2}(a_0 b_2 + a_1 b_1 + a_2 b_0) \tag{5.41}$$

We focus now on the interesting case of having a black hole horizon at $\bar{\rho}$. Using the freedom to redene Ω we can set the product $a_0 b_1$ to any desired value. For convenience we choose

$$a_0 b_1 = 8 \tag{5.42}$$

Relation (5.36) xes then $\xi = 4$, eliminating a parameter with respect to the generic case.

Every Ω-family of $f_{1,2}$ functions giving rise to static spacetimes with a (non-extremal) Killing horizon, has an associated smooth solitonic solution with a center. (Similar conclusions hold for stationary solutions.) This solution is obtained by exchanging the roles of the input functions

$$f_{1s} = f_2 \qquad f_{2s} = f_1 \tag{5.43}$$

and demanding the absence of a conical defect. The absence of a conical defect species uniquely the value of Ω to

$$\Omega_s = \frac{a_0}{16} \tag{5.44}$$

Therefore, for any $(n+1)$-parameter family of static black holes there is a smooth n-parameter family of static solitonic solutions with a center. The simplest example is the 1-parameter family of static BTZ black holes, which has a 0-parameter family of solitons, namely the global AdS solution. It is suggestive to consider these solitonic solutions as possible ground states of a given theory. To decide which geometry is the ground state we have to calculate the free energy.

Integration constants

We have completely understood the role that each of the integration constants of the EOMs plays in parametrizing solutions.

- One is related to an arbitrary number we can add to the radial coordinate. We fixed it by choosing the value of the radial coordinate at the center/singularity, ρ_0;
- Two are related fixed by chosing the boundary metric. We fix them by demanding that the solution be asymptotically AdS — $f_{1,2}$ both grow linearly at infinity and $f_1 \to f_2$;
- One more is related to identification of the bulk x^μ coordinates with the physical t, φ coordinates. It thus generates rotations:

$$t = x^0 \cosh\eta - x^1 \sinh\eta \qquad \varphi = -x^0 \sinh\eta + x^1 \cosh\eta \tag{5.45}$$

- The parameter Ω generates families of solutions with the same potential $V(\phi)$;
- The parameter λ is the choice of the boundary conditions for the scalar ϕ as we will see when we discuss holographic renormalization;
- The parameter ξ will be fixed by demanding that solutions be regular, also discussed together with holographic renormalization.

5.3 Holographic renormalization

We now discuss the addition of different classes of counterterms.

From (5.19) we can see that asymptotically AdS solutions with Minkowski boundary metric require

$$f_{1,2} = 2\rho + \dots \tag{5.46}$$

This fixes the boundary metric and so it corresponds to Dirichlet boundary conditions for the metric.

In general we need to add counterterms at the boundary of AdS. These counterterms should be specified once and for all (indeed, they can be seen as part of the definition of the theory, much like the potential $V(\phi)$) and should after that cancel all divergences of *all* solutions. This means that from the beginning one should define exactly what kinds of divergences the counterterms he's looking for are suppose to cancel. This question depends on the chosen boundary conditions. That is, (5.46) selects exclusively the leading term not saying anything about the sub-leading terms. These terms will in part be determined by solving the EOMs of the theory. But for these we need to select the leading terms of the scalar field that we are interested in considering.

The EDG generalization of the Brown-Henneaux [10] boundary conditions is

$$f_{1,2} = 2\rho + C_{1,2} + \mathcal{O}(\rho^{-\epsilon}) \tag{5.47a}$$

$$\phi(\rho) = \mathcal{O}(\rho^{-\frac{1+\epsilon}{2}}) \tag{5.47b}$$

where $\epsilon > 0$, $C_{1,2}$ are arbitrary constants that determine j (5.6) and the asymptotic form of the scalar was chosen from the EOMs. Further playing with substitutions into the EOMs we find that around $\phi = 0$

$$V = \frac{1}{2}m^2\phi^2 + \dots\,, \qquad m^2 = -(1-\epsilon^2) \tag{5.48}$$

and there for $0 \leq \epsilon \leq 1$ since the lower limit corresponds to the Breitenlohner-Freedman (BF) bound $m^2_{\text{BF}} = -1$ and the upper limit corresponds to $m^2 = 0$.

At this point we can suspect that we are missing something. The common AdS/CFT lore tells us that for a scalar mass between the BF bound and zero we usually have two possible boundary conditions: Dirichlet or Neumann (or mixed) corresponding to fixing the leading or sub-leading terms respectively (or linear combinations thereof). However, according to (5.47b) this is already fixed and we have no such freedom. It seems like we are accidentally excluding acceptable solutions. Once we pick the scalar mass we always have two possible asymptotic behaviors,

$$\phi(\rho) = \mathcal{O}(\rho^{-\frac{\Delta_\pm}{2}})\,, \qquad \Delta_\pm = 1 \pm \epsilon \tag{5.49}$$

The reason why this shows up here but not in (5.47b), is that the ansatz (5.47a) is actually too constraining.

Below we present a larger generalization of the Brown-Henneaux boundary conditions for EDG if we want to allow for the important freedom described above. We have started with a certain generalization of f_1 and used the EOMs to obtained behavior of the remaining things. We see in particular that in this case we recover (5.49):

$$f_1 = 2\rho + A\Omega^{1-\epsilon}\rho^\epsilon + B\Omega\log\rho + C\Omega + \dots \tag{5.50a}$$
$$f_2 = f_1 - \xi\Omega + \dots \tag{5.50b}$$
$$\phi = \phi_-\rho^{-\Delta_-/2} + \phi_+\rho^{-\Delta_+/2} + \dots \tag{5.50c}$$
$$\phi_- = \alpha\Omega^{\Delta_-/2}\,, \qquad \phi_+ = \frac{B}{\alpha\Delta_-\Delta_+}\Omega^{\Delta_+/2} \tag{5.50d}$$

with

$$\alpha \equiv \sqrt{\frac{2A\epsilon}{1-\epsilon}} \tag{5.51a}$$
$$B = \Delta_-\Delta_+\alpha^{2/\Delta_-}\lambda \tag{5.51b}$$

where A, B, C and $\Omega \neq 0$ are constants, the dots stand for vanishing terms at the boundary, λ is the integration constant of (5.34).

Note that we are already writing f_1 (5.50a) in a way that is convenient according to our discussion about the independence of the potential on Ω. Accordingly, f_2 depends on j only through $\xi\Omega = j$. Following our discussion of boundary conditions, we have the additional requirement on our Ω-families that the *boundary conditions* too be independent of Ω. Fortunately we already have that the integration constant λ of (5.34) naturally fix the $\phi_\pm$ boundary conditions in an Ω-invariant way.

Cancelling divergences

To cancel divergences we add to (5.1) a counterterm at the boundary:

$$\Gamma_+ = \int d^3x\sqrt{-g}\left(R+2-\frac{1}{2}(\partial\phi)^2-V(\phi)\right)+2\int_\partial d^2x\sqrt{-\gamma}\,(K-U(\phi)) \tag{5.52}$$

where the boundary ∂ is a surface at constant radius, has induced metric γ and the trace of the extrinsic curvature of γ is K. Below we will see what the $(+)$ subscript means. A counterterm like

$$U(\phi) = 1+\frac{\Delta_-}{4}\phi^2 \tag{5.53}$$

cancels all divergences [29] for any solution that could come up if we have an asymptotic behavior like (5.47). To the original action plus counterterms we call Γ_+, our new renormalized action. We can now use the usual AdS/CFT lore to calculate expected values: the derivative of the renormalized on-shell action with respect to the boundary metric is the expected value of the stress-tensor and its derivative with respect to the leading mode of ϕ, ϕ_- is the expected value of the field theory operator dual to ϕ:

$$\begin{aligned}
\Gamma_+|_{\text{EOM}} &= \frac{\text{Vol}}{2}\left(\partial_\rho(f_1f_2)|_{\rho_h}+\lim_{\rho\to\infty}\left[\partial(f_1f_2)-4U(\phi)\sqrt{f_1f_2}\right]\right)\\
&= \text{Vol}\,(|j|+\Delta_-(\Delta_+-\Delta_-)\phi_-\phi_+) && (5.54)\\
\delta_\gamma\Gamma_+|_{\text{EOM}} &= \int_\partial d^2x\sqrt{-\gamma}\,(K_{ij}-(K-U(\phi))\gamma_{ij})\,\delta\gamma^{ij} && (5.55)\\
\delta_\phi\Gamma_+|_{\text{EOM}} &= -\int_\partial d^2x\sqrt{-\gamma}\left(n^\mu\partial_\mu\phi+2U'(\phi)\right)\delta\phi && (5.56)
\end{aligned}$$

And so we obtain the expected values of the stress-energy tensor and of the operator dual to ϕ,

$$\begin{aligned}
\langle T_{ij}\rangle_+ &= j\delta_{ij}+\Delta_-(\Delta_+-\Delta_-)\phi_+\phi_+\eta_{ij} && (5.57)\\
\langle\mathcal{O}_{\Delta_+}\rangle &= -(\Delta_+-\Delta_-)\phi_+ && (5.58)
\end{aligned}$$

and the trace Ward identity

$$\langle T^i{}_i\rangle_+ = -\Delta_-\phi_-\langle\mathcal{O}_{\Delta_+}\rangle \tag{5.59}$$

In the above the boundary metric is $\gamma_{ij} = g^{(0)}_{ij}\rho+\ldots$, and $g^{(0)}_{ij} = 2\eta_{ij}$.

However note that when we computed the variation of the on-shell action with respect to the scalar, (5.56), the ϕ_+ vanishes asymptotically and so $\delta\phi = \delta\phi_-\rho^{-\Delta_-/2}$. Furthermore, the result of this variation comes proportional to $\delta\phi_-$ and therefore Γ_+ poses a well defined variational problem for fixed ϕ_-. However we would like to be to able to keep the λ of (5.34) fixed instead. To do this we will have to add new boundary terms to keep the variational problem well defined.

The variational problem

For the variational problem to be well defined, we want that the variation of the on-shell action Γ with respect to the source be proportional to the variation of the source. Call $\mathcal{J}(\phi_-,\phi_+)$ the combination of leading and sub-leading scalar modes that we decide to keep fixed, i.e. the source. This are called mixed boundary conditions.

Specifically write

$$\mathcal{J} \equiv (\Delta_+ - \Delta_-)\phi_+ - \mathcal{W}'(\phi_-) \tag{5.60}$$

where $\mathcal{W}$ is an arbtirary function. The new boundary terms necessary are

$$S_{\mathcal{W}} = -\int d^2x\sqrt{-g^{(0)}}\left((\Delta_+ - \Delta_-)\phi_+\phi_- + \mathcal{W}(\phi_-) - \phi_-\mathcal{W}'(\phi_-)\right) \tag{5.61}$$

because then we can define a new action which has the required variational property:

$$\delta\Gamma_- = \delta(\Gamma_+ + S_{\mathcal{W}}) = -\int d^2x\sqrt{-g^{(0)}}\phi_-\delta\mathcal{J} \tag{5.62}$$

i.e. it is proportional to δJ. Therefore Γ_- defines a variational problem for the mixed boundary conditions source $\mathcal{J}$. We see that the factor multiplying $\delta\mathcal{J}$ is ϕ_- which means this is the expectation value of the operator dual to ϕ, as expected [65].

Lets put the above to use. Putting together (5.60) and the definition of λ which we want to keep fixed, (5.34), we learn that we should use in the definition of the source $\mathcal{J}$ the function

$$\mathcal{W}(\phi_-) = \lambda\frac{\Delta_-(\Delta_+ - \Delta_-)}{2}\phi_-^{2/\Delta_-} \tag{5.63}$$

The free parameter Ω will label physically different solutions and so physical observables like expected values of the stress-energy tensor and of the dual operator $\mathcal{O}_{\Delta_-}$ will depend on Ω. However, as we wanted Ω is labeling solutions within a family solutions of the same Ω-independent boundary conditions:

$$\langle T_{ij}\rangle_- = \langle T_{ij}\rangle_+ - (\mathcal{W}(\phi_-) + \phi_+\mathcal{J})g^{(0)}_{ij} \tag{5.64}$$

$$\langle \mathcal{O}_{\Delta_-}\rangle = \phi_- \tag{5.65}$$

$$\langle T^i{}_i\rangle_- = -\Delta_+\mathcal{J}\langle\mathcal{O}_{\Delta_-}\rangle \tag{5.66}$$

It is known [66] that boundary conditions like (5.34) correspond to deforming the dual CFT with Neumann boundary conditions by a marginal multitrace deformation

$$\Delta L = \lambda\mathcal{O}_{\Delta_-}^{\frac{2}{\Delta_-}} \tag{5.67}$$

Therefore this is what our algorithm has been generating: solutions for a multitrace-deformed EDG. Of course, before we properly defined the variational problem this was far from obvious by just looking at the algorithm

Having introduced all boundary counterterms to first cancel all divergences and then guaranteee a well-defined the variational problem, the thermodynamical properties of black holes can be obtained from the general methods of [67].

5.4 Thermodynamics

Black hole thermodynamics provides some key insights into semi-classical and quantum gravity. Of particular importance is the black hole entropy and its microscopic description, for instance from a CFT perspective by virtue of the Cardy formula. In this section we address these issues for EDG.

Below we discuss basic thermodynamical quantities, like temperature, entropy, etc. We derive a formula for entropy in terms of curvature invariants, focus on black hole families and their associated solitons. We prove that these solitons can never have a (free) energy lower than global AdS for marginal boundary conditions. In section 6.3 we show the validity of the Cardy formula in EDG, again for marginal boundary conditions.

5.4.1 Basic thermodynamical quantities

Black hole thermodynamics can be studied efficiently on the gravity side in the Euclidean path integral approach, by exploiting results from the previous sections. We refer to [67] for a general analysis of black hole thermodynamics in the context of holography in asymptotically locally AdS backgrounds. This section is a particular application of the results there to the 3-dimensional case we are discussing here, taking into account the modifications required by the possibility of generalized boundary conditions. See also [68] for a similar analysis of black hole thermodynamics in 2-dimensional EDG.

Temperature

Demanding the absence of a conical defect at the horizon $\rho = \rho_h$ leads to a periodicity in Euclidean time $\tau \sim \tau + \beta$ that is identified with the inverse temperature. From the line-element (5.24) we obtain

$$\beta = T^{-1} = \frac{4\pi}{R\partial_\rho N^2}\bigg|_{\rho_h} = \frac{2\pi R_h}{j} \tag{5.68}$$

Notice that for black hole solutions the particle angular momentum j is positive.

Entropy

To derive entropy from scratch we could evaluate first the on-shell action, extract from there the free energy and then obtain entropy by taking the appropriate partial derivative of the free energy with respect to temperature. We shall provide these results below. Alternatively, for a two-derivative gravity theory it is known that the black hole entropy simply is given by the Bekenstein-Hawking formula

$$S = 4\pi A_h \tag{5.69}$$

where $A_h = 2\pi R_h$ is the horizon area. Using (5.68), an interesting reformulation of the result for entropy is

$$S = 2\mathrm{Vol}_E j \tag{5.70}$$

where $\mathrm{Vol}_3 = \int d\tau d\varphi$. The entropy formula (5.70) highlights the physical importance of the constant of motion j from (5.6).

Angular velocity

Since a black hole is a localized object, its angular velocity is measured with respect to that at infinity, which is a property of the asymptotic region

$$\omega = N_{\varphi h} - N_{\varphi\infty} \tag{5.71}$$

In the AdS case we are currently considering and without loss of generality, we then fix the asymptotic form of the spacetime by requiring the boundary metric to be Minkowski. Namely, $N_{\varphi\infty} = 0$ and $R_\infty^2 = 2$. This reduces the map between the local and physical coordinates (5.18) to (5.45). This restriction yields

$$\omega = \tanh \eta \tag{5.72}$$

with η as defined in (5.45).

Mass and angular momentum

The holographic conserved charges associated with a boundary conformal Killing vector k^i are given by

$$\mathcal{Q}[k] = \int_0^{2\pi} d\varphi \langle T_{ti} k^i \tag{5.73}$$

Since we know the renormalized holographic stress tensor, it is straightforward to evaluate these conserved charges. The black hole mass is obtained for $k = \partial_t$

$$M = \int_0^{2\pi} d\varphi (\langle T_{00} \rangle \cosh^2 \eta + \langle T_{11} \rangle \sinh^2 \eta \tag{5.74}$$

where the stress tensor should be evaluated with the appropriate boundary conditions, and the subindices here refer to the local coordinates (x^0, x^1). Substituting (5.57) for Dirichlet, or (5.64) for Neumann or Mixed boundary conditions, we obtain

$$M = 2\pi j \cosh 2\eta - 2\pi \langle T^i{}_i \rangle \tag{5.75}$$

The black hole angular momentum is obtained for $k = \partial_\varphi$

$$J = \int_0^{2\pi} d\varphi \langle T_{t\varphi} \rangle = \pi (\langle T_{00} \rangle + \langle T_{11} \rangle) \sinh 2\eta = 2\pi j \sinh 2\eta \tag{5.76}$$

Gibbs free energy and the first law of black hole mechanics

The renormalized Euclidean on-shell action gives the Gibbs free energy [69]

$$I = \beta G(T, \omega) \tag{5.77}$$

where $I = -\Gamma$ is the renormalized Euclidean on-shell action and

$$G(T, \omega) \equiv M - TS - \omega J \tag{5.78}$$

is the Gibbs free energy. This coincides with the Helmholtz free energy for vanishing angular velocity and angular momentum. Evaluating the Euclidean on-shell action we get

$$G(T, \omega) = -2\pi j - 2\pi \langle T^i{}_i \rangle \tag{5.79}$$

Indeed, using the relations derived above, this expression reproduces the right hand side of (5.78), and $-\partial G / \partial T|_\omega$ reproduces the Bekenstein-Hawking entropy (5.69). Finally, as is shown in general in [67] these quantities satisfy the first law of black hole mechanics

$$\delta M = T \delta S + \omega \delta J \tag{5.80}$$

where the variations are taken at fixed source J and fixed boundary condition for the scalar field.

5.4.2 Black hole families and their solitons

We have seen in previous sections how to systematically construct black hole families by varying, besides the rotation parameter η, the integration constant Ω. We analyze here their thermodynamic properties. The black hole temperature, (5.68), is

$$T = \frac{1}{2}\pi \cosh\eta \sqrt{\frac{\Omega}{\Omega_s}} \tag{5.81}$$

with Ω_s the value of Ω for the unique static soliton solution associated to each black hole family, given in (++++2.51). As we have discussed, only marginal boundary conditions with vanishing source allow to freely vary the parameter Ω. Namely, this is the boundary condition for which the $\{\Omega, \eta\}$-black hole family can be interpreted as thermal states in the same boundary CFT. Since for marginal boundary conditions the trace of the stress tensor is proportional to the sources, (5.59), the field theory energy and angular momentum are given by

$$M = 8\pi\Omega \cosh 2\eta \qquad J = 8\pi\Omega \sinh 2\eta \tag{5.82}$$

We have chosen Ω satisfying (++++2.49), such that $j = 4\Omega$ for simplicity. The entropy is

$$S = 32\pi^2 \cosh\eta \sqrt{\Omega_s \Omega} \tag{5.83}$$

The charges of the solitonic solution are

$$M_s = -8\pi\Omega_s \qquad J = 0 \tag{5.84}$$

Any of these 2-parameter families of stationary hairy black holes includes a 1-parameter family of extremal solutions. It is obtained by performing the double scaling limit $\Omega \to 0, |\eta| \to \infty$ while keeping fixed $\Omega e^{2|\eta|} \to \bar{\Omega}$. We then have

$$M = |J| = 4\pi\bar{\Omega} \qquad S = 16\pi^2\sqrt{\Omega_s \bar{\Omega}} \qquad T = 0 \tag{5.85}$$

Stability of the hairy sector

In addition to solutions with non-trivial scalar profile, the boundary condition (5.34) clearly allows solutions with vanishing scalar: the BTZ black hole family and its associated soliton, global AdS. The preferred solution will be that with smaller free energy for a given temperature.

The free energy for hairy or BTZ black holes and their respective solitons is given by

$$G = -8\pi\Omega \qquad G_s = M_s = -8\pi\Omega_s \tag{5.86}$$

A first interesting implication is that inside each family there is a Hawking-Page phase transition at $T = \frac{1}{2\pi}$. For $T < \frac{1}{2\pi}$, or equivalentely $\Omega < \Omega_s$, the soliton geometry with a thermal circle is preferred, while for $T > \frac{1}{2\pi}$ the preferred one is the black hole. Comparing members of the hairy and BTZ families with the same temperature (5.81), we obtain

$$G = \frac{\Omega_s}{\Omega_{\rm AdS}} G_{\rm BTZ} \qquad M_s = \frac{\Omega_s}{\Omega_{\rm AdS}} M_{\rm AdS} \tag{5.87}$$

Which family dominates just depends on the quotient $\Omega_s/\Omega_{\rm AdS}$.

We show now that $\Omega_s < \Omega_{\text{AdS}}$ for any smooth solution with a center in EDG with non-trivial scalar profile. Relation (5.32) can be rewritten as

$$\Omega_s = \frac{1}{2\dot{f}_{1c}} \tag{5.88}$$

where the subindex 'c' indicates that the function should be evaluated at the center. We are assuming f_1 to be asymptotically positive, in particular $\dot{f}_1 = 2$ at infinity. The inequality (5.14) requires then its second derivative to be negative for all values of the radial coordinate. Hence $\dot{f}_1$ is a decreasing function, and we obtain

$$\Omega_s \leq \frac{1}{4} \tag{5.89}$$

The inequality is saturated only when $\ddot{f}_1$ vanishes for all radial values, which implies that the solution is global AdS. We can state the following interesting result: any smooth solution of EDG with vanishing trace of the boundary stress tensor has bigger mass than global AdS. Given that the free energy (5.87) is negative, the previous result ensures that a BTZ black hole has smaller free energy than the corresponding hairy one (for marginal boundary conditions).

5.4.3 Cardy formula

The Cardy formula for specific hairy black holes in EDG was considered in [70, 71].

$$S_{\text{Cardy}} = 4\pi\sqrt{-\Delta_0^+\Delta *+} + 4\pi\sqrt{-\Delta_0^-\Delta *-} \tag{5.90}$$

where $\Delta^\pm = (M \pm J)/2$ are the Virasoro zero mode eigenvalues of the black hole states, and $\Delta_0^\pm$ are the lowest eigenvalues. The non-trivial question is what those lowest eigenvalues should be. Rewriting the entropy formula (5.82) in a suggestive way,

$$S = 2\pi\sqrt{-M_s(M+J)} + 2\pi\sqrt{-M_s(M_J)} \tag{5.91}$$

we see that the Cardy formula is satisfied, $S = S_{\text{Cardy}}$, provided we identify $\Delta_0^\pm = \frac{1}{2}M_s$ as proposed in [70]. Since our conclusions hold for any (Ω, η)-family of stationary black hole solutions we have generalized the results by Correa, Martinez and Troncoso from a set of specific examples to generic EDG.

The fact that a Cardy formula holds for hairy black holes is remarkable and may indicate that the hairy sector is actually stable against tunneling into the BTZ sector.

Summary and conclusions

In this work we used the AdS/CFT correspondence to study time evolution of generic strongly coupled systems. Our results can be summarized in the following way:

- We proposed that the gravitation collapse, specifically as described by the asymptotically AdS Vaidya metric, be the holographic dual of a quench where we turn on a homogeneous density of sources for a short interval. These type of quenches have since been dubbed "thermal quenches". We argued that in these situations the interesting observables to examine are non-local observables.

- We used the Ryu-Takayanagi conjecture to calculate one of these non-local observables called the entanglement entropy. We studied the corresponding gravitational objects, equal boundary time extremal surfaces, to draw conclusions about the time evolution of the entanglement entropy following a thermal quench. We identified a time scale t_0 derived from the extremal surfaces living in time evolving geometries. We argued that in the field theory description, this time scale is associated with the thermal wavelength of the excitations in the final state of the quench. We also argued that at least in the first moments after the quench, it seems that the apparent horizon plays no role in the process of thermalization.

- We used the gravitational WKB approximation to argued that non-equal time spacelike 2-point functions in the field theory are described by spacelike sepparated extremal surfaces anchored in the boundary. We found that these observables also contain information about the time scale t_0. We also proposed another time scale $\bar{t}$, associated with the equilibration of the occupation numbers of the excitations.

- In these last two points we our holographic results match to the CFT results of Calabrese and Cardy.

- In order to generalize the types of quenches available, we went looking for new solutions to asymptotically AdS 3-dimensional Einstein-dilaton gravity. For this we proposed an algorithm that allows us to generate such solutions from which we demanded certain physical properties. We used this to obtain all asymptotically AdS stationary axi-symmetric solutions. We obtained a 1-parameter family of black hole solutions whose thermodynamics we studied, and showed that they can never have a free energy lower than global AdS. We also showed that they always come with an associated solitonic solution.

Resumén y conclusiones

En este trabajo hemos usado la correspondencia AdS/CFT para estudiar la evolución temporal de sistemas en acoplo fuerte. Nuestros resultados pueden ser resumidos de la siguiente forma:

- Hemos propuesto que el colapso gravitatorio, especificamente como descrito por una métrica Vaidya asimptoticamente AdS, sea el dual holográfico a un quench en el cual encendemos una fuente uniforme durante un corto intervalo de tiempo. A este tipo de quenches se llamó quenches térmicos. Hemos argumentado que en estas situaciones los observables interesantes a examinar son observables no-locales.

- Hemos usado la conyectura de Ryu-Takayanagi para calcular uno de estos observables no-locales llamado entropía de entrelazamiento. Hemos estudiado los objectos gravitatorios correspondientes, que son surperficies extremales a tiempo igual, para obtener conclusiones sobre la evolución temporal de la entropía de entrelazamiento despues de un quench térmico. Hemos identificado una escala de tiempo t_0 que se puede derivar de las surperfícies extremales que viven en geometrias que evolucionan en el tiempo. Hemos argumentado que en la descripción de la teoria de campos esta escala de tiempo está asociada con la longitud de onda térmica de las excitaciones que viven en el estado final del quench. También hemos argumentado que por lo menos en lo que dice respecto a los momentos iniciales después del quench, el horizonte aparente no juega un papel en el proceso de termalización.

- Hemos usado la versión gravitatória de la aproximacíon WKB para argumentar que las funciones a dos puntos de tipo espacio en la teoria de campos son descritas por surperfícies extremas del tipo espacio que terminan en la frontera. Hemos encontrado que estos observables también contienen información sobre la escala de tiempo t_0. También hemos propuesto otra escala de tiempo $\bar{t}$, asociada con la equilibración de los numeros de ocupación de las excitaciones.

- En estos dos últimos puntos nuestros cálculos holográficos están de acuerdo con los resultados de CFT de Calabrese y Cardy.

- Para generalizar el tipo de quenches disponibles, hemos buscado nuevas soluciones de gravedad tres-dimensional asimptoticamente AdS. Para ello hemos propuesto un algoritmo que nos permite generar nuevas soluciones de las cuales podemos exigir ciertas propriedades físicas. Hemos usado esto para obtener todas las soluciones estacionárias y axi-simétricas. Hemos obtenido famílias de soluciones de agujeros negros cuya termodinamica hemos estudiamos, y hemos probado que nunca pueden tener una energía libre por debajo de AdS global. También hemos probado que estas famílias de agujeros negros siempre vienen acompañadas por una solución solitónica correspondiente.

Bibliography

[1] Juan Martin Maldacena. The Large N limit of superconformal field theories and supergravity. *Adv.Theor.Math.Phys.*, 2:231–252, 1998.

[2] Edward Witten. Anti-de Sitter space and holography. *Adv.Theor.Math.Phys.*, 2:253–291, 1998.

[3] S.S. Gubser, Igor R. Klebanov, and Alexander M. Polyakov. Gauge theory correlators from noncritical string theory. *Phys.Lett.*, B428:105–114, 1998.

[4] C. Orzel, A.K. Tuchman, M.L. Fenselau, M. Yasuda, and M. A. Kasevich. Squeezed States in a Bose-Einstein Condensate. *Science*, 291:2386–2389, 2001.

[5] Markus Greiner, Olaf Mandel, Tilman Esslinger, Theodor W. Hnsch, and Immanuel Bloch. Quantum phase transition from a superfluid to a Mott insulator in a gas of ultracold atoms. *Nature*, 415:39–44, 2001.

[6] Ofer Aharony, Steven S. Gubser, Juan Martin Maldacena, Hirosi Ooguri, and Yaron Oz. Large N field theories, string theory and gravity. *Phys.Rept.*, 323:183–386, 2000.

[7] Eric D'Hoker and Daniel Z. Freedman. Supersymmetric gauge theories and the AdS / CFT correspondence. pages 3–158, 2002.

[8] Edward Witten. (2+1)-Dimensional Gravity as an Exactly Soluble System. *Nucl.Phys.*, B311:46, 1988.

[9] Edward Witten. Three-Dimensional Gravity Revisited. 2007.

[10] J. David Brown and M. Henneaux. Central Charges in the Canonical Realization of Asymptotic Symmetries: An Example from Three-Dimensional Gravity. *Commun.Math.Phys.*, 104:207–226, 1986.

[11] A.A. Belavin, Alexander M. Polyakov, and A.B. Zamolodchikov. Infinite Conformal Symmetry in Two-Dimensional Quantum Field Theory. *Nucl.Phys.*, B241:333–380, 1984.

[12] Ulrich W. Heinz. Thermalization at RHIC. *AIP Conf.Proc.*, 739:163–180, 2005.

[13] John C. Collins and M.J. Perry. Superdense Matter: Neutrons Or Asymptotically Free Quarks? *Phys.Rev.Lett.*, 34:1353, 1975.

[14] Edward V. Shuryak. What RHIC experiments and theory tell us about properties of quark-gluon plasma? *Nucl.Phys.*, A750:64–83, 2005.

[15] Matthew Luzum and Paul Romatschke. Conformal Relativistic Viscous Hydrodynamics: Applications to RHIC results at s(NN)**(1/2) = 200-GeV. *Phys.Rev.*, C78:034915, 2008.

[16] Paul M. Chesler and Laurence G. Yaffe. Horizon formation and far-from-equilibrium isotropization in supersymmetric Yang-Mills plasma. *Phys.Rev.Lett.*, 102:211601, 2009.

[17] Guillaume Beuf, Michal P. Heller, Romuald A. Janik, and Robi Peschanski. Boost-invariant early time dynamics from AdS/CFT. *JHEP*, 0910:043, 2009.

[18] Paul M. Chesler and Laurence G. Yaffe. Boost invariant flow, black hole formation, and far-from-equilibrium dynamics in N = 4 supersymmetric Yang-Mills theory. *Phys.Rev.*, D82:026006, 2010.

[19] Irene Amado, Carlos Hoyos-Badajoz, Karl Landsteiner, and Sergio Montero. Hydrodynamics and beyond in the strongly coupled N=4 plasma. *JHEP*, 0807:133, 2008.

[20] Ulf H. Danielsson, Esko Keski-Vakkuri, and Martin Kruczenski. Spherically collapsing matter in AdS, holography, and shellons. *Nucl.Phys.*, B563:279–292, 1999.

[21] Ulf H. Danielsson, Esko Keski-Vakkuri, and Martin Kruczenski. Black hole formation in AdS and thermalization on the boundary. *JHEP*, 0002:039, 2000.

[22] Yoav Peleg and Alan R. Steif. Phase transition for gravitationally collapsing dust shells in (2+1)-dimensions. *Phys.Rev.*, D51:3992–3996, 1995.

[23] Vijay Balasubramanian and Simon F. Ross. Holographic particle detection. *Phys.Rev.*, D61:044007, 2000.

[24] Leonard Susskind and Edward Witten. The Holographic bound in anti-de Sitter space. 1998.

[25] Vijay Balasubramanian, Per Kraus, Albion E. Lawrence, and Sandip P. Trivedi. Holographic probes of anti-de Sitter space-times. *Phys.Rev.*, D59:104021, 1999.

[26] Tom Banks, Michael R. Douglas, Gary T. Horowitz, and Emil J. Martinec. AdS dynamics from conformal field theory. 1998.

[27] Javier Abajo-Arrastia, Joao Aparicio, and Esperanza Lopez. Holographic Evolution of Entanglement Entropy. *JHEP*, 1011:149, 2010.

[28] Joao Aparicio and Esperanza Lopez. Evolution of Two-Point Functions from Holography. *JHEP*, 1112:082, 2011.

[29] Joao Aparicio, Daniel Grumiller, Esperanza Lopez, Ioannis Papadimitriou, and Stefan Stricker. Bootstrapping gravity solutions. *JHEP*, 1305:128, 2013.

[30] P. Di Francesco, P. Mathieu, and D. Senechal. Conformal field theory. 1997.

[31] John L. Cardy. Conformal Invariance and Surface Critical Behavior. *Nucl.Phys.*, B240:514–532, 1984.

[32] Pasquale Calabrese and John L. Cardy. Time-dependence of correlation functions following a quantum quench. *Phys.Rev.Lett.*, 96:136801, 2006.

[33] Jean-Marie Stéphan and Jérôme Dubail. Logarithmic corrections to the free energy from sharp corners with angle 2π. 2013.

[34] C. Domb and J.L. Lebowitz. PHASE TRANSITIONS AND CRITICAL PHENOMENA. VOL. 10. 1986.

[35] H.W. Diehl. The Theory of boundary critical phenomena. *Int.J.Mod.Phys.*, B11:3503–3523, 1997.

[36] Pasquale Calabrese and John Cardy. Quantum Quenches in Extended Systems. *J.Stat.Mech.*, 0706:P06008, 2007.

[37] Christoph Holzhey, Finn Larsen, and Frank Wilczek. Geometric and renormalized entropy in conformal field theory. *Nucl.Phys.*, B424:443–467, 1994.

[38] Luca Bombelli, Rabinder K. Koul, Joohan Lee, and Rafael D. Sorkin. A Quantum Source of Entropy for Black Holes. *Phys.Rev.*, D34:373–383, 1986.

[39] Mark Srednicki. Entropy and area. *Phys.Rev.Lett.*, 71:666–669, 1993.

[40] Pasquale Calabrese and John L. Cardy. Entanglement entropy and quantum field theory. *J.Stat.Mech.*, 0406:P06002, 2004.

[41] M. Le Bellac. Thermal field theory. 1996.

[42] J.L. Cardy, O.A. Castro-Alvaredo, and B. Doyon. Form factors of branch-point twist fields in quantum integrable models and entanglement entropy. *J.Statist.Phys.*, 130:129–168, 2008.

[43] Pasquale Calabrese and John Cardy. Entanglement entropy and conformal field theory. *J.Phys.*, A42:504005, 2009.

[44] Pasquale Calabrese and John L. Cardy. Evolution of entanglement entropy in one-dimensional systems. *J.Stat.Mech.*, 0504:P04010, 2005.

[45] Stanley Deser and R. Jackiw. Three-Dimensional Cosmological Gravity: Dynamics of Constant Curvature. *Annals Phys.*, 153:405–416, 1984.

[46] Maximo Banados, Claudio Teitelboim, and Jorge Zanelli. The Black hole in three-dimensional space-time. *Phys.Rev.Lett.*, 69:1849–1851, 1992.

[47] Maximo Banados, Marc Henneaux, Claudio Teitelboim, and Jorge Zanelli. Geometry of the (2+1) black hole. *Phys.Rev.*, D48:1506–1525, 1993.

[48] P. Vaidya. The Gravitational Field of a Radiating Star. *Proc.Indian Acad.Sci.*, A33:264, 1951.

[49] S. Weinberg. Gravitation and Cosmology: Principle and Applications of the General Theory of Relativity. 1972.

[50] Per Kraus, Hirosi Ooguri, and Stephen Shenker. Inside the horizon with AdS / CFT. *Phys.Rev.*, D67:124022, 2003.

[51] Juan Martin Maldacena. Eternal black holes in anti-de Sitter. *JHEP*, 0304:021, 2003.

[52] Jorma Louko, Donald Marolf, and Simon F. Ross. On geodesic propagators and black hole holography. *Phys.Rev.*, D62:044041, 2000.

[53] C.P. Herzog and D.T. Son. Schwinger-Keldysh propagators from AdS/CFT correspondence. *JHEP*, 0303:046, 2003.

[54] Shinsei Ryu and Tadashi Takayanagi. Holographic derivation of entanglement entropy from AdS/CFT. *Phys.Rev.Lett.*, 96:181602, 2006.

[55] Shinsei Ryu and Tadashi Takayanagi. Aspects of Holographic Entanglement Entropy. *JHEP*, 0608:045, 2006.

[56] Veronika E. Hubeny, Mukund Rangamani, and Tadashi Takayanagi. A Covariant holographic entanglement entropy proposal. *JHEP*, 0707:062, 2007.

[57] Shouvik Datta and Justin R. David. Renyi entropies of free bosons on the torus and holography. 2013.

[58] Ivan Booth. Black hole boundaries. *Can.J.Phys.*, 83:1073–1099, 2005.

[59] S. W. Hawking and Ellis G. F. R. The large scale structure of space-time. 1973.

[60] Vijay Balasubramanian and Per Kraus. A Stress tensor for Anti-de Sitter gravity. *Commun.Math.Phys.*, 208:413–428, 1999.

[61] Sebastian de Haro, Sergey N. Solodukhin, and Kostas Skenderis. Holographic reconstruction of space-time and renormalization in the AdS / CFT correspondence. *Commun.Math.Phys.*, 217:595–622, 2001.

[62] V. Balasubramanian, A. Bernamonti, J. de Boer, N. Copland, B. Craps, et al. Holographic Thermalization. *Phys.Rev.*, D84:026010, 2011.

[63] Gerard Clement. Particle - like solutions to topologically massive gravity. *Class.Quant.Grav.*, 11:L115–L120, 1994.

[64] Robert M. Wald. General Relativity. 1984.

[65] Ioannis Papadimitriou. Multi-Trace Deformations in AdS/CFT: Exploring the Vacuum Structure of the Deformed CFT. *JHEP*, 0705:075, 2007.

[66] Edward Witten. Multitrace operators, boundary conditions, and AdS / CFT correspondence. 2001.

[67] Ioannis Papadimitriou and Kostas Skenderis. Thermodynamics of asymptotically locally AdS spacetimes. *JHEP*, 0508:004, 2005.

[68] Daniel Grumiller and Robert McNees. Thermodynamics of black holes in two (and higher) dimensions. *JHEP*, 0704:074, 2007.

[69] G.W. Gibbons and S.W. Hawking. Action Integrals and Partition Functions in Quantum Gravity. *Phys.Rev.*, D15:2752–2756, 1977.

[70] Francisco Correa, Cristian Martinez, and Ricardo Troncoso. Hairy Black Hole Entropy and the Role of Solitons in Three Dimensions. *JHEP*, 1202:136, 2012.

[71] Mu-In Park. Fate of three-dimensional black holes coupled to a scalar field and the Bekenstein-Hawking entropy. *Phys.Lett.*, B597:237–242, 2004.